ADDIS ABABA UNIVERSITY

ADDIS ABABA INSTITUTE OF TECHNOLOGY

SCHOOL OF CHEMICAL AND BIO ENGINEERING

Isolation and Performance Evalaution of Microcrystalline Cellulose from Ethiopian *Teff* (*Eragrostis tef*) Straw for the Enhancement of Thermo-Mechanical Properties of Polyvinyl Alcohol Based Bio-Degradable Polymer

By : Equar Gebre Assefa

A PhD Dissertation Submitted to the School of Chemical and Bio Engineering in partial Fulfillment of the Requirements for the Degree of Doctor of Philosophy in Chemical Engineering (Process Engineering)

Supervisors: Prof. Zebene Kiflie

Dr. Eng. Hundessa Dessalegn

Addis Ababa, Ethiopia

July, 2024

DECLARATION

This doctoral dissertation represents my own original work. I confirm that it has not been submitted previously for any academic degree. All information and ideas borrowed from other sources have been properly acknowledged and referenced. Additionally, I have included a list of publications based on research conducted for this dissertation. .

Equar Gebre Assefa

Signature:

Date:

APPROVAL SHEET

ADDIS ABABA UNIVERSITY

ADDIS ABABA INSTITUTE OF TECHNOLOGY

SCHOOL OF CHEMICAL AND BIO ENGINEERING

This is to certify that the PhD Dissertation prepared by Equar Gebre Assefa, entitled: **"Isolation and Performance Evalaution of Microcrystalline Cellulose from Ethiopian *Teff* (Eragrostis tef) Straw for the Enhancement of Thermo- Mechanical Properties of Polyvinyl Alcohol Based Bio-Degradable Polymer"** and submitted in partial fulfillment of the requirements for Degree of Doctor of Philosophy in Chemical Engineering (Process Engineering Stream) complies with the regulations of the university and meets the accepted standards with respect to originality and quality.

Examining Committee:

Internal Examiner	**Signature**	**Date**
External Examiner	**Signature**	**Date**

Supervisors

Major Advisor	**Signature**	**Date**
Co- Advisor	**Signature**	**Date**

School Dean/ Graduate Program Coordinator

EXECUTIVE SUMMARY

Traditional plastics come from fossil fuels, harm the environment, and don't break down easily. Here, the study explores using a natural material, microcrystalline cellulose (MCC), from *Teff* straw (TS), an abundant agricultural residue in Ethiopia. The research aims to isolate MCC from TS and evaluate its effectiveness as a reinforcing agent in PVA to create improved eco-friendly plastic. This research is divided into three main parts.

In the first part of this study, developing a method to produce cellulose-rich pulp from TS and characterization of the achieved material was done. A two stage pre-treatment(alkaline and chlorine-free bleaching treatments) for TS fibers was used which can bring about internal defibrillation in the fibers through cleavage of the hydrogen bonding that holds the hemicellulose - cellulose micro fibril network. The first alkaline treatment stage termed as the alkaline delignification was optimized by a single effect design with a three independent variables [i.e. temperature (60–95 °C at the interval of 10°C except for the last level (at 5°C interval)), time (30–150 min at the interval of 30 min), and NaOH concentration (2–8 wt. % at the interval of 1.5 wt. %)] targeted at predict their effect on lignin decomposition and fiber yield. The second stage bleaching treatment was conducted using a preheated mixture of hydrogen peroxide (20%) and sodium hydroxide (5%) at a temperature of 65 °C for 90 min. The bleaching treatment was focused on obtaining a cellulose-rich pulp with minimal lignin content for microcrystalline cellulose production.

Chemical composition analysis shows that the raw TS has 40.44%, 29.44%, and 18.05% of cellulose, hemicellulose, and lignin respectively. Furthermore, the TS cellulose-rich pulp obtained after the two-stage pre-treatment had cellulose, hemicelluloses, and lignin content of 85.5%, 11.98%, and 2.52%, respectively, which confirmed the significant decrease in the percentage of non-cellulosic components. In addition, the extraction procedure yielded purified cellulose with crystallinity, Onset temperature (T_{on}), and maximum decomposition temperature (T_{max}), of 65.51%, 255 °C, and 365.5 °C. The results indicated that two-stage alkali hydrogen peroxide treatment was beneficial for producing cellulose-rich pulp, while TS is a promising new source of raw material to produce cellulose for application in microcrystalline cellulose production.

In the second part, the cellulose was converted to microcrystalline cellulose via transition metal salts assisted dilute acid hydrolysis. The products were characterized by FT-IR, SEM, XRD, and TGA. XRD results indicated that Cr $(NO_3)_3$ assisted acid hydrolysis produced MCCs presented the highest crystallinity index (CrI) values (73.34%), as compared to both $FeCl_3$ (67.58%), and Fe $(NO_3)_3$ (66.69%) catalyzed acid treatments. Furthermore, from the TGA analysis, It was interesting to note that, the thermal degradation starting temperature (T_{on}) obtained for Cr $(NO_3)_3$, $FeCl_3$, and Fe $(NO_3)_3$ assisted dilute acid hydrolysis were 285, 273, and 275 °C, respectively which indicate the higher thermal stability of these fibers.

After successfully isolating MCC from *Teff* straw, its ability was further explored to act as a reinforcing agent in PVA polymer in the last part of this research work. The processing of PVA /MCCs composites employed solvent based fabrication methods (solution casting) by mixing the pre-dispersing MCCs in a 5% PVA solution and then performing a film. The effects of filler-matrix compatibility on the composites mechanical, thermal properties were investigated. The mechanical properties of the composites were remarkably enhanced by the incorporation of MCC into the PVA matrix at lower MCC content without negatively affecting its important properties. The tensile strength of the PVA films increased by up to 49%, 71%, and 67% when Cr(III)-MCC, Fe(III)Cl-MCC and Fe(III)-MCC was incorporated at a level of 5%, respectively. Additionally, MCCs obtained using different catalysts (Cr(III)-MCC, Fe(III)Cl-MCC, and Fe(III)-MCC) showed different reinforcement effects for the PVA composite films.

MCC addition also increased the thermal stability of the composites compared to pure PVA (295°C). Notably, the onset temperatures reached 305°C for Cr(III)-MCC, 308°C for Fe(III)Cl-MCC, and 303°C for Fe(III)-MCC-based PVA films. SEM analysis also revealed that the MCC fibers were dispersed in the PVA matrix, indicating that there was good interaction between the two materials. Overall, the results of this study suggest that *Teff* straw MCCs could be used as a low-cost reinforcement additive to produce biodegradable films with enhanced mechanical properties and thermal stability. These films could be used for a variety of applications, such as food packaging.

Keywords: *Teff* straw; cellulose; microcrystalline cellulose; composites; hydrolysis; polyvinyl alcohol; pre-treatments; characterization

ACKNOWLEDGMENT

Above all, I thank the Almighty God, for giving me the strength, health, and his blessing throughout my research work to complete the research successfully. I am also thankful to all those who have assisted me in completing my doctoral study. Some of these great people are mentioned below and without them I couldn't have achieved what I have done so far.

First and foremost, I'd like to express my heartfelt gratitude to my supervisor, Prof. Zebene Kiflie for his continuous guidance, support, and patience that were critical to my success as a graduate student. I appreciate his brilliant insight and I feel honored to have worked under his supervision. I also would like to thank my co-supervisor, Dr.Eng Hundessa Dessalegn, who has been supportive starting from the development of the proposal and throughout my Ph.D studies. I am deeply indebted to thank Professor Nigus Gabbiye, for allowing me to use his lab, valuable suggestions and all-rounded support throughout my study. Besides, I would like to thank to Dr. Yallow W/amanuel, Mr. Zinabu Tassew, and Leulseged Belay for their helps in laboratory works.

I am very thankful to the staff members of School of Chemical and Bio-engineering (AAiT) for their hospitality, willingness to help and encouragement. Acknowledgment is also extended to the staffs of the Faculty of Chemical and Food engineering (BiT), Alebel Abebaw, Neima Ahmed, Tadele Mihiret, and Addisu Getahun for their technical support with instruments and for supplying the necessary consumables and devices for my experimental work at BiT. I would like to thank my friends Mr. Agimasie Agasie, Dr. Tsegahun mekonen and Mahilet Minwuyelet for their encouragement, friendship and empathy. I really appreciate you all. I would like to say a big thank to my brother Dr. Nigus G/medhin for his financial and professional support!

I am extremely grateful to my families and very special thanks to Selamawit Teferi, my wife, for her steadfast love, tolerance and endless support during my long period of study. She and my three little angels, Samuel, Mahilet, and Kidist Equar have been the inspiration of my life. Their unconditional love and guidance has made me the man that I am today, for which I am deeply grateful. Finally, I would like to thank Addis Ababa Institute of Technology and Bahir Dar Institute of Technology, for granting me the scholarship, providing financial support for this research, and allowing me laboratory facilities that helps me to finalize my Ph.D. studies.

TABLE OF CONTENTS

LIST OF FIGURES

LIST OF TABLES

LIST OF PUBLICATIONS

1. **Assefa, E.G.,** Kiflie, Z. & Demsash, H.D. (2023) Valorization of Abundantly Available Ethiopian *Teff* Eragrostis Tef) Straw for the Isolation of Cellulose Fibrils by Alkaline Hydrogen Peroxide Treatment Method. J Polym Environ 31, 900–912. https://doi.org/10.1007/s10924-022-02646-4
2. **Assefa, E. G.,** Kiflie, Z., & Demsash, H. D. (2023). Transition metal salt assisted dilute acid hydrolysis for synthesis of microcrystalline cellulose from Teff Straw. Cellulose, 30(10), 6289-6301.https://doi.org/10.1007/s10570-023-05270-0
3. **Assefa, E. G.,** Kiflie, Z., Demsash, H. D., & Habtu, N. G. (2024). Effect of Teff Straw (Eragrostis Tef) Based Microcrystalline Cellulose on Enhancement of Thermo-Mechanical and Microstructural Properties of PVA Bio-Degradable Polymers. Waste and Biomass Valorization, 1-12. https://doi.org/10.1007/s12649-024-02553-w

LIST OF ABBREVIATIONS

AHP	Alkali hydrogen peroxide
CCD	Central composite design
CNF	Cellulose nanofiber
CrI	Crystallinity Index
CW	Cellulose nano-whiskers

DTG	Derivative Thermogravimetry
Eb	Elongation at Break
FAO	Food and Agriculture Organization
FTIR	Fourier Transform Infrared Spectroscopy
ILs	Ionic Liquids
LCB	Lignocellulosic biomass
MCC	Microcrystalline cellulose
MFC	Micro fibrillated cellulose
OPEFB	Oil palm empty-fruit-bunches
NREL	National Renewable Energy Laboratory
PBS	Polybutylene Succinate
PGA	Polyglycolic Acid
PCL	Polycaprolactone
PLA	Polylactic acid
PVA	Polyvinyl alcohol
PVAc	Polyvinyl acetate
RW	residual weight
RSM	Response surface methodology
SA	Sulfuric Acid
SEM	Scanning Electronic Microscope
TGA	Thermo Gravimetric Analysis

TONC	TEMPO-oxidized nanocellulose
T_{on}	Onset degradation temperature
T_{max}	Maximum degradation temperature
TS	*Teff* straw
XRD	X-Ray Diffraction

CHAPTER 1: INTRODUCTION

1.1. Background

Polymer materials are widely used across various industries due to their affordability, accessibility, lightness, resistance to chemicals, durability, and easy manufacturing [1]. On the other hand, the rapid increase in plastic production and fossil fuel use has resulted in environmental pollution generated by plastic waste, ever-depleting non-renewable sources, and generating greenhouse gases. Synthetic plastics often require decades, or even centuries, to degrade. Packaging industries are the primary source of plastic production, making them the biggest contributor to environmental issues [2]. Consequently, the depletion of fossil resources and the increasing emphasis on environmental protection and public well-being have pushed a great number of academicians to focus on the development of biodegradable polymers for use in packaging, fields of construction, automobile manufacturing, and healthcare that satisfy the environmental concerns [3]. Biodegradable polymers are generally defined as those that decompose in natural aerobic and anaerobic environments. Based on their source, these can be categorized into two groups: natural polymers whose components are derived from renewable raw materials, while synthetic biodegradable polymers are derived from petroleum-based resources.

Polyvinyl alcohol (PVA) is a synthetic biodegradable polymer that has a relatively simple chemical structure possessing a hydroxyl group attached to a side chain. Because of the hydroxyl (-OH) groups on alternating carbon atoms, PVA is strongly hydrophilic which helps to promote its degradation through hydrolysis. It is an odorless and tasteless, translucent, white granular powder [4]. PVA demonstrates good properties at blocking substances like oils and fats, aromas and perfumes, and tiny particles (nitrogen, oxygen, etc.) due to a combination of factors. The combination of some crystallinity, extensive hydrogen bonding, and hydrophilicity makes PVA an effective barrier material [4–6]. The crystalline regions within the polymer matrix act like densely packed stopgaps. Extensive hydrogen bonding between PVA chains creates a maze-like path for permeating molecules. Additionally, PVA's hydrophilicity repels non-polar oils and fats. This combined effect makes PVA to successfully block the passage of oils, fats, aromas, and perfumes.

Moreover, this biopolymer has excellent film-forming and adhesive properties. PVA's structure contains multiple hydroxyl groups capable of hydrogen bonding with other materials. These properties have made PVA a promising material for creating eco-friendly alternatives to disposable plastic products. However, the PVA film has the defects of poor mechanical properties, low decomposition, and glass transition temperature [4]. PVA's hydrogen bonding network and low crystallinity contribute to poor mechanical properties [7]. Additionally, PVA consists of a carbon backbone with hydroxyl groups attached [8]. These hydroxyl groups are susceptible to thermal degradation at relatively low temperatures (around 200°C) [9]. During decomposition, the chain breaks down, releasing water vapor and other volatile compounds. The defects affect the application of PVA widely, compared with any other known polymers. Thus, the mechanical properties of PVA should be significantly enhanced while maintaining its valuable characteristics.

The emergence of composites has brought a revolution in materials science. Composites are a class of materials that combine the properties of two or more materials (reinforcing and matrix components) to create a new one with enhanced properties. The reinforcement in a composite is the material that provides strength and stiffness, while the matrix is the material that binds the reinforcement together and provides toughness. Growing concerns over sustainability and environmental damage has led to focus on the development biodegradable polymer composites.

Lignocellulosic biomass (LCB) is the most abundant and continuously produced on Earth. It includes woody residues from forests, grasses, agricultural waste, and municipal solid waste. LCB is primarily made up of three polymers: cellulose, hemicellulose, and lignin. Among them, cellulose is the most widely available renewable polymer resource at present. It is considered as a material that can provide an abundant supply to fulfill the rising demand for environmentally friendly and biocompatible products [1, 10]. Wood and cotton are the primary sources of cellulose, a purified form of lignocellulosic biomass. However, competition from other industries, such as furniture, pulp and paper, building products, and the burning of wood for energy, as well as the use of cotton for fabric production, makes it challenging to supply sufficient wood and cotton to all industries at affordable prices. Additionally, wood and cotton are not available in many regions. The need for a cheaper source of cellulosic fibers has prompted investigation into other lignocellulosic materials. Most of the low-value biomass, such as herbaceous plants, grass,

aquatic plants, agricultural crops, and their by-products are called lignocellulosic, referring to their main constituent: cellulose, hemicelluloses, and lignin.

Although there are multiple sources for cellulosic fiber production, agricultural residue stand out as a particularly economical choice for commercial applications. This is because these residues are often available at low or zero cost. Extracting cellulose from agricultural residues also requires less chemicals and energy compared to extracting it from wood. This is because agricultural waste naturally contains less lignin, a substance that makes cellulose extraction more difficult and energy-intensive [11, 12]. Currently, the growing global population has necessitated increased food production to keep up with food demands. [13]. Modern farming methods have dramatically increased crop yields, leading to a surge in agricultural waste. This includes large amounts of plant matter left over from harvesting. Unfortunately, much of this valuable material is underused. However, these residues are rich in cellulose, a substance that can be extracted and used to create new environmentally friendly products [13]. In Ethiopia, cereal crop production and marketing are the main means of livelihood for millions of smallholder households, where, *Teff* (*Eragrostis teff*) is the most important crop by area planted. It is well-suited to a wide range of environments and is presently cultivated under diverse agro-climatic conditions. Now, Ethiopia is the biggest *Teff*-producing country and the country produces more than 90% of the *Teff* produced in the world [14]. Consequently, a large quantity of *Teff* straw (TS), which could contain a high fraction of lignocellulosic compounds, is also being produced.

The use of agricultural materials to create environmentally friendly products has significantly driven scientific exploration into green composites [15]. Nevertheless, challenges such as poor bonding with polymer materials, clumping during production, and the tendency of cellulose to absorb water, particularly in its disordered areas [16], hinder the use of natural fibers for strengthening polymers. To overcome these issues, scientists have focused on isolating the highly organized parts of cellulose, known as microcrystalline cellulose (MCC). This is achieved by breaking down the less structured parts of cellulose through hydrolysis and depolymerisation. MCC is obtained by hydrolyzing and depolymerizing the amorphous region of cellulose. MCC is an ideal material for creating bio-composites due to its various beneficial qualities. These include being environmentally friendly, safe, biodegradable, strong, lightweight, and compatible with

living organisms. Additionally, it is inexpensive [17]. In recent years, MCC has been used to develop bio-composites that are eco-friendly, economical, and have high performance.

MCC contains a very small particle size, while PVA has relatively lower stiffness and strength. Fabricating biodegradable MCC-reinforced PVA composite may be a potential way to address the application limitations of MCC and PVA. Strong interfacial interaction between MCC and PVA leads to inter-chain hydrogen bonding, enhancing modulus and tensile strength compared to pure PVA [4].

Various agricultural residues have been studied for their potential in MCC extraction. According to our knowledge, the responses of TS for MCC preparation and as a potential reinforcement have not been studied so far. However, TS could be a competitive biomass resource like other agricultural residues. Considering this opportunity, in this study, TS was characterized for its physico-chemical characteristics and thereafter it was used for the synthesis of MCC. The main aim of this study was to prepare PVA and MCC composite films using the solvent casting method by varying the percentage of MCC. These films were subsequently tested for their mechanical and thermal properties. It is believed that this research has the potential to lead to the development of new and innovative bio-based materials with a wide range of applications.

1.2. Statement of the Problem

Biodegradable plastics could offer a solution to protect the environment from the hazards caused by conventional petroleum-based plastics. Biodegradable plastics offer environmental benefits, but come with drawbacks compared to traditional plastics. Their mechanical properties, such as tensile strength, elasticity, and impact resistance, are often lower, limiting their use in high-durability applications like car parts or construction materials. While biodegradable, their breakdown rates vary depending on environment and type. Some may degrade slower than desired, especially in non-industrial composting conditions. Additionally, they can be more brittle, particularly at lower temperatures. Production costs can also be higher, and some may offer weaker barriers against moisture or gases compared to traditional plastics [18, 19].

The emergence of composites has brought in a revolution in materials science. Composite materials are formed by combining two or more distinct materials. One component, called the reinforcement, provides strength and stiffness. The other component, called the matrix, binds the reinforcement together and provides toughness and dimensional stability. Different classes of fibers are used to reinforce polymeric matrices; the most common fibers being carbon fibers, aramid fibers, and glass fibers. These fibers have some serious drawbacks: they are non-renewable resources, non-recyclable, abrasive to equipment, require a high energy input to manufacture, and can pose a health risk. In addition, the production of glass fibers releases carbon dioxide and other harmful chemicals into the environment.

The exploitation of biomass for the processing of novel biodegradable composites will be attractive because of its ecological and renewable characteristics. Cellulosic fibers have sparked a special interest because of their high specific mechanical properties and biocompatibility. They are a feasible alternative for some applications to replace synthetic reinforcement in polymers. MCC is a type of cellulose that has been refined to be highly crystalline and purified. It is obtained from lignocellulosic biomass such as wood pulp, and has several advantageous properties, including being odorless, light, stiff, strong, fibrous, non-toxic, insoluble in water,

crystalline, biodegradable, and renewable. To extract MCC from lignocellulosic materials, the first step is to remove lignin and hemicellulose.

Once lignin and hemicellulose have been removed, a controlled hydrolysis treatment is performed. This treatment typically uses a mineral acid to cleave the amorphous regions of the cellulose polymer while maintaining the crystal domains. The particle size, crystallinity, and morphology of MCC are strongly affected by the acid type, treatment duration, and temperature. The most commonly used acid for MCC extraction is sulfuric acid, typically at a concentration of 65% [20, 21]. However, this can cause problems such as corrosion of equipment, the need for large amounts of water, the difficulty of acid recovery, and over-degradation of cellulose. To address these challenges, researchers have been exploring the use of alternative acids, such as hydrochloric acid and nitric acid [22, 23]. These acids are less corrosive than sulfuric acid and can be more easily recovered. However, they are also less effective at cleaving the amorphous regions of cellulose, so they may not produce MCC with the same properties such as higher crystallinity and thermal stability. Recently, researchers have been investigating the use of catalysts to facilitate the hydrolysis reaction. Catalysts can help to reduce the concentration of acid required, which can minimize the problems associated with using concentrated acids.

Transition metal salt catalysts have been explored recently for the conversion of biomass to cellulose derivatives to solve the problems associated with mineral acids [24, 25]. They are more efficient, selective, environmentally friendly, and cause minimum equipment corrosion. Moreover, transition metal salts can be isolated from the liquid blend following the reaction, consequently allowing for possible reuse many times with minimum performance loss [24–26]. As a result, they are a promising option for the production of high-quality MCC. Nevertheless, the acid and catalyst system for MCC extraction depends on the specific source of lignocellulosic material and the desired properties of the MCC (higher crystallinity and thermal stability). Thus, the development of more sustainable and efficient MCC extraction methods is an active area of research.

Therefore, in this research work, an alternative alkali hydrogen peroxide pretreatment of TS followed by transition metal salts assisted dilute acid hydrolysis was used to investigate for

efficient MCC separation from TS. The MCC obtained was then evaluated for its ability to enhance the mechanical and thermal properties of PVA biopolymers.

1.3. Objectives of the Study

1.3.1. General objective

The main objective of the present research work is to develop a new hydrolysis technique for isolating microcrystalline cellulose from *Teff* straw and evaluate its effectiveness in enhancing polyvinyl alcohol properties.

1.3.2. Specific Objectives

- To characterize the physicochemical properties of TS
- To isolate and characterize cellulose fibrils from TS by alkaline hydrogen peroxide treatment method
- To synthesize and characterize MCC obtained from TS cellulose fiber using transition metal salts assisted dilute acid hydrolysis
- To fabricate and characterize polyvinyl alcohol/MCC biocomposite films.

1.4. Scope and Limitation of the Study

The scope of this research is to extract and characterize microcrystalline cellulose from *Teff* straw and to study the enhancement of the thermal and mechanical properties of PVA polymers using the produced MCC as a reinforcement material.

The production of *Teff* in Ethiopia is spatially distributed under diverse agro-climatic conditions adapted to a wide range of environments. Moreover, there are two types of *Teff* varieties (red and white *Teff*). As a result, there could be potential morphological differences in their straw. However, it is not in the scope of this study, to consider these specific variations.

The isolation of MCC from cellulose fibers by acid hydrolysis process depends on the processing conditions such as the temperature and time of hydrolysis, and the concentration of acid. According to different previously studied data on the isolation of MCC via acid hydrolysis, the reaction conditions have a significant role in the yield and crystallinity of MCC. Optimal conditions reported in these studies may not be directly applicable to TS.

Therefore, the best conditions for maximizing TS's MCC yield and crystallinity must be identified independently. However, this study was limited by time and resources. As a result, the following factors during the transition metal salt catalysts assisted dilute acid hydrolysis process were not addressed:

- The effect of temperature and time of hydrolysis
- The effect of concentration of acid and catalyst
- The effect of fiber-to-acid ratio on yield and crystallinity of MCC

These factors are known to affect the properties of MCC, and their investigation would have been valuable. However, due to time and resource constraints, they were not included in this study. Future work could investigate the factors listed above to further understand the properties of MCC obtained from *Teff* straw.

1.5. Rationale and Significance of the Study

Emerging trends in materials technology have revealed the significance of industrial and agricultural waste as a potential source of raw materials. Recycling and reusing waste can help to minimize environmental problems associated with its accumulation. Agro-industries produce a large amount of cellulosic waste each year. As a result, there is a growing demand for new uses for these agricultural cellulosic wastes [27, 28].

In Ethiopia, *Teff* is the main cultivated cereal crop and it is the major staple food. As a result, a lot of TS is generated each year throughout the country and it is mainly used for animal feed. Because of its less familiarity in the scientific community, only very few Ethiopian scholars have tried to investigate the use of TS for biogas production [29], nano silica synthesis [30, 31], and as adsorbent for chrome removal [32].TS could be a viable alternative for value-added MCC production. Therefore, the utilization of this biomass residue (TS) for processing novel composites will be attractive.

Moreover, it is expected that by combining the dilute acid with catalysts, can effectively extract MCC from feedstock. No studies have been reported on the use of TS as an MCC source because of its less familiarity in the scientific research community. Hence, in this research work more ecofriendly alkali hydrogen peroxide pretreatment of the raw TS, followed by transmission metal salts catalyzed dilute acid hydrolysis process were investigated. The findings of this study could significantly advance the development of new biocomposite produced from agricultural waste.

1.6. Organization of the Dissertation

This dissertation is organized in six chapters.

Chapter 1 provides the background, brief overview of the problem, objectives, potential contributions, and an outline of the dissertation.

Chapter 2 gives the *"Literature Review"* which presents an overview on lignocellulosic biomass, and different MCC synthesis techniques. This chapter also provides the potential us of TS and other agriculture residues as source of microcrystalline cellulose, and the latest insight on the micro and nano scale cellulose reinforcement on PVA based composite.

Chapter 3 presents a published article on the isolation of cellulose fibrils from TS using alkali hydrogen peroxide treatment. During the alkali treatment, different alkali treatment parameters were analyzed to determine their influence on lignin decomposition and fiber production. In addition, the methods for sample preparation, characterization of the raw and extracted cellulose fibers, and calculations for data analysis are outlined in this chapter.

Chapter 4 describes the synthesis of MCC from TS using catalyzed dilute acid hydrolysis. The catalytic performance of the transmission metal salts has been compared in terms of physic-chemical analysis (FTIR, Thermogravimetry, X-ray diffraction and scanning electron microscopy) of the synthesized MCC samples. Furthermore, the presence of chrome (Cr (III)) and iron (Fe (III)) ions in the prepared MCCs was investigated using atomic absorption spectroscopy (AAS) analysis, and discussed in this chapter.

Chapter 5 focuses on the processing of PVA / MCC composites using the solution casting method. This includes incorporation of MCCs (produced using different approaches as presented in Chapters *4*) into the PVA. The enhancement on the thermo-mechanical properties of PVA / MCC composites, including mechanical properties and thermal stability were evaluated.

Chapter 6, the concluding chapter of the dissertation, presents the general conclusions of the research work and gives recommendations for further study.

CHAPTER 2: LITERATURE REVIEW

2.1. Biodegradable Polymers: An Overview

Traditional plastics derived from petroleum are persistent environmental pollutants. They don't break down easily and accumulate in the natural world due to their resistance to microbial decomposition. Coupled with recent sharp increases in oil prices, these factors have driven growing interest in developing plastics that can decompose naturally. Biodegradable polymers or plastics are plastics that can be decomposed by the action of living organisms, usually bacteria. Biodegradable polymeric materials break down when their chemical bonds are weakened or broken down by water (hydrolysis) or enzymes. This process, called polymer erosion, gradually wears away the material.

In recent times, a substantial number of biodegradable polymers have been developed, and scientists have identified certain microorganisms and enzymes capable of breaking them down. Biodegradable polymers can be categorized into two main groups: natural polymers derived from renewable resources and synthetic polymers produced from fossil fuels [33]. Natural polymers, also known as biopolymers, are produced naturally by living organisms during their growth processes. These polymers are formed through enzyme-driven reactions involving activated monomers, which are created within cells through complex biochemical pathways.

Poly lactic acid (PLA) is a standout among naturally derived, biodegradable plastics. It's made from renewable materials like starch and is gaining significant attention. PLA is not only safe but also performs similarly to traditional, synthetic plastics [34]. PLA is widely used to create various plastic films because it's environmentally friendly, clear, and safe for living things [35]. Despite its advantages, PLA is hindered by its high hardness, fragility, low strength, and inability to withstand high temperatures, limiting its potential applications. In addition, PLA's low glass transition temperature, ranging from 65 to 70 °C, restricts its use in packaging that undergoes heat processing. Due to its pliability and low melting point, it excels in heat-sealing and thermoforming processes . Therefore, the modification of the PLA matrix is required to broaden its use.

Most synthetic polymers cannot be broken down naturally. Nevertheless, certain types of polymers, including those made from materials like polyester, polyamide, and polyurethane, can be decomposed by water or living organisms under specific conditions. This is because these polymers have structures that are more vulnerable to breaking down [36]. Polyglycolic Acid (PGA), Polybutylene Succinate (PBS), and Poly Vinyl Alcohol are widely used synthetic degradable polymers.

The escalating plastic pollution problem has prompted intensive research into environmentally friendly alternatives. Synthetic biodegradable polymers have emerged as a promising solution, offering the functionality of traditional plastics with the added benefit of environmental degradation. Unlike traditional plastics that linger in landfills for centuries, these innovative materials degrade into harmless components like water, CO_2, and biomass under specific conditions. This significantly reduces plastic pollution in the environment and its detrimental effects.

Beyond their environmental benefits, synthetic biodegradable polymers offer a range of applications [37]. In packaging, they're replacing traditional plastics in food containers, bottles, and films, diverting waste from landfills and promoting a circular economy. The medical field utilizes synthetic biodegradable polymers for sutures, drug delivery systems, and tissue engineering scaffolds. Their degradability allows for controlled drug release and eventual absorption by the body, minimizing foreign object reactions. Agriculture benefits from synthetic biodegradable mulch films that retain moisture, suppress weeds, and then degrade after use, eliminating the need for removal and potential soil contamination. Finally, Synthetic biodegradable bags aid in waste management by facilitating organic waste collection and composting, ultimately reducing the overall waste burden.

Synthetic biodegradable polymers, while promising, face some limitations [38]. Their mechanical properties like strength, stiffness, and gas barriers can be lower compared to traditional plastics, making them unsuitable for demanding applications. Additionally, production costs are often higher, hindering widespread adoption. Effective breakdown can also be a challenge. Some require specific composting facilities, which may not be universally available. Even in ideal

conditions, degradation rates can vary depending on the material, and some may break down slower than desired, especially in home composting setups.

The future of synthetic biodegradable polymers is bright, with ongoing research dedicated to improving their performance and affordability [18]. One promising area lies in enhancing mechanical properties. New processing techniques and the incorporation of reinforcing agents like MCC and NCC hold the key to creating stronger and more durable biodegradable materials. Additionally, cost reduction efforts are underway, focusing on optimizing production processes and utilizing readily available renewable resources to make these polymers more competitive with traditional plastics. Furthermore, research is tackling biodegradation rates. Tailoring the chemical structure and enzymatic degradation of these polymers can lead to faster and more consistent breakdown across various environments [36, 39, 40]. These advancements will solidify the position of synthetic biodegradable polymers as a sustainable and effective alternative to traditional plastics.

Overall synthetic biodegradable polymers offer a sustainable alternative to traditional plastics. While challenges remain in terms of performance and cost, on-going research holds promise for overcoming these limitations. By addressing these concerns and promoting advancements, synthetic biodegradable polymers can play a crucial role in creating a more sustainable future for plastic use and waste management.

2.2. Polyvinyl alcohol (PVA)

Polyvinyl alcohol is well known as a synthetic biodegradable polymer derived from polyvinyl acetate [41]. This synthetic material is partially crystalline, has no smell or taste, and completely breaks down naturally. It's safe for living things, dissolves in water, and is primarily made up of carbon-carbon bonds [42]. PVA excels in film formation, emulsification, and adhesion, while demonstrating high flexibility, and barrier properties against oxygen and aromas. These versatile attributes make PVA a compelling alternative for disposable and biodegradable plastics. Compared with any other known polymer, PVA significantly outperforms superior features in blocking oxygen; however, its ability to maintain this barrier depends on protecting it from moisture [43]. The chemical structure of PVA is as shown in Figure 2-1. PVA can degrade under aerobic and anaerobic conditions in a microbial active environment within 5–6 weeks. The

biodegradation mechanism involves a two-step pathway: hydroxyl group oxidation followed by hydrolysis.

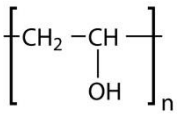

Fig. 2-1 Chemical structure of polyvinyl Alcohol

Herrman and Haehnel first synthesized PVA in 1924 by subjecting a polyvinyl acetate (PVAc) solution to alkaline hydrolysis [44]. The production of PVA does not follow the standard polymerization route used for many other vinyl polymers. PVA's synthesis skips the traditional route of monomer polymerization due to the inherent instability of vinyl alcohol. PVA instead is prepared by partial or complete hydrolysis of polyvinyl acetate. The method involves hydrolysis of polyvinyl acetate, essentially replacing its acetate groups with hydroxyl groups via a chemical transformation. Methanolysis, the traditional method for polyvinyl acetate hydrolysis, involves dissolving it in methanol and introducing a base or acid catalyst. This facilitates the conversion of acetate groups into hydroxyl groups, ultimately leading to the formation of PVA, which precipitates out of the solution [41]. Polyvinyl Alcohol synthesis is shown in Fig. 2-2.

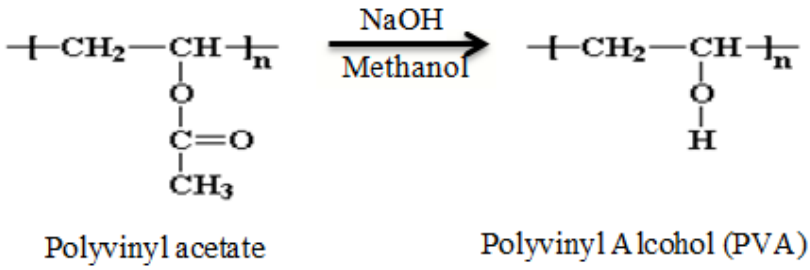

Fig. 2-2 Polyvinyl Alcohol syntheses

PVA is used in a variety of industries, including paper coatings, mats, films, textile, adhesive, cosmetic, food, drug, paper and packaging. Its film-forming ability makes it ideal for packaging in food supplements and other sensitive products. PVA is benign to living tissues, harmless, and nontoxic. In medicine, PVA membranes serve as platforms for drug delivery and cell culture. Its ability to bind nanoparticles and remove metal ions finds use in water purification. Additionally,

PVA's surface properties and adhesive characteristics lead to its widespread use in film coatings, packaging, and various industrial applications.

2.3. Lignocellulosic Biomass (LCB)

Lignocellulosic biomass is a non-edible plant material that is abundant and continuously produced. It includes woody residues from forests, grasses, agricultural waste, and municipal solid waste. Figure 2-3 below shows different sources of lignocellulosic biomass.

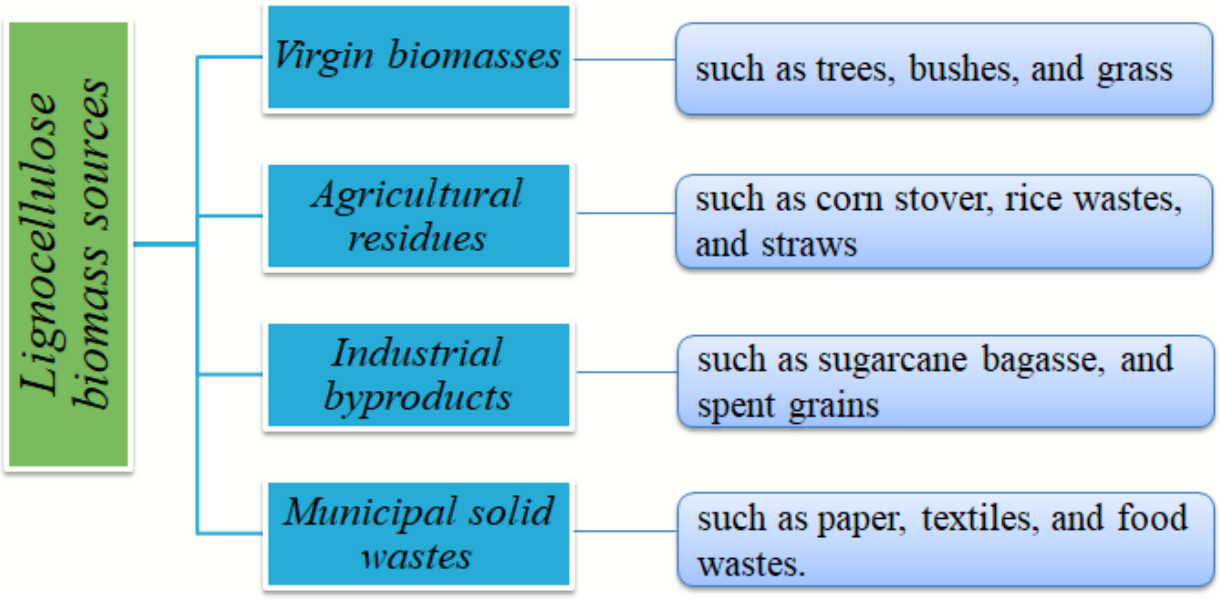

Fig. 2-3 Sources of lignocellulosic biomass as adapted in Abo, Bodjui Olivier, et al [45]

Lignocellulose is primarily composed of three main substances: cellulose, hemicellulose, and lignin. While these three make up the bulk of the material, natural lignocellulose also contains small amounts of other components such as pectin, nitrogen-based compounds, and ash. Figure 2-4 below shows the components of lignocellulosic materials. The chemical composition of lignocellulosic biomass fibers can vary depending on a number of factors, including genotype, environment, physiological conditions, and harvest techniques.

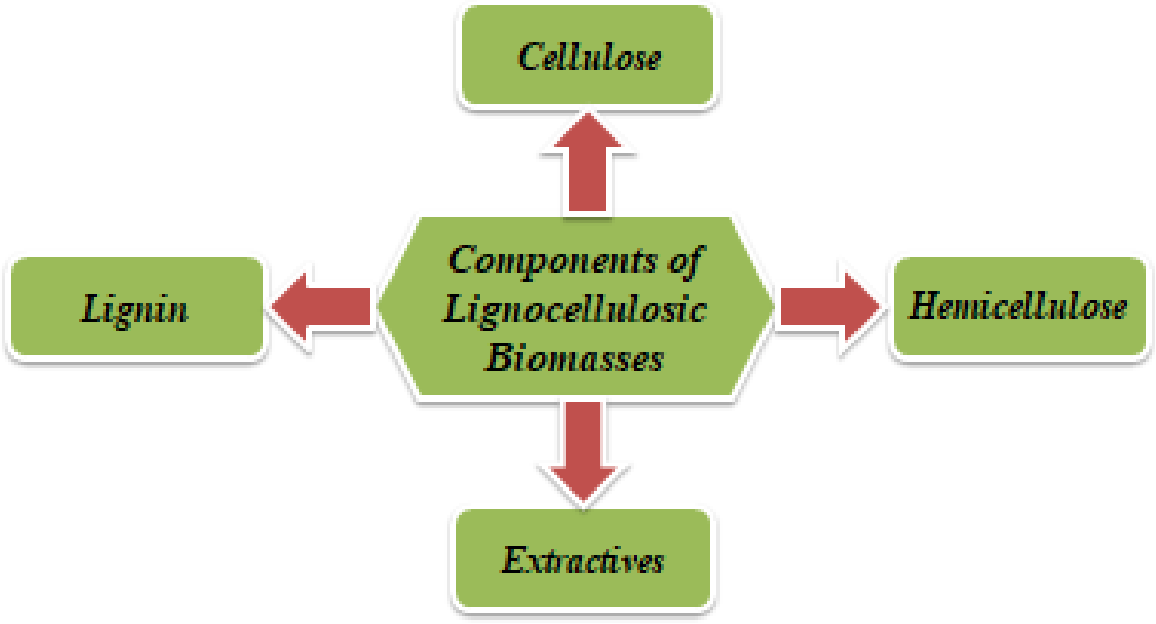

Fig. 2-4 Components of lignocellulosic biomass based on the figure in [46]

Plant cell walls are tightly packed structures composed of cellulose, hemicellulose, and lignin. Cellulose and hemicellulose molecules are primarily held together by hydrogen bonds, while lignin is more strongly attached to both cellulose and hemicellulose through covalent bonds. The cell wall's strength and flexibility come from the hydrogen bonds linking cellulose and hemicellulose. The covalent bonds between lignin, cellulose and hemicellulose provide additional strength and rigidity.

Lignocellulosic biomass offers a sustainable and versatile source material for creating valuable, eco-friendly products. Its chemical makeup makes it suitable for producing a variety of biotechnological goods.

a) Cellulose

Cellulose is the planet's most plentiful renewable organic material. It can be sourced from a wide range of organisms, including plants, bacteria, and marine algae. Produced in vast quantities annually, amounting to billions of tons, cellulose is a highly valuable natural substance. Several biomass sources, including hardwood stems (40-55%) and softwood stems (45-50%), offer a rich source of cellulose. Grasses vary in cellulose content from 25-40%. Leaves have the lowest cellulose content, ranging from 15-20% [47].

Cellulose molecules form organized structures that combine in to bundles, and determine the framework of the cell wall. Figure 2-5 shows the molecular chain structure of cellulose.

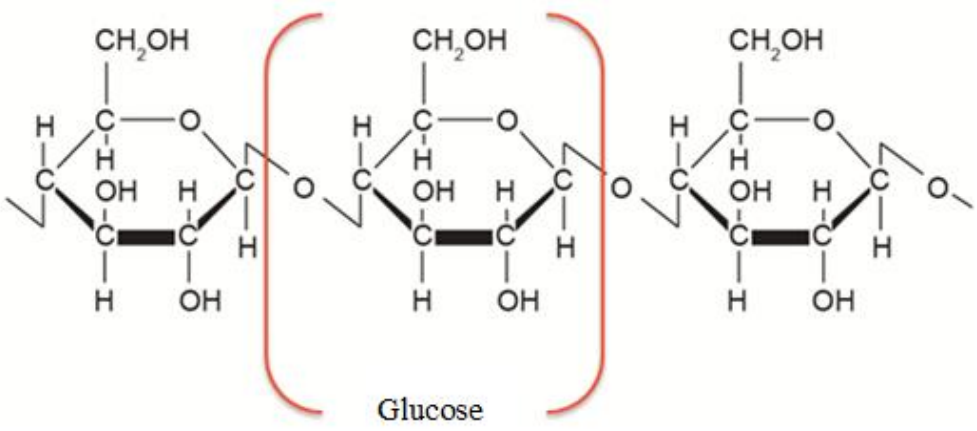

Fig. 2-5 Molecular chain structure of cellulose [48]

The disordered areas of cellulose exhibit greater chain separation, facilitating hydrogen bond formation with molecules such as water. This makes cellulose hygroscopic. However, the cellulose chains are still held together by hydrogen bonds, so cellulose does not dissolve in water. Instead, it swells as it absorbs water.

Cellulose is a key ingredient in various industries, including paper, textiles, and chemicals. It also has diverse uses in renewable energy, biodegradable materials, and composite products. This versatile substance can be obtained from plant matter through mechanical, chemical, or biological processes.

b) Lignin

Lignin is a crucial building block of plant matter, alongside cellulose and hemicellulose. It is an amorphous and highly complex polymer that forms the cell walls of plants. Lignin is made up of aryl propyl units linked together by β-O-4 bonds, as well as other C-C and C-O linkages. Unlike cellulose, lignin does not have a single repeating unit. Instead, it is a complex arrangement of substituted phenolic units.

Lignin contents differ from species to species and from one tissue to the next in the same plant, even within different parts of the same cell wall. Softwoods generally have lower lignin levels, ranging from 18% to 25%, compared to hardwoods, which have a higher lignin content of 25% to

35%. Moreover, ecological conditions like the wood's age, weather, plant nutrients, and sun exposure also influence lignin's chemical makeup [49].

After cellulose, it is the most abundant renewable carbon source on Earth. These polymers are extremely resistant to degradation and difficult to use directly as substrates in industrial fermentation. Most of the biorefinery schemes have focused on utilizing easily convertible fractions (cellulose and hemicellulose), while lignin remains relatively underutilized compared to its potential. To make lignin more useful, it must be depolymerized into low-molecular-weight phenolics and aromatics. These compounds can then be used to synthesize a variety of products, such as fuels, chemicals, and materials. Various techniques, such as chemical, enzymatic, and thermal methods, can be employed to decompose lignin. As the technology continues to develop, lignin is likely to become a more widely used resource.

c) Hemicellulose

Hemicelluloses are a group of complex heteropolysaccharides that are found in plant cell walls. Unlike cellulose, which is a polymer of glucose only, hemicelluloses are not chemically homogeneous. They are made up of a variety of different sugars, including D-xylose, L-arabinose, D-mannose, D-glucose, D-galactose, and sugar acids (D-glucuronic and D-galacturonic acids). Hemicelluloses are typically branched heteropolymers. This branching gives hemicelluloses a more flexible structure than cellulose, which is why they are not as strong or as rigid.

Hemicelluloses are also more easily hydrolyzed than cellulose [50]. This is because the bonds between the sugar molecules in hemicelluloses are not as strong as the bonds between the sugar molecules in cellulose. Hemicelluloses provide strength and flexibility to the cell wall, and they also help to bind cellulose and lignin together. They are also a valuable source of energy for microorganisms.

2.4. Microcrystalline Cellulose

Microcrystalline cellulose was first identified in 1955 by researchers Battista and Smith [51] and was subsequently introduced to the market under the name Avicel. Interestingly, the discovery of MCC commenced from a failed experiment [51]. The authors explored the use of a Waring blender to disintegrate hydrolyzed cellulose into smaller fragments within a water solution. They

believed that the high-speed blender would break down the clustered tiny crystals within the chemically treated cellulose into even smaller pieces. These extremely small crystal pieces would then separate from the water and sink to the bottom. Instead of the desired outcome, they produced a stable colloidal suspension commonly known as Avicel. This substance, also referred to as MCC, was first introduced to the market in 1962 by FMC Corporation, a U.S. chemical company, under the brand name Avicel [1]. Subsequently, a rapidly increasing number of scientists have dedicated their research efforts to this material. Initially, wood and cotton were the primary sources used to extract cellulose for the production of MCC.

Microcrystalline cellulose (MCC) is a natural compound derived from cellulose that has undergone partial breakdown. Traditionally, it's produced by treating a pure form of cellulose with a large amount of mineral acid. Cellulose itself is made up of tiny fibers containing both ordered (crystalline) and disordered (amorphous) sections. The crystalline parts, known as cellulose crystallites, are tightly packed bundles of cellulose molecules held together by weak chemical bonds. When cellulose is exposed to acid, the disordered parts break down more easily, leaving behind smaller, more crystalline pieces, which is MCC.

MCC has several advantageous properties, including being odorless, light, stiff, strong, fibrous, non-toxic, insoluble in water, crystalline, biodegradable, and renewable. These properties make MCC a versatile and attractive material for use in a wide range of industrial fields. MCC offers a broad spectrum of potential applications. Its unique structure and diverse physical and chemical properties make it well-suited for various industries. Consequently, MCC has garnered significant attention as a promising material for industrial, technological, and biomedical applications.

Ongoing research focuses on exploring MCC's potential in diverse industries, including construction, food, pharmaceuticals, medicine, automotive, packaging, and smart materials. Microcrystalline cellulose has various applications based on its form. In powder form, it serves as a binding and filling agent in food and pharmaceuticals, and is crucial for strengthening polymer composites. When in colloidal form, MCC acts as a stabilizer for suspensions, retains water, controls viscosity, and emulsifies substances in products like pastes and creams.

MCC plays a vital role in the development of bio-composites, which combine MCC with a polymer. It can improve the strength, stiffness, and toughness of these materials. These bio-composites offer advantages over traditional materials, such as biodegradability and sustainability. MCC has already been successfully used in the production of bio-composites in conjunction with starch, chitosan, poly(lactic acid), poly(3-hydroxybutyrate), and poly(vinyl alcohol). Compared to conventional composites based on synthetic non-biodegradable materials, the utilization of MCC in polymer bio-composite formulations is still somewhat limited. This is primarily due to challenges in achieving optimal distribution of filler particles within the polymeric matrix. Achieving uniform dispersion of MCC in polymers can be challenging due to several factors [52]. MCC fillers often have different polarities and surface energies compared to the polymer, leading to weak interactions. This encourages filler particles to clump together (agglomerate) rather than disperse evenly throughout the material. Additionally, the processing technique itself can also play a role. Methods like melt blending or solution casting can inadvertently trap air bubbles or create shear forces that contribute to aggregation [53]. These combined factors necessitate careful consideration when aiming for a well-dispersed filler-polymer composite. Despite these limitations, MCC holds great promise as a material for bio-composites.

Microcrystalline cellulose obtained from different sources can vary in particle size and crystallinity. The properties of MCC are affected by its crystallinity, particle size, and other factors. The particle size of MCC affects its flowability, solubility, and other properties. Smaller particles have a higher surface area, which can lead to increased water absorption and swelling. The crystallinity of MCC affects its strength, stiffness, and other properties. MCC exhibits a notably high level of crystallinity, usually falling within the 55% to 80% range [54]. MCC with high crystallinity is strong and stiff, while MCC with low crystallinity is more absorbent and swells more in water.

As the demand for MCC continues to grow, the development of new and innovative methods for producing and processing MCC will be essential. Different sources and extraction methods can affect the overall performance of the product. For example, the source of the cellulose and extraction methods can affect the molar mass, particle size, crystallinity, surface area, moisture

content, and porous structure of the MCC. These properties can in turn affect the MCC's performance in different applications.

2.4.1 Isolation of Microcrystalline Cellulose from Lignocellulosic Biomasses

To extract microcrystalline cellulose from lignocellulosic materials, the first step is to remove lignin and hemicellulose. Lignin is the most difficult component to remove, and it can be done using physical, biological, chemical, or combined methods. These methods are commonly employed as a pretreatment to facilitate the hydrolysis stage of the raw materials into MCC. Once lignin and hemicellulose have been removed, a controlled hydrolysis treatment is performed. This treatment typically uses a mineral acid to cleave the amorphous regions of the cellulose polymer while maintaining the crystal domains.

This part of the text provides a comprehensive overview of different methods used to produce MCC. It examines the advantages and drawbacks of these techniques, as well as key challenges associated with isolating cellulose for MCC production.

2.4.1.1. Pretreatment of lignocellulosic biomasses for the production of microcrystalline cellulose

The goal of pretreatment is to break down the complex structure of lignocellulose and make the cellulose more accessible to hydrolysis [55, 56] as shown in Figure 2-6. The Pretreatment of fibers from different lignocellulosic biomass generally follows a three-step protocol. First, milling which increases the surface area of the fibers, enhancing the effectiveness of subsequent treatments, ensures uniform size and improves water absorption [57]. Next, washing with deionized water removes soluble impurities [58]. Finally, the fibers undergo chemical, enzymatic, or mechanical treatment to break down the lignocellulose structure.

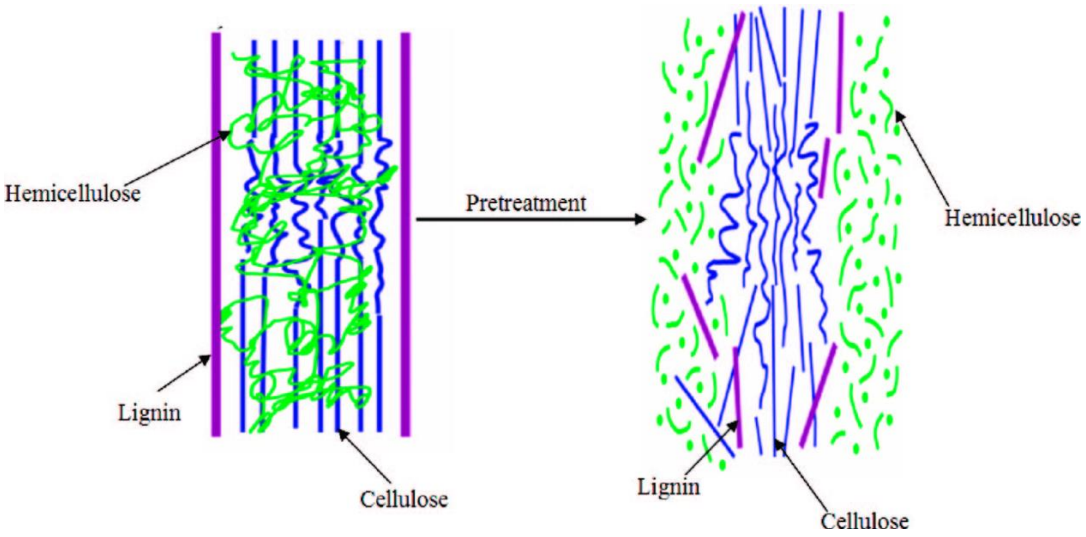

Fig. 2-6 Schematic representation of pre-treatment of biomass adapted from Rajendran, Karthik, et al., and Ji, Xiao-Jun, et al. [59, 60]

Lignin is a rigid polymer that forms a protective layer around the cellulose fibers. It is difficult to remove lignin, but it is essential for the production of MCC. Hemicellulose is a water-insoluble polymer that is also difficult to remove. It is important to remove hemicellulose because it can inhibit the hydrolysis of cellulose. Figure 2-7 shows methods that can be used to pretreat lignocellulosic biomass.

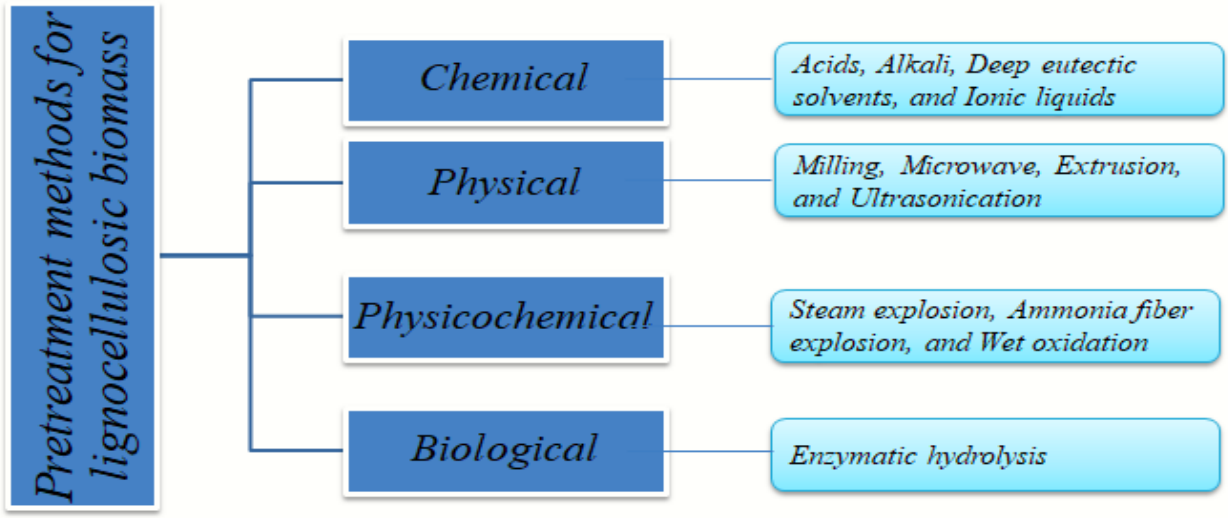

Fig. 2-7 Pretreatment methods for lignocellulosic biomass [61]

The choice of pretreatment method depends on a number of factors, such as the type of biomass, the desired properties of the MCC, and the cost of the process [57]. Physical pretreatment methods are environmentally friendly as they don't generate harmful substances. However, they can be energy-intensive. The amount of energy needed for this process varies depending on the type of plant material used. For example, breaking down soft plants like corn stalks and switchgrass requires less energy than processing hard plants like pine and poplar. Specifically, corn stalks need 11 kilowatt-hours per ton, switchgrass needs 27.6, while pine and poplar require a much higher energy input of 85.4 and 118.5 kilowatt-hours per ton, respectively [59]. The most common physical pretreatment methods include: milling, extrusion, microwave and ultrasonication [62]. New physico-chemical pretreatment approaches, such as steam explosion, have also shown great results in eliminating lignin fraction while leaving cellulose structure intact and therefore purer. For example, in a study done by Song, Yan, et al [63], kenaf bast lignin was removed and cellulose fibers were isolated from the material through a combined process of steam explosion and fenton oxidation degumming.

Among various purification methods, chemical pretreatment is the most promising method for preparing microcrystalline cellulose. Acid pretreatment in particular by using sulfuric acid, alkaline, ionic liquids (ILs)-based, and organosolv pretreatment are the commonly employed chemical pretreatments for lignocellulosic biomass [62]. Acid pretreatment can be performed either under low acid concentration and high temperature or under higher acid concentration and lower temperature. Using concentrated acid is more economic as the process is performed at low temperature; however, toxicity, corrosiveness of equipment, and acid recovery are major drawbacks preventing the widespread application of this method. On the other hand, ionic liquids exhibit specific chemical properties but come with the drawbacks of high cost and toxicity towards microorganisms and enzymes. Additional research is required to create affordable methods for recovering ionic liquids and to evaluate their potential harm for widespread commercial use. Alkali-bleaching pretreatment is preferred over classical chemical treatments for cellulose fiber purification because NaOH/KOH, sodium chlorite, and acetic acid are readily available in limited conditions.

- ***Alkaline treatment (mercerization)***

Alkaline pretreatment is a versatile and effective method for breaking down lignocellulosic biomass. Sodium hydroxide (NaOH), potassium hydroxide (KOH), and calcium hydroxide ($CaOH_2$) are mostly used in this pretreatment method. It is a chemical process that uses an alkaline solution to break down glycosidic ether bonds in lignin, disrupting the lignin structure in biomass [64]. A saponification reaction during alkaline treatment causes disruption of the ester bonds linking hemicellulose and lignin molecules. This results in the solubilization of lignin and hemicellulose components in the alkaline solution. After lignin solubilization, the lignin no longer acts as a protective shield to the cellulose. This exposes the cellulose crystals for further processing, and more susceptible to other treatments, such as acid hydrolysis [65]. This makes the extracted cellulose more susceptible to micro and nano synthesis. Additionally, alkaline treatment removes residual waxes, pectin, silica ash, and natural fats at the pre-treatment stage. This is important because these contaminants can interfere with the micro and nano cellulose production processes. Alkaline processing also causes the cellulose component of the lignocellulosic material to swell, modifying its structure. This swelling causes a decline in both crystallinity and polymer chain size, resulting in a larger internal space [66]. Previous studies indicates that alkaline pretreatment commonly utilizes strong base solutions with specific conditions tailored to different biomass feedstock as presented in Table 2-1.

Table 2-1 Alkaline and bleaching pretreatments for different lignocellulosic fibers carried out at varying conditions using different reagents.

No	Raw material	Pretreatment reagents and conditions		Ref.
		alkali treatment	**bleaching treatment**	
1	Calotropis procera fiber	NaOH (2wt. %) at room temperature for 3 h	H_2O_2 (5 wt. %) and NaOH (3.8 wt. %) at room temperature for 3 h	[67]
2	coconut fiber	NaOH (2 wt.%) at 80 °C for 2 h	$NaClO_2$ glacial acetic acid at 70 °C for 1 h	[68]
3	Bagasse	NaOH (10 wt.% for 1.5	$NaClO_2$/glacial CH_3COOH	[69]

		h, 20 wt.% for 1.5 h and 20 wt.% for 1 h) at 98 °C	at 75 °C for 2 h	
4	Rice husk	NaOH (5 wt.%) at 80 °C for 4 h	H_2O_2 (5%), NaOH (0.1%) and $MgSO_4$ (0.1%) at 70 °C for 4 h	[70]
5	Citrus waste	NaOH (6 wt. %) at room temperature overnight.	H_2O_2 at 80 °C.	[71]
6	Rape straw	NaOH (2 wt.%) at 75°C for 1 h	H_2O_2 (5%) at 75 °C for 2.5 h,	[72]
7	Coconut palm	NaOH (2 wt%) at 90 °C for 2 h	$NaClO_2$ (1wt. %) at 75 °C for 1h	[73]
8	Rice straw	4%, 6%, and 8% (w/v) of NaOH at 70 °C for 5 min to up to 120 min	----------	[74]
9	Jute fibres	NaOH (2 wt.%) at 30 °C for 6 h	($NaClO_2$) solution (at pH 2.3) for 1 h at 50 °C	[75]
10	Jack bean skin	NaOH (4, 6, 8, 10 and 20%) at 100 °C for 3 h	First bleaching using NaOCl (0, 3 and 6%) at 60 °C for 3 h, and second bleaching using 3% sodium bisulfite at 60 °C for 3 h	[76]
11	Pineapple leaf	NaOH (2 wt. %)	(NaClO, 4% w/v) with the mixture of acetic acid and NaOH (2% w/v) for (1, 2, 3 and 4 h)	[77]

Various studies have shown that alkaline pretreatment is an effective technique for removing lignin and making lignocellulosic fibers more accessible for downstream processing. However, there are some disadvantages to this technique, such as the need to recover the added alkalis, which can be difficult and expensive. Additionally, alkaline pretreatment is particularly suited to

breaking down plants with low lignin levels, such as herbaceous crops and agricultural byproducts, while its effectiveness decreases for hardwoods. Despite the disadvantages, alkaline pretreatment is a promising technique for the production of micro or nanocellulose from lignocellulosic biomass.

- ***Bleaching treatment (mercerization)***

Following alkaline treatment, the bleaching process takes place. This process is necessary to remove components such as residual lignin and hemicellulose. There are two main types of bleaching treatments chlorine-based, and hydrogen peroxide bleaching treatments**.** Chlorine-based bleaching uses chlorine compounds under acidic conditions to remove lignin and other impurities from the fabric. This treatment is more effective than hydrogen peroxide bleaching, but it is also more environmentally harmful. Hydrogen peroxide bleaching treatment is less effective than chlorine-based bleaching, but it is also more environmentally friendly. Hydrogen peroxide bleaching uses hydrogen peroxide under alkaline conditions to remove lignin and other impurities from the biomass [78]. The bleaching process is typically repeated multiple times, or in stages, until the desired whiteness is achieved. The resulting white color of the bleached material indicates that a significant amount of lignin has been removed, confirming that the bleaching process has been successful. Currently, there's a growing trend towards using hydrogen peroxide instead of chlorine contain compounds for bleaching, due to its lower environmental impact.

Overall, alkali-bleaching pretreatment is a crucial step in microcrystalline cellulose production, offering several key benefits: Firstly, it disrupts the complex lignocellulose structure, making the cellulose more accessible for hydrolysis. Secondly, pretreatment streamlines the hydrolysis process, reducing the energy required for MCC production [79]. Lastly, it can even enhance the intrinsic properties of MCC, improving its crystallinity, solubility, and mechanical strength [58, 80].

2.4.1.2. Hydrolysis of purified cellulose for MCC isolation

Even though pure cellulose has been extracted through earlier processing steps, additional treatment is necessary to produce microcrystalline cellulose. This is because the cellulose still contains disordered regions that can weaken its heat resistance and overall structure. The isolation of MCC requires intensive hydrolysis, which can be done using a mechanical or chemical

process. The mechanical hydrolysis process uses high-pressure homogenization or ultrasonication to break down the cellulose fibers into smaller particles. The mechanical hydrolysis process is less effective than chemical hydrolysis at producing MCC with high crystallinity. However, it is a more environmentally friendly process and it can be used to produce MCC from a wider variety of cellulose sources. The chemical hydrolysis is the most common method for isolating MCC. In this process, a strong acid, such as hydrochloric acid or sulfuric acid, is used to break down the amorphous regions of the cellulose. The crystalline regions, which are more resistant to acid hydrolysis, remain intact and can be isolated as MCC particles [1, 81].

The physical and chemical properties of MCC are determined by the conditions under which it's produced. Factors such as temperature, processing time, type and amount of acid, and the proportion of fiber to acid used to extract cellulose from raw materials all influence the final properties of the MCC. These factors influence the physical and chemical characteristics of MCC, including its particle size, shape, structure, thermal stability, and strength. After hydrolysis, a number of downstream processes, including neutralization, washing, and drying, are used to produce fine, powdered MCC. The properties of MCC can be tailored to meet the specific needs of different applications.

The strong acid hydrolysis process is a versatile method for preparing MCC from a variety of biomass sources. The process is relatively simple and can be scaled up to produce large quantities of MCC. Sulfuric acid is the most widely used acid because it is easily obtainable and relatively cheap. Hydrochloric acid is also used, but it is more expensive than sulfuric acid. Unfortunately, the sulfated cellulose produced by sulfuric acid hydrolysis has low yield and less thermal stability than the starting material. This is because the presence of active sulfate ester groups on the fiber surface can negatively impact the treated material's ability to withstand heat. Despite this, the extraction of MCC from various natural materials employing the acid hydrolysis process continues to be investigated in research laboratories. This is because MCC can be further developed and processed into functional and high-value-added products. There are other methods for preparing MCC, such as enzymatic hydrolysis and steam explosion. These methods are less harmful to the environment and do not require the use of strong acids. However, they are more expensive and less efficient than strong acid hydrolysis.. Enzymatic hydrolysis, though environmentally friendly, suffers from its selectivity, leading to lower yields and slower speeds

[82]. Steam explosion, though faster than enzymes, breaks down some cellulose itself and yields a wider range of particle sizes, requiring further processing [83].

Further research is needed to develop methods for mitigating these drawbacks and to improve the efficiency and cost-effectiveness of the acid hydrolysis process. Jahan et al. [84] isolated MCC from jute using a high acid concentration method. The MCC produced using this method had good thermal stability and crystallinity of 74%. The authors attributed these properties to the use of formic acid, which is an organic acid. The higher acidity of formic acid may have led to a more complete hydrolysis of the cellulose fibers, resulting in MCC with higher crystallinity and thermal stability. The authors also noted that the use of formic acid resulted in a lower yield of MCC than the use of hydrochloric acid. However, they considered this to be a worthwhile trade-off, given the improved properties of the MCC produced using formic acid. The results of this study suggest that the use of organic acids, such as formic acid, may be a promising approach for the production of high-quality MCC. However, further study is needed to confirm these findings and to optimize the process conditions for the production of MCC using organic acids.

2.4.1.3. Metal Salt Catalysis for Cellulose Hydrolysis

As previously mentioned, MCC is primarily produced by the use of strong acids. Beyond these methods, only a limited number of combined approaches have been effectively implemented to create microcrystalline cellulose from various biomass sources. Metal salts have been employed to process cellulose-based materials due to their ability to break down cellulose structures and weaken the bonds holding them together [85, 86]. Recently, transition metal salts have taken on a new role as acidic catalysts for efficient cellulose hydrolysis.

Transition metal salt catalysts can be categorized as trivalent and divalent catalysts based on their valence state. Trivalent catalysts, such as $FeCl_3$, $Fe_2(SO_4)_3$, $CrCl_3$, and $AlCl_3$, are more effective than divalent catalysts, such as $FeCl_2$, $FeSO_4$, and $CuCl_2$. This is because the higher valence state of the metal ion produces more H^+ ions, which are more effective at catalyzing the hydrolysis reaction. The hydrolysis of cellulose catalyzed by transition metal salts has several advantages over conventional methods, such as using organic solvents or inorganic acids. Metal salts can more efficiently disrupt the hydrogen bonds that hold cellulose fibers together. This makes it easier for the cellulose to be hydrolyzed into smaller molecules [87]. Metal salts have a higher

selectivity for disordered regions of cellulose, which means that they are less likely to degrade the crystalline regions [88]. They are less corrosive and more environmentally friendly than organic solvents or inorganic acids. This makes them a safer and more sustainable option for cellulose hydrolysis. Metal salts can help to reduce the energy consumption required for cellulose hydrolysis. Furthermore, metal salts have a larger surface area than solid-phase catalysts. This allows for more efficient contact between the catalyst and the cellulose, which leads to a faster and more complete hydrolysis reaction [87]. The supernatant produced during cellulose hydrolysis can be converted into another useful byproduct by chemical precipitation. This prevents the supernatant from being discharged into wastewater treatment plants, where it would be a waste product.

Overall, to extract MCC from lignocellulosic materials, the first step is to remove lignin and hemicellulose. As discussed above, alkaline pretreatment is an effective technique for removing lignin and making lignocellulosic fibers more accessible for downstream processing. This treatment occurs at milder conditions (below 140 °C) and lower severity as compared to other pretreatment technologies. Additionally, alkaline pretreatment is more effective for low lignin content biomass, such as herbaceous crops and agricultural residues like *Teff* straw. However, further research is needed to improve the efficiency and cost-effectiveness of alkaline pretreatment. The conditions, such as temperature, time, and concentration of the alkaline solution, should be optimized to achieve the desired results for different agricultural residues. Furthermore, currently, there is a growing interest in the use of hydrogen peroxide bleaching as a more environmentally friendly alternative to chlorine-based bleaching.

As discussed above, transition metal salts catalysts offer a number of advantages over conventional methods for cellulose hydrolysis. They are more efficient, selective, environmentally friendly, and cost-effective. As a result, they are a promising option for the production of high-quality MCC. Thus, in this study, alkaline hydrogen peroxide pretreatment followed by transition metal salts assisted dilute acid hydrolysis were selected to isolate MCC from TS.

2.4.2 Potential of Agricultural Residues as Source of MCC

Microcrystalline cellulose comes from various plant sources, with wood and cotton being the main ones. However, these materials are also in high demand for other uses like furniture, paper, and textiles. This competition, along with limited availability in some regions, drives the search for alternative, more affordable sources of cellulosic fibers. The need for a cheaper source of cellulosic fibers has led to the exploration of other forms of lignocellulosic materials, such as herbaceous plants, grasses, aquatic plants, agricultural crops, and even their byproducts. These alternative sources hold promise for meeting the growing demand for MCC in a more sustainable and cost-effective way.

While various plant-based materials can be used to make cellulose fibers, agricultural waste products offer a significant financial benefit as a source of these fibers for commercial production. This is because these residues are practically free or even a burden to dispose, and they can be transformed into cellulose with minimal processing. Compared to other sources, agricultural residues have additional benefits: they contain naturally lower amounts of hemicellulose and lignin [89]. This means that they require less chemicals and energy to bleach, making them a more sustainable source of cellulose. As a result, agricultural residues hold immense potential as a sustainable and cost-effective source of cellulose. Such resources include: leaves, stems and stalks from a variety of agricultural residues.

The source of MCC significantly impacts its overall quality and performance. As MCC can be derived from various cellulose-rich materials, exploring different extraction methods is crucial for optimizing its properties. From the relevant literatures, a variety of agricultural residues are investigated as feedstock materials for the manufacture of MCC. For example, rice straw [90], palm fibers [91], giant reed [92], cotton stalk waste [17], tea waste [93], lagenaria siceraria (bottle gourd) [94], Orange mesocarp [95], rice husk [96], and corn residues [97] have been investigated as potential sources of MCC. The development of MCC from agricultural residues has the potential to create new value-added products, while also solving disposal problems [1].

Ethiopia's agricultural landscape is primarily composed of countless small farms that predominantly grow grains to feed their families and generate income. The five cereals (*Teff*,

Wheat, Maize, Sorghum, and Barley) are the core of Ethiopia's agriculture accounting almost three-fourths of the total area cultivated [98, 99]. Moreover, there has been substantial growth in cereals in terms of area cultivated, yields, and production. Because of the country's agricultural strength, a substantial amount of agricultural residue is produced.

The food culture of *Teff* in Ethiopia is historical and a major part of the country's national identity with high socio-cultural values and high prices among cereal crops [100]. *Teff* is an ancient grain that was first domesticated in Ethiopia between 4000 and 1000 BC [101]. It is well-adapted to the highland areas of Ethiopia, where it is grown on heavy, well-drained, clay soils. *Teff* is used to make *injera*, a traditional Ethiopian flatbread, as well as a variety of other dishes. It is a versatile and sustainable crop, and it is an important part of Ethiopia's economy.

Teff straw is the main solid residue after *Teff* grain is harvested. As a result, a lot of TS is generated each year throughout the country, which is primarily used for livestock diet, to plaster mud when constructing residential huts, and to make local grain storage silos in rural areas [102]. Except for these mentioned uses, TS has no other commercial value. However, this agricultural residue contains lignocellulosic compounds that could be a potential resource for value-added materials such as cellulose fibrils

2.5. Biodegradable Polymers in Composites

While biodegradable polymers are environmentally friendly, they have drawbacks in terms of thermal resistance, barrier properties, and strength, as detailed in section 2.1.The emergence of composites has brought in a revolution in materials science. A composite material is made up of two or more different components. One component, called the reinforcement, provides strength and stiffness. The other component, called the matrix, binds the reinforcement together and provides toughness and dimensional stability. The properties of the composite depend on the properties of the reinforcement and the matrix. Several articles have highlighted the importance of biodegradable polymer matrix in the development and use of composite materials [36, 103, 104].

Bio-composites can be prepared using two main techniques: solvent casting and melt compounding. Melt compounding is an extrusion process that involves the incorporation of thermoplastic particles using thermo mechanical mixing (compounding), and then extruded

through a die to form a film. The main advantage of melt compounding is that it is a solvent-free process. It is a good choice for applications where no organic solvent system is required. This eliminates the need to use toxic and hazardous solvents, which can be harmful to the environment and to human health. The main disadvantage of melt compounding is that it can be difficult to control the dispersion of the fillers in the polymer matrix. This can lead to poor mechanical properties and a lack of uniformity in the film. Careful control of the process parameters is essential to minimize degradation of the fillers and to ensure that the fillers are uniformly dispersed in the polymer matrix [105].

Among the techniques of film manufacturing, solvent casting is a feasible, preferable, and undoubtedly widely used method mainly due to the straightforward manufacturing process (involving no specialized equipment) and low cost of processing. The quality of the film produced by solvent casting can be controlled by monitoring the parameters of each step in the process. For example, the concentration of the polymer solution, the casting speed, and the drying temperature can all affect the thickness, uniformity, and mechanical properties of the film [106].

Different classes of fibers are used to reinforce polymeric matrices. The most common fibers used in industry are carbon fibers, aramid fibers, and glass fibers. However, these fibers have some serious drawbacks: They are non-renewable resources, non-recyclable, abrasive to equipment, require a high energy input to manufacture, and they can pose a health risk. In addition, the production of glass fibers releases carbon dioxide and other harmful chemicals into the environment. New technologies are being developed to address some of the drawbacks of fibers. For example, researchers are developing ways to make fibers from renewable resources and to recycle them more easily [107]. They are also working on ways to reduce the energy input required to manufacture fibers and to make the manufacturing process more environmentally friendly [108–110].

Cellulosic fibers have sparked a special interest because of their high specific mechanical properties, biocompatibility, and bio-resource. They are a feasible alternative for some applications to replace synthetic reinforcement in polymers. In addition to these advantages, cellulosic fibers also have a lower density than glass fibers, yet they offer higher mechanical strength and stiffness. This makes them a more attractive option for many applications. As a result

of these advantages, and the demand for more environmentally friendly and sustainable materials increases, cellulosic fibers are becoming increasingly popular as a reinforcement material for polymers [111].

Many approaches with different cellulosic fibers have been considered to improve the physical characteristics of polymers. The use of macro and nano cellulose fibers as either additives or reinforcements in diverse polymer systems to modify their characteristics has become a popular research area. For instance, combining nanocelluloses with polylactic acid creates a material that not only breaks down naturally but is also significantly improved the mechanical properties. Wang et al. [112], extracted cellulose nanocrystals from waste cotton using a mixed H_2SO_4 & HCl, and subsequently used as filler to reinforce a PLA polymer matrix. The researchers created composite films by combining different amounts (0%, 0.1%, 0.3%, 0.5%, and 0.7%) of CNCs with PLA. They found that films with small amounts of CNCs (0.1% and 0.3%) had desirable qualities such as a smooth surface, high crystallinity, and good strength and flexibility. However, when the CNC content was increased to 0.7%, the CNCs were unevenly distributed within the PLA, resulting in poor light transmission, reduced crystallinity, and decreased strength and elasticity.

Qian et al. [113], also studied effects of bamboo cellulose nanowhisker (BCNW) content on the morphology, crystallization, mechanical, and thermal properties of PLA matrix biocomposite. Biofilms made from PLA combined with varying amounts of BCNW were created using a solution casting method. The amount of BCNW in these biofilms ranged from 0 to 4%. The resulting biofilms were then analyzed. The study found that the strongest and most flexible biofilm was produced when BCNW made up 2.5% of the material, achieving a maximum tensile modulus of 427 MPa. However, the biofilm with the greatest ability to stretch before breaking contained 1.0% BCNW, with an elongation at break of 22%. Additionally, the addition of BCNW significantly increased the size of the crystalline structures within the biofilm, reaching a peak crystallinity of 30.7% when BCNW was 2.5% of the material. Furthermore with the increase in BCNW content, tensile strength of the composites reduced gradually. The literature also presents biodegradable composites using other polymers, like polyacrylamide/TEMPO-oxidized cellulose nanofibril [114], Poly(ε-caprolactone)(PCL) /cellulose fibers [115], Polyhydroxybutyrate (PHB)

reinforced with natural fibers [116], and natural renewable polymers like starch-based composites [117].

2.6. Performance Enhancement of PVA Polymer by Cellulosic Micro and Nano Reinforcement

The PVA structure has many hydroxyl groups attached to its carbon backbone, which allows other substances to be incorporated into it through hydrogen bonding. Over last years, the productions of the PVA based composite using cellulosic fibers from different lignocellulosic biomass have been reported by several research groups as shown in Table 2-4. Previous studies have shown that adding reinforcing fillers to a polyvinyl alcohol matrix can improve its water resistance, mechanical properties, and thermal stability. Some of the fillers that have been studied include graphene oxide [118], montmorillonite [119], bamboo charcoal [120], and cellulose [121].

Natural fibers offer a more environmentally friendly approach to strengthening composite materials. Cellulose, the primary component of these fibers, is inherently robust due to its highly ordered structure and the strong bonds between its molecules. The obtained cellulosic structures are usually at the micro or nano scale, and can demonstrate special properties when used as reinforcement in polymer composites

2.6.1. Cellulosic micro - reinforcement

As discussed above, by reinforcing PVA with natural fibers, it is possible to improve its strength, stiffness, and toughness. Chakraborty et al. [122], investigated the impact of micro-fibrillated cellulose (MFC) on the tensile strength of PVA composites. They found that adding 5% MFC significantly improved the composite's strength. However, exceeding this amount led to MFC fiber clumping, reducing the strengthening effect. The researchers concluded that MFC's superior strength and shape made it an effective reinforcement. In another study, Qiu and Netravali enhanced the properties of MFC/PVA composites by chemically linking MFC and PVA with glyoxal [3]. This crosslinking boosted the composite's mechanical strength, thermal stability, and glass transition temperature. However, the composite's melting point and crystallinity decreased. In a study by Santi et al. [123], PVA/MCC composites were prepared using mechano-chemically activated MCC. Six different formulations were developed, with increasing ratios of MCC

content (from 0% to 55% w/w) in PVA. The composites were then extruded using a co-rotating twin-screw extruder. The PVA/MCC composites exhibited a good stress–strain behavior, as well as a close correlation between MCC content and tensile, thermal, and degradation properties. The results showed that the addition of MCC to PVA can improve its mechanical properties, thermal stability, and biodegradability. In another study, Hasan et al. [124] developed PVA composite films using MCC derived from jute fiber. They oxidized the jute fiber with ammonium persulfate to introduce carboxylic groups. The composite films were produced in varying ratios of MCC and PVA. The researchers found that the composite films exhibited improved thermal stability, suggesting their potential as flame-retardant materials.

2.6.2. Cellulosic nano - reinforcement

Asad et al., [42] used TEMPO-oxidized nanocellulose (TONC) suspension from oil palm empty-fruit-bunches (OPEFB) to reinforce PVA polymer with varying weight percentages from 0.5 to 6% (w/w) using the casting method. They found that the 4% (w/w) TONC content reinforced nanocomposite had the highest tensile strength and modulus, increasing by 122% and 291% respectively, compared to neat PVA. However, the elongation at break decreased by about 42.7%. The thermal stability of PVA-based nanocomposite films was also improved.

Table 2-2 Tensile strength, Modulus and Elongation at break of PVA/TONC composite with increasing TONC content [42]

Weight percentage of TONC (%)	**Tensile strength (MPa)**	**Modulus (GPa)**	**Elongation at break (%)**
0	63.2	0.9	6.2
0.5	121	2.1	5.4
1	125	2.75	4.5
2	137	3.3	4.25
4	140.3	3.9	3.65
6	130	3.7	3.5

Table 2-2 demonstrates that the tensile strength and modulus of the nanocomposite films increased with increasing TONC content, while the elongation at break decreased. This suggests that the TONC reinforcement improved the strength and stiffness of the films, but decreased their ductility. These findings suggest that TONC reinforcement enhanced the films' strength and stiffness while compromising their ductility, as shown in Table 2-2. The thermal stability of the films was also improved with increasing TONC content. These findings demonstrate the effectiveness of TONC in reinforcing PVA polymer, leading to the creation of films with not only enhanced mechanical strength and stiffness but also superior thermal stability.

In 2018, Wang and his team [125] produced cellulose nanofibrils (CNFs) from steam-exploded rice straw fibers using a TEMPO-mediated system. They then used these CNFs to prepare reinforced PVA composite films by solution casting. The resulting films demonstrated improved flexibility, transparency, and heat tolerance compared to the original PVA films. However, they also showed weaker water resistance due to the existence of more polar groups in the rice straw CNFs. Here is a table (Table 2-3) summarizing the results of the study:

Table 2-3 Mechanical properties, transparency, and thermal stability of rice straw CNFs/PVA composite films at 3% CNF content and pure PVA films [125].

Property	**Pure PVA films**	**Rice straw CNFs/PVA composite films at 3% CNF content**
Tensile strength (MPa)	40	60
Elongation at break (%)	150	110
Thermal stability (T_{max} (°C))	255	270
Water resistance (% water absorption)	118	108

The data presented in Table 2-3 shows that composite films made from rice straw cellulose nanofibers (CNFs) and PVA are significantly stronger than pure PVA films. The researchers explain that this improvement in strength and stiffness is due to the CNFs' long, thin shape. These

nanofibers create a reinforcing network within the PVA material. Additionally, the inclusion of CNFs also enhanced the composite films' resistance to heat. The CNFs acted as a barrier to heat, preventing it from reaching the PVA matrix. Furthermore the PVA composite films are more water-resistant than pure PVA film. Increasing the cellulose fiber content in these composites further reduces their water absorption. The authors concluded that the rice straw CNFs/PVA composite films could be used as a potential alternative to conventional materials in a variety of applications, such as packaging, membranes, and composites. However, they noted that the weak water resistance of the films would need to be addressed before they could be used in applications where water resistance is important.

In other research work, Spagnol et. al., [126] have demonstrated the successful isolation of highly crystalline cellulose nanowhiskers (CW) from cotton. These nanowhiskers were then incorporated into PVA films at varying concentrations (3, 6, and 9%). The resulting nanocomposite films exhibited significant enhancements in both tensile strength (up to 33%) and elastic modulus (up to 140%), with the degree of improvement dependent on the specific chemical treatment of the nanowhiskers and their concentration within the film. The authors of the study attributed the improved mechanical properties of the CW-reinforced PVA films to the high aspect ratio of the CWs, the good dispersion of the CWs in the PVA matrix, and the chemical modification of the CWs. The authors concluded that CWs are a promising reinforcement material for PVA polymer. They suggest that further research is needed to optimize the processing conditions and CW loading to achieve the best possible mechanical properties. Focusing on mechanical properties, Table 2-4 presents a comparative analysis of PVA composites reinforced with various cellulose fibrils, identifying their optimal fiber loading percentages for achieving superior mechanical properties.

Table 2-4 Summary of studies on mechanical properties of PVA-based composites reinforced by cellulose fibrils from different fiber sources with their optimum fiber loading.

Formulation	**Fiber source**	**MCC/NC extraction method**	**Tensile str.(MPa)**	**Elongation (%)**	**Ref.**
PVA/6% CNF	Wood chips	ultrasonication	57	-------	[127]
PVA/ 6 % CWMA	cotton fibers	Concentrated HCl (37%)	33% Increment	-------	[126]
PVA/4% TONC	oil palm pulp	TEMPO-oxidization	140.3	3.75	[42]
PVA /3% CNF	Rice straw	TEMPO-oxidization	60	110	[128]
PVA/7.5% CNC	sugarcane bagasse	Acid hydro. (60%) H_2SO_4	60	180	[129]
PVA/ 5%NC	MCC	Acid hydro. (95%) H_2SO_4	82	------	[130]
PVA/7.5%MCC	Rice straw	alkali-bleaching treatment	31	15	[90]
PVA/2.5%cellulose	Palm Fruit Bunch	Acid hydro. (H_2SO_4)	36.09	119.96	[131]
PVA/ 1%MCC	sago seed shell	------	22.5	----	[132]

* TONC = TEMPO-oxidize nanocellulose, CWMA=cellulose whiskers modified by maleic anhydride

Overall, PVA's diverse character is defined by its flexibility, water solubility and remarkable chemical resistance against oils, greases, and solvents. Additionally; PVA is also biodegradable, making it an environmentally friendly choice. However, its highly hydrophilic nature and poor mechanical strength limit its wider application. The above studies clearly demonstrate that natural fibers such as MCC and NCC enhance the mechanical, thermal, and degradation properties of PVA. This holds immense potential for developing sustainable and high-performance materials.

Further research can optimize PVA's utilization for specific applications within automotive, construction, packaging and medical industries. Thus, in this study, PVA is selected as a polymer matrix for biodegradable composite preparation.

2.7. Conclusions

Significant studies have been conducted in recent decades on the conversion of lignocellulosic biomass into cellulose derivatives. This review provides an overview of different techniques used to extract microcrystalline cellulose from various materials. It also explores how MCC is used to create composite materials and their current applications.

Solid waste disposal is a major problem facing modern society. Among the solid wastes, agricultural residues are produced in large quantities in Ethiopia and other countries. Using agricultural residues as starting materials to synthesize various compounds can help to solve the disposal problem and also provide a value-added product. MCC is one such product that can be obtained from various lignocellulosic biomass wastes. Typically, it is produced by subjecting alpha cellulose to an abundance of mineral acids. MCC has gained significant attention as a promising material for industrial, technological, and biomedical applications. The source of the cellulose and extraction methods can affect the particle size, crystallinity, surface area, moisture content, and porous structure of the MCC. These properties can in turn affect the MCC's performance in different applications.

Microcrystalline cellulose is currently made from various plant-based materials. To reduce production costs, researchers are exploring the use of alternative sources like grasses, aquatic plants, and agricultural waste products. While many materials can be used to produce MCC, agricultural waste is particularly attractive due to its potential economic benefits. This is because these residues are often available at low or even negative cost, and they can be used to produce cellulose without the need for additional processing. Compared to other sources, agricultural residues have additional benefits: lower hemicellulose and lignin content. This means that they require less chemicals and energy to bleach, making them a more sustainable source of cellulose. As a result, agricultural residues are a promising source of cellulose.

Ethiopia’s crop agriculture continues to be dominated by the country’s numerous small farms, which cultivate mainly cereals for both their own consumption and sales. Due to the country's extensive farming activities, a massive quantity of agricultural residue is produced. *Teff* is versatile and sustainable crop, and the straw from *Teff* crop is a valuable agricultural residue that

has a variety of potential uses. Therefore, this research will focus on the production and characterization of MCC from TS as a bio-filler for enhancing the mechanical and thermal properties of biopolymers.

To extract microcrystalline cellulose from lignocellulosic materials, the first step is to remove lignin and hemicellulose. The goal of pretreatment is to break down the complex structure of lignocellulose and make the cellulose more accessible to acid hydrolysis. Alkali-bleaching treatments are preferred over classical chemical treatments for cellulose fiber purification because NaOH/KOH, sodium chlorite, and acetic acid are readily available in limited conditions. A saponification reaction during alkaline pretreatment causes the cleavage of the intermolecular ester linkages between hemicelluloses and lignin. This results in the solubilization of lignin and hemicellulose fragments in the alkaline solution. After lignin solubilization, the lignin no longer acts as a protective shield to the cellulose. This exposes the cellulose crystals for further processing, and more susceptible to other treatments. Additionally, alkaline pretreatment is more effective for low lignin content biomass, such as agricultural residues. The conditions, such as temperature, time, and concentration of the alkaline solution, should be optimized to achieve the desired results.

Once lignin and hemicellulose have been removed, a controlled hydrolysis treatment is performed. Sulfuric acid is the most widely used acid because it is easily obtainable and relatively cheap. The process is relatively simple and can be scaled up to produce large quantities of MCC. Unfortunately, the sulfated cellulose produced by sulfuric acid hydrolysis has low yield and less thermal stability than the starting material. Further research is needed to develop methods for mitigating these drawbacks and to improve the efficiency of the acid hydrolysis process. Recently, transition metal salts have taken on a new role as acidic catalysts for efficient cellulose hydrolysis. Transition metal salt catalysts offer a number of advantages over conventional methods for cellulose hydrolysis. They are more efficient, selective, environmentally friendly, and cost-effective. As a result, they are a promising option for the production of high-quality MCC.

The main motivation for developing bio-composites is to create a new generation of composites that are environmentally friendly in terms of manufacturing, application, and recycling. The development of continuous native cellulose fibers is an emerging technology that is believed to be

important when bio-composites with light weight and targeted properties are required. MCC plays a vital role in the development of bio-composites, which combine MCC with a polymer. It can improve the strength, stiffness, and toughness of these materials. Polyvinyl alcohol is the most readily biodegradable of vinyl polymers. This odorless and tasteless material excels in film formation, and adhesion, while demonstrating flexibility, and barrier properties against oxygen and aromas. Moreover, the PVA structure has many hydroxyl groups linked to its carbon backbone, enabling the integration of other substances through hydrogen bonds. These versatile attributes make PVA a compelling alternative for disposable and biodegradable plastics. However, its highly hydrophilic nature and poor mechanical strength limit its wider application.

In conclusion, the path towards utilizing *Teff* straw as a sustainable source of MCC and its incorporation into bio-composites is laden with possibilities. More research and development are crucial to optimizing extraction methods, exploring diverse sources of cellulose, and evaluating the performance of these bio-composites across various applications. By embracing this novel approach, we can not only address waste management concerns but also pave the way for a future driven by environmentally responsible and high-performance materials.

CHAPTER 3: VALORIZATION OF ABUNDANTLY AVAILABLE ETHIOPIAN *TEFF* (*ERAGROSTIS TEF*) STRAW FOR THE ISOLATION OF CELLULOSE FIBRILS BY ALKALINE HYDROGEN PEROXIDE TREATMENT METHOD

Based on the published paper: *Assefa, E.G., Kiflie, Z. & Demsash, H.D (2023). Valorization of Abundantly Available Ethiopian Teff (Eragrostis Tef) Straw for the Isolation of Cellulose Fibrils by Alkaline Hydrogen Peroxide Treatment Method. J Polym Environ 31, 900–912.* https://doi.org/10.1007/s10924-022-02646-4

Abstract

Teff is the main cereal crop in Ethiopia, where *Teff* straw is the solid residue after the grain is harvested. Therefore, the valorization of such abundant agricultural residue for isolating cellulose could be a viable fiber source. This study characterized cellulose fiber isolated from TS by alkaline and chlorine-free bleaching treatments for bio-filler applications. During the alkali treatment, three independent variables [i.e. temperature (60–95 °C at the interval of 10°C except for the last level (at 5°C interval)), time (30–150 minute at the interval of 30 min), and NaOH concentration (2–8 wt. % at the interval of 1.5 wt. %)] were examined to predict their effect on lignin decomposition and fiber yield. Chemical composition analysis showed that the raw *Teff* straw has 40.44%, 29.44%, and 18.05% of cellulose, hemicellulose, and lignin respectively. Based on the single-factor alkali treatment results the percentage of lignin removal and the yield of cellulose were influenced by the NaOH concentration, treatment time, and temperature of the treatment. Furthermore, the final bleached fibers had cellulose, hemicellulose, and lignin contents of 85.5%, 11.98%, and 2.52 % respectively, which confirmed the significant decrease in the percentage of non-cellulosic components. As a result, the isolated cellulose has high crystallinity (65.51%) and thermal stability (T_{on} (255 °C) and T_{max} (365.5 °C)). SEM images of the obtained cellulose showed a long rod-like structure with an average diameter of 4.5 µm. Overall, the results of this study indicated that *Teff* straw is a promising new source of raw material to produce cellulose, which could be used as a bio-filler in bio-composite preparation.

Keywords: *Teff* straw; Biomasses valorization; Cellulose isolation; Chlorine-Free Bleaching; Characterization.

3.1. Introduction

Being environmentally friendly, natural fiber-reinforced polymers have been significantly used in many applications, such as automobiles, packaging, and the furniture industry as alternatives to synthetic polymers which pollute the environment. Cellulose, primary component of natural fibers, plays a vital role in providing mechanical strength and structural support [133]. It has excellent mechanical properties, and thermal resistance, as well as degradability, which is unobtainable in synthetic fillers. This makes it an excellent bio-filler for both synthetic and natural polymer matrices [134–136]. Cellulose is a natural, partially crystalline material made up of repeating glucose units linked together in a specific pattern. It's the most common organic compound on Earth and can be produced sustainably from a variety of living things [137, 138]. Plant fibers vary widely in their makeup and structure based on factors such as the plant type, its age, which part of the plant it comes from (root, stem, or leaf), where it was grown, and the local climate [139–141]. Consequently, cellulose derived from different sources and growing conditions exhibits distinct chemical, mechanical, and thermal characteristics. Therefore, the isolation and characterization of cellulose fibrils from different lignocellulose sources in different geological regions for various applications is a major area of study to compare and efficiently exploit these resources.

Due to the increasing demand for cellulose fibers, alternative sources such as agricultural residues are currently being investigated. Furthermore, agricultural sources are particularly promising because they usually have lower lignin and higher holocellulose contents compared to wood materials [142]. For this reason, delignification and fiber purification of such agricultural residues may require lower energy and chemical consumption. The cultivation of *Teff* as a cereal crop produces a large quantity of TS annually as discussed in the previous chapters. Physically, *Teff* is a tufted annual grass where its culm is fine, and erect that reaches a height of 150–200 cm at maturity [102, 143]. Recently, different studies have been reported on TS valorization such as for activated carbon, bio-silica, and bio-char preparation [144–147]. Gabriel et al. [148] also isolated cellulose from TS and other plant by-products using three stages of chemical treatments at different NaOH concentrations. However, this work did not study the effects of process variables like reaction time and temperature on alkali-treated fiber yield and lignin removal, which are crucial factors when the yielded fiber is to be used for reinforcement application.

So far, different methods for isolating cellulose from lignocellulosic materials have been reported: mechanical, biological, chemo-mechanical, and chemical [149–154]. The main purpose of these treatment methods is to break down the carbohydrate polymers of the biomass, reduce the proportions of hemicellulose and lignin, accompanied by a greater cellulose proportion [155]. Among these, chemical methods have been widely used for isolating cellulose as they are cheaper and more efficient. Chemical methods such as alkali and acid hydrolysis are often considered cheaper for cellulose isolation due to simpler equipment needs, faster processing times, and potentially higher yields [156]. Compared to mechanical or biological methods, they often require simpler equipment. setting up and maintaining complex machinery like grinders or bioreactors can be expensive, making chemical methods more cost-effective. Additionally, chemical methods boast faster processing times, leading to lower energy consumption and reduced operational costs. Furthermore, these methods can achieve higher cellulose yields from the raw material compared to some alternatives. This translates to needing less starting material for the same amount of cellulose, ultimately resulting in cost savings.

Alkali treatment increases cellulose content by removing the outer non-cellulosic layers, hemicelluloses, and lignin from the raw fiber. Additionally, alkali treatment removes residual waxes, as well as pectin [157]. Alkali-based methods are particularly effective for processing lignocellulosic biomass with a lower lignin content, like that found in agricultural residues [158]. In the literature, alkali treatments of different lignocellulosic biomass at different process conditions have been reported. For instance, Gu, J., & Hsieh, Y. [74], successfully isolated cellulose from rice straw by alkali treatment with 4%, 6%, and 8% (w/v) of NaOH at 70 °C for 5 to 120 min treatment time, to find the optimal conditions. Yue, Yiying, et al. [69], treated energy cane bagasse with NaOH under different conditions (10 wt.% for 1.5 h, 20 wt.% for 1.5 h, and 20 wt.% for 10 h) at 98 °C. Similarly, in the study of Aurelia, et al. [76], dried jack bean skin was treated with NaOH solution in several concentrations (4, 6, 8, 10, and 20%) at 100 °C for 3 h to extract cellulose. All the above studies report different optimal conditions for cellulose yield as well as lignin removal efficiency from the lignocellulosic biomass. Moreover, the three parameters (reaction temperature, time, and NaOH concentration) are the main factors in the alkali treatment of biomass for cellulose isolation.

An alkali hydrogen peroxide treatment was chosen for this study as it is an inexpensive and effective method to isolate cellulose fibers [159, 160]. Additionally, the use of hydrogen peroxide bleaching treatment has less environmental impact compared to the chlorine-containing bleaching agents. Alkaline treatment strips away some of the hemicellulose, lignin, wax, and oils on the outside of the fiber cell. Following this, bleaching breaks down and dissolves the colored parts of the remaining lignin and any natural dyes within the fiber [75]. The conditions of the alkali and bleaching treatments, including the strength of the sodium hydroxide solution, treatment duration, and temperature, significantly impact the quantity and purity of the cellulose fiber produced.

Therefore, this study aims to isolate and characterize cellulose fibrils from TS using alkali hydrogen peroxide treatment and investigate the effect of alkali treatment conditions on the yield and percentage of lignin removal on the obtained fiber. All samples at each stage of treatment were characterized through chemical composition, X-ray diffraction, Thermogravimetry, and Scanning electron microscopy analysis.

3.2. Materials and Methods

3.2.1. Materials

Teff straw was collected from a local farm in the northern part of Ethiopia, Amhara region, near Bahir Dar city, Ethiopia.

The chemical reagents used were sodium hydroxide (NaOH, 98%), and sulfuric acid (H_2SO_4, 98%) (HiMedia, Mumbai, India), hydrogen peroxide (H_2O_2, 30%), (Fisher Scientific, Loughborough, UK), glacial acetic acid, ethanol (98%) (Research-Lab, Mumbai, India), and Nitric acid 65% (Loba Chemie, Mumbai, India). All chemical reagents were of analytical grade.

3.2.2. Experimental Methods

3.2.2.1. Isolation of Cellulose Fibers

a) Sample preparation

The preparation of cellulose fibers from natural fibers requires the removal of extractives, lignin, and hemicellulose. The existence of extractives in natural fibers reduces the penetration of the alkali solution as they shield the fibers' reactive functional groups. Thus, size reduction and

extractive removal are performed to increase the delignification efficiency. Extractive removal is mainly performed through treatment with a mixture of benzene/ethanol, toluene/ethanol, or hot water. Due to environmental and economic considerations, this study utilized hot water to extract and remove components including waxes, fats, resins, tannins, gums, sugars, and starches that were not chemically linked to the material [68].

The collected TS was washed several times to remove dirt and sand before being milled. It was then placed under sunlight drying for about 3 days to remove the excess moisture. After sun drying, it was milled using a cutter mill (Fritsch, D-55743, Germany) to reduce the size of fibers to a size that could pass the 850 µm sieve size and retained in the 250 µm sieve. 10 g of milled *TS* fiber (dry weight) was soaked in 500 ml of distilled water and stirred for 120 min at 70 °C as per the method used by Yue, Yiying, et al. [69]. Then, the slurry was filtered and washed with distilled water repeatedly to remove soluble extractives. Finally, it was dried in a hot air oven (PH-030A, China) to constant weight.

b) Alkali and bleaching treatment

Among various purification methods, alkali hydrogen peroxide (AHP) treatment is a preferred chemical treatment method for the purification of cellulose fibers. NaOH and H_2O_2 are widely available in the industry at a reasonable cost and have lower environmental impact. Different solid to liquid ratios (g/ml) in alkali/bleaching treatment of biomass have been reported in the literature [54, 70, 93, 161]. It is essential to make the treatment at high solid concentration since on an industrial scale higher solid loadings are desirable as they lead to lower production costs. However, the higher fiber content might increase the viscosity, which hinders the mixing procedure. Whereas, lower fiber content might cause wastage of chemicals and lower the cellulose fiber yield due to chemical degradation [162]. Based on the preliminary experimental work results of this study (Appendix A1), the solid-to-liquid ratio of 1:30 (g/ml) was used throughout the alkali and bleaching treatments.

- ***Alkali treatment***

In this study alkali treatment of the obtained hot water-treated TS was carried out using sodium hydroxide on a hot plate under a constant magnetic stirring (magnetic stirrer hotplate, Stuart Scientific, UK). In order to investigate the effect of reaction temperature, reaction time, and

NaOH concentration on the yield and lignin removal efficiency of the fiber from TS, the treatment was conducted under different process conditions, as shown in Table 3-1 with a one-variable-at-a-time approach. Preliminary work at a higher temperature (100 °C) resulted in the drying of the working solution, causing the fibers to burn before the reaction was complete. Consequently, the temperature was reduced in 5 °C intervals from level 4 to 5.

At the end of each reaction, the mixtures were filtered using vacuum filtration and washed with distilled water repeatedly. Then, the obtained residue was rinsed with distilled water and mixed manually with a dilute acetic acid solution using stirring rods to neutralize any alkali solution attached to the fiber. Chemical treatment creates pores in lignocellulosic fibers by removing lignin. These pores, filled with water in a wet state, collapse upon drying due to fiber shrinkage. This structural change reduces porosity and hinders subsequent treatments. Oven drying at lower temperatures is a common approach to minimize shrinkage. Based on literature, in this research work drying at lower temperature (60 °C) was chosen for alkali and bleaching treated fibers drying. Thus, the samples were oven-dried at 60 °C till constant weight. Finally, the yield and residual lignin content were then determined for each sample.

Table 3-1 Process parameters and levels for the alkali treatment

No.	**Factor**	**Level**				
		1	**2**	**3**	**4**	**5**
1	Reaction temperature (°C)	60	70	80	90	95
2	Reaction time (min)	30	60	90	120	150
3	Sodium hydroxide concentration (%)	2	3.5	5	6.5	8

- ***Bleaching treatment***

This study utilized hydrogen peroxide under alkaline conditions for oxidation because it offers a more environmentally sound and chlorine-free bleaching process [163]. The alkali-treated fiber was bleached using a preheated mixture of hydrogen peroxide (20%) and sodium hydroxide (5%) to remove the remaining lignin and hemicelluloses using a hot plate under constant magnetic

stirring. Based on the preliminary experimental work results (Appendix A2) and literature surveys, bleaching treatment was conducted at a temperature of 65 °C for 90 min. The remaining material, high in cellulose, was filtered and repeatedly rinsed with pure water until neutrality. Previous studies indicate that bleaching treatment by H_2O_2 at alkali conditions needs repeating the process to provide a higher level of lignin removal because the lignin does not readily withdraw from the first stage of bleaching. Thus, the bleaching process was repeated twice to produce purer cellulose. Finally, it was oven dried at 60 °C and milled to powder using a high-speed universal disintegrator (FW100, China) as shown in Figure 3-1.

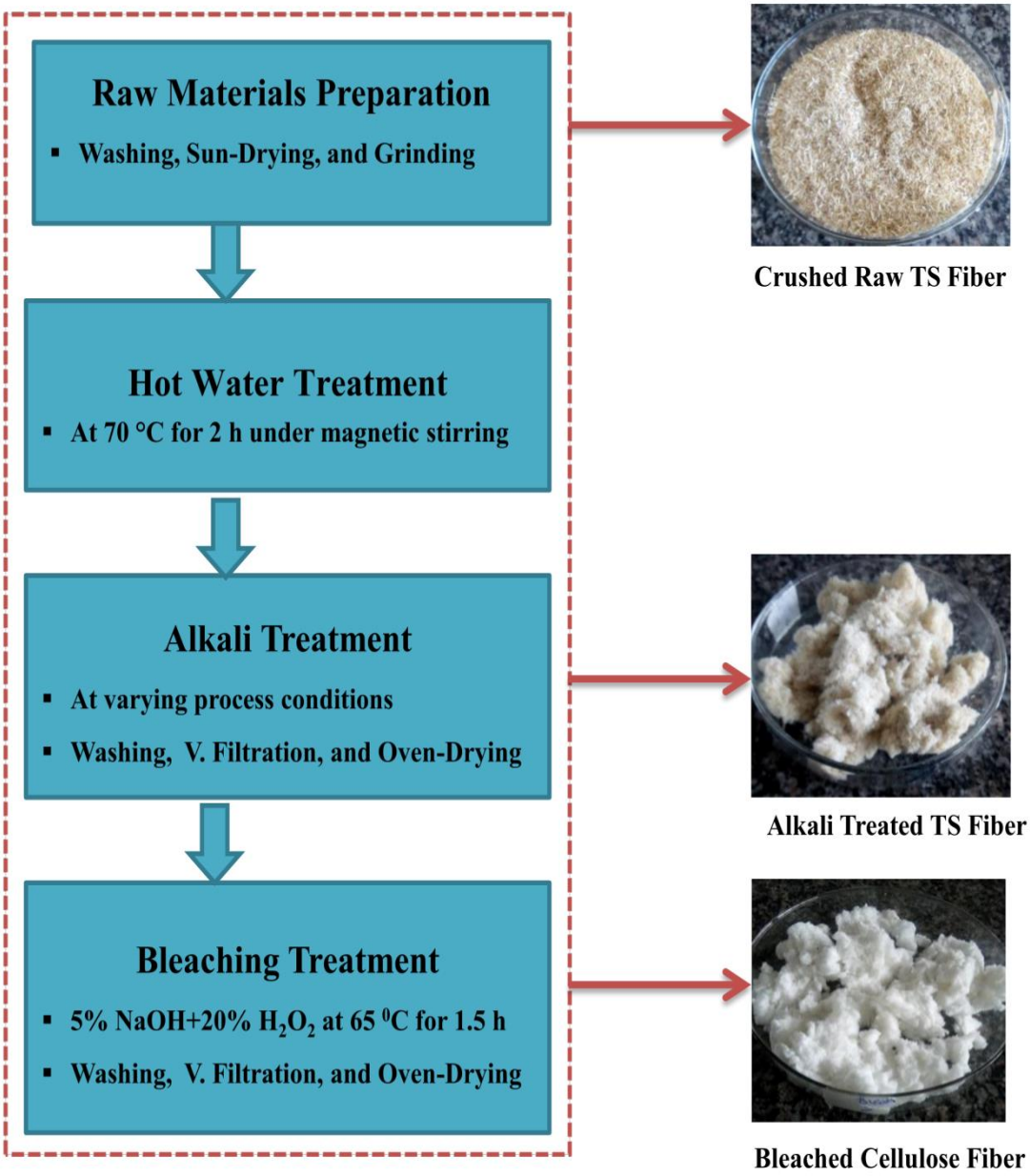

Fig. 3-1 Schematic flow diagram for the isolation of cellulose from *Teff* straw.

3.2.2.2. Characterization

a) Chemical composition analysis

The chemical conformations of raw and chemically treated TS fibers were investigated using the National Renewable Energy Laboratory (NREL) protocol (for ash, extractive, and lignin content) [164–166], and the *Kurschner-Hoffer* method (for cellulose content) [167]. The amount of

extractive was determined by the water/alcohol treatment method [165], and the amount of inorganic material (ash) content was determined by placing the sample in a muffle furnace at 575 °C based on the NREL [164] laboratory analytical procedure.

- ***Determination of lignin content***

The lignin content of the samples was determined based on the NREL method using a two-step acid hydrolysis [166]. The water/ethanol isolated dried raw biomass was weighed (0.3 g) and placed in glass test tubes onto which 3 ml of 72 % H_2SO_4 was added. Then, the sample was placed in a water bath (CU – 420, China) set to 30 °C for 60 min. The sample was manually stirred every five minutes using a stirring rod. Following this initial acid hydrolysis process, the sample was mixed with 84 milliliters of pure water. The second hydrolysis stage was carried out in a pressurized autoclave (portable autoclave, Sentwin, RKB-496B, India) for 60 min at 121°C to ensure complete breakdown of the material. The resulting mixture was then cooled and filtered to separate the solid residue. The amount of insoluble lignin was determined determined by drying the residues at 105 °C and accounting for ash by incinerating the hydrolyzed samples at 575 °C in a muffle furnace (Nabertherm, LT 3/12/B180, Germany), while the amount of soluble lignin was measured by analyzing the liquid portion using a UV spectrophotometer (PerkinElmer lambda 35, USA) at 320 nm. The lignin content of the samples was then calculated as the summation of acid-insoluble lignin and acid-soluble lignin.

To determine the lignin content of the chemically treated fibers, firstly the obtained fiber from each process treatment was ground to powder and then soaked in distilled water in a 250 ml Erlenmeyer flask. Drops of 5 % acetic acid were added and stirred manually with stirring roads for 15 min to adjust the pH of the suspension to below 4 to neutralize any remaining alkali attached to the fiber. Then, it was washed with distilled water to neutrality, and finally oven-dried. The dry powder was then used to determine the lignin content using the NREL procedure.

- ***Determination of cellulose content***

The cellulose content was determined using *Kurschner-Hoffer* gravimetrical method [167]. A sample of the dry fiber free of extractives (water/ethanol extracted) was weighed (2 g) and placed in a 250 ml Erlenmeyer flask containing 100 mL of a solution, prepared from nitric acid: ethanol 20:80 v/v [168]. The flask was equipped with a reflux condenser and boiled for 60 min. After

boiling, the contents of the flask were filtered and washed with distilled water. The same process was repeated for 60 min with the same mixture. Subsequently, impurities were removed by filtering, and the substance was cleaned with distilled water. Finally, the prepared cellulose from the Kürschner–Hoffer was dried in an oven at 105±3 °C until reaching constant weight. The cellulose content was calculated according to equation 3-1 shown below.

$$\%Cellulose = \frac{W_1}{W_0} * 100 \qquad (3-1)$$

Where W_0 is initial dry sample weight and W_1dry sample weight after the treatment

- ***Determination of hemicellulose content***

The hemicellulose fraction was calculated by the difference between ash, extractive, cellulose, and lignin content.

$$\%hemicelluloses = 100\% - \%Lignin - \%Cellulose - \%Extractives - \%Ash \qquad (3-2)$$

b) X-Ray Diffraction (XRD)

Lignocellulosic fibers consist of two types of components: amorphous components (lignin, hemicellulose, and extractive fractions) and crystalline components (cellulose). XRD analysis has been widely used to identify crystalline components by determining the parameters, such as the percentage of crystalline, nature of cellulose polymorphism, and size of crystallites of lignocellulosic fibers before and after treatment [169]. Thus, in this study, X-ray diffraction analysis was conducted to evaluate the degree of crystallinity of the raw TS, alkali-treated, and the yielded cellulose fibrils.

XRD data were collected using an X-ray diffractometer (D2 phaser, Bruker, Germany) equipped with Cu Kα radiation operated at 30 kV and 10 mA to investigate the XRD spectra of the cellulosic sample. Samples were placed on the specimen holder and scanned over the range 2θ =10° - 40° with a step interval of 0.02° and a scanning speed of 1°/min. The crystallinity of the samples was then calculated from the diffraction intensity data by using the empirical Segal's method [169] according to the following equation.

$$CrI\,(\%) = \frac{I_{200} - I_{am}}{I_{200}} * 100 \qquad (3-3)$$

Where I_{200} represents to the maximum peak intensity at the lattice diffraction (200) of the crystalline regions and I_{am} is the minimum value between planar reflections (200) and (110), which refers to reflection intensity of the amorphous parts of the samples.

c) Thermogravimetry Analysis

Fundamental information regarding the thermal stability of the fibers can be obtained from Thermogravimetry analysis. Thermal Gravimetric Analyzer (HCT-1, BJHENVEN, China) was used to characterize the thermal stability of the samples. 8 mg of the samples were placed in a crucible, and then the operating temperature was elevated from room temperature to 700 °C with a constant heating rate of 20 °C/min. To prevent the rapid breakdown and oxidation of the cellulosic materials, all experiments were conducted in a nitrogen environment.

d) Scanning Electron Microscopy

Surface morphology changes of the samples were characterized by a scanning electronic microscope (JEOL JSM-6010 LV, Japan). To prepare the samples for examination, a thin coating of gold and palladium alloy was applied using a specialized machine (JEOL JFC-1300 Smart Coater, USA) in a vacuum chamber. This coating prevented the samples from becoming electrically charged when exposed to the electron beam during the analysis process. The diameter of the bleached fiber from the SEM images was analyzed using ImageJ software. A minimum of 100 measurements was taken to plot the size distribution curve of the bleached fiber.

3.3. Results and Discussion

3.3.1. Chemical Compositions Analysis

The chemical compositions of untreated and chemically treated TS fibers were investigated. Ash, extractive, lignin, cellulose, and hemicellulose content of the untreated and chemically treated TS fibers are listed in Table 3-2, where the average values were calculated from the data of three samples. The results showed that the raw fibers contained 40.44% cellulose, 29.44% hemicellulose, and 18.05% lignin that indicates cellulose, hemicellulose, and lignin are the main components of *Teff* straw fiber. The cellulose content in the untreated TS (40.44%) obtained in this study was higher as compared to khat waste (39%) [170], however, lower than the cellulose content of garlic straw residues (41%) [171], sugarcane bagasse (43%) [69], and cotton stalk

waste (54%) [17]. Whereas, the lignin content (18.5%) of TS determined in this study (Table 3-2) is much lower than reported in other studies elsewhere, such as 28.67% for khat waste [170], 24.5% for cotton stalk waste [17], and 24.09% for sugarcane bagasse [69].

After treatment with 5% NaOH for 90 min at 80 °C, the lignin and the hemicellulose contents were reduced to 7.02% and 21.4%, respectively, as compared to the raw TS (Table 3-2). The extractives content was also extremely low because of the treatments. In contrast, the cellulose content increased from 40.44% to 68.59 after alkaline treatment. Other studies also reported a rise in the cellulose content following chemical processing of the raw lignocellulosic materials. However, from the alkali treatment alone, it was found that hemicellulose and lignin could not be thoroughly removed by the NaOH-treated. Hence, to further eliminate the residual lignin, the NaOH-treated samples were subjected to a hydrogen peroxide treatment under alkaline conditions. As a result, the bleaching treatment of the fiber increased the cellulose content and decreased other components, with the final bleached fibers having cellulose, hemicellulose, and lignin contents of 85.5, 11.9, and 2.52%, respectively. The second stage of bleaching was expected to remove the remaining lignin completely. Despite the completion of the bleaching process, traces of lignin persisted. Lignin has a tendency to bind tightly with other carbohydrate molecules, creating intricate structures that are nearly impossible to eliminate entirely [172, 173].

Figure 3-1 shows, the photograph of the raw, alkali treated, and bleached TS fiber. As can be observed from Figure 3-1, after NaOH treatment, the color of the TS fiber was changed from brown to yellow, which indicates the reduction in the amount of lignin. Similarly, after the repeated bleaching treatment, the fiber color is changed to pure white on the produced fiber. This suggests the removal of most of the initial non-cellulosic components that remained after the NaOH treatment stage, which is in agreement with the composition analysis results.

In conclusion, the TS fibers had a high amount of holocellulose and relatively low lignin content, which could be viewed as a potential source of cellulosic fibers for the production of fiber-reinforced composite materials.

Table 3-2 Chemical composition of the untreated and treated TS and other lignocellulosic fibers (wt. % on dry matter)

Fiber source	**Sample**	**Composition (%)**					**Ref.**
		Lignin	**Cellulose**	**Hemicellulose**	**Extractives**	**Ashes**	
Teff straw	R	18.05 ±0.2	40.4 ±1.8	29.4 ±1.6	5.8±0.25	6.3±0.4	**This work**
	AT	7.02 ±0.7	68.6 ±3.01	20.8 ±3.5	nd	3.6 ±0.13	
	PCF	2.5 ±0.5	85.5 ±3.6	11.9 ±3.3	nd	0.1 ±0.03	
Wheat Straw	AT	17±2	44 ± 0.5	36± 0.5	---	7.2±0.05	[159]
	PCF	8± 0.5	79 ± 1.0	14± 1.0	---	---	
Rice Straw	AT	30.9	53.02	22.77	4.2	12.00	[150]
	PCF	1.03	84.90	12.50	1.3	0.27	
Khat Waste	AT	28.7 ± 2.5	39.4 ± 0.4	12.8 ± 0.5	14.7±0.35	3.4 ± 0.1	[170]
	PCF	10.9 ± 0.21	82.7 ± 1.4	5.8 ± 0.5	2.3±0.13	1.3 ± 0.2	
Palm	AT	21	33± 1.0	17	---	---	[138]
	PCF	---	73.8± 1.0	---	---	---	
Napier grass	AT	21.6	47.1	31.2	---	---	[174]
	PCF	3.4	93.5	2.9	---	---	

*nd, not detected: R, raw: AT, alkali treated: PCF, purified cellulose fiber

3.3.2. Effect of Process Parameters of Alkali Treatment on Lignin Removal and Cellulose Yield

This experiment was performed to observe the influence of process variables (temperature, time, and NaOH concentration) on the responses (the lignin removal and fiber yield) based on a single factor effect. Each individual variable has its effect on lignin decomposition (lignin removal). Time and temperature are necessary to make the fiber swell, and alkali concentration is a must to decompose the non-cellulosic components from the fiber [175]. In this study, the variation of these parameters has shown their effect on the percentage of lignin removal and fiber yield during the alkali treatment of *Teff* straw, as presented in Figure 3-2.

Figure 3-2 (a) shows the effect of treatment time on lignin decomposition and alkali-treated fiber yield where the reaction time varies from 30 min to 150 min, and the other factors (temperature and sodium hydroxide concentration) were maintained at constant values of 80 °C and 5%, respectively. From the obtained results, at lower time durations (30 min), lignin removal was found poor, which could be due to the alkali treatment does not have enough contact time to attack and decompose the lignin. The raw TS fiber requires some time to swell so that the alkali reagents can enter the fiber. The improvement in the extent of delignification reached its maximum at 120 min duration (64.44%). This result could imply that the reaction had reached its completion and any further increase in reaction time would only lead to a little or negligible effect on the extent of TS delignification. In addition to the reaction time, other factors (the reaction temperature and NaOH concentration) play a role in the isolation of cellulose fiber.

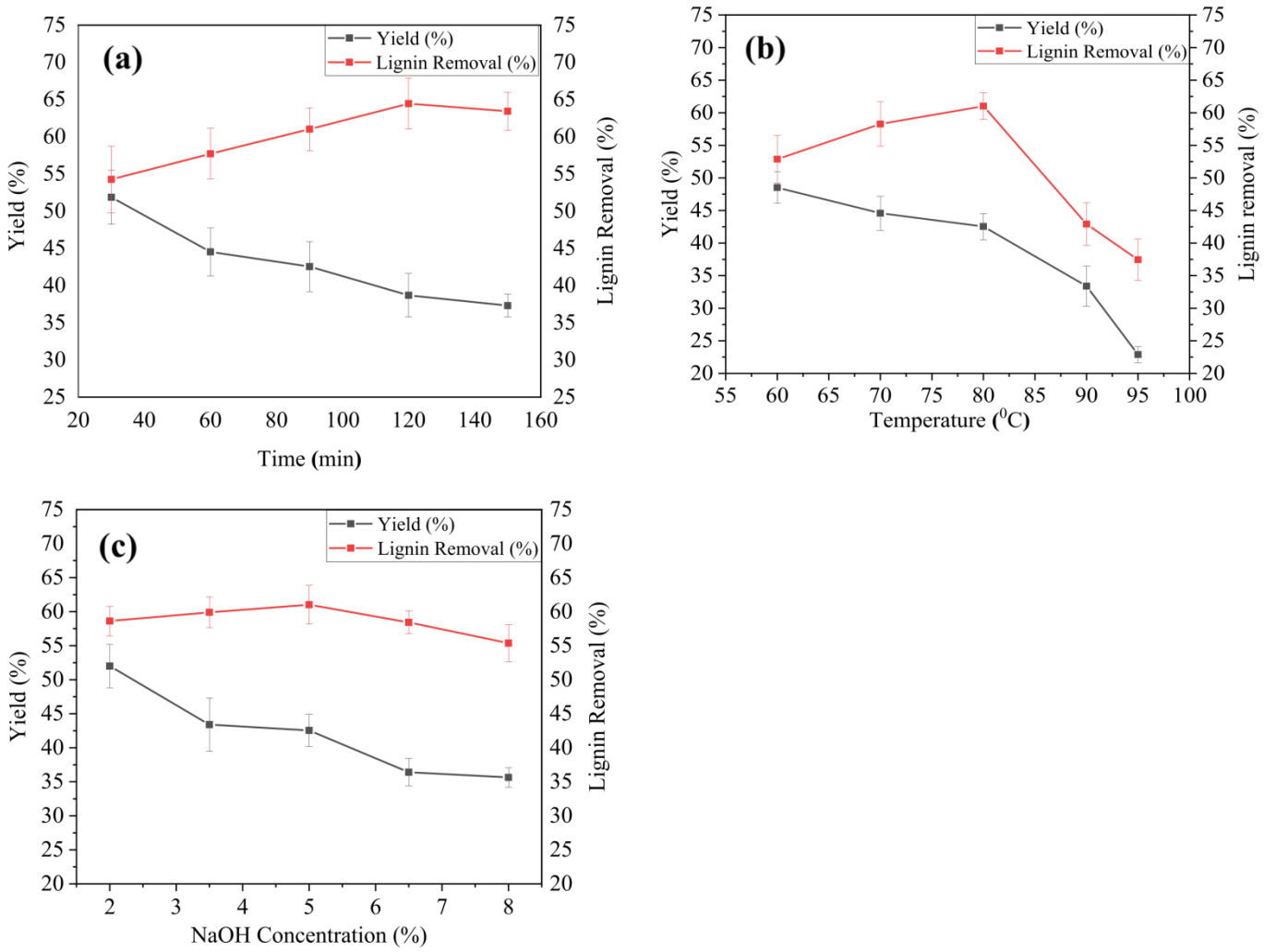

Fig. 3-2 Effect of (a) time , (b) temperature, and (c) NaOH concentration on lignin removal and cellulose yield from TS

The influence of treatment temperature on the percentage of lignin removal can be seen in Figure 3-2 (b). The reaction temperature varied from 60 to 95 °C, and time and sodium hydroxide concentration were kept at constant values of 90 min and 5%, respectively. The degradation of lignin by NaOH on the fiber was very slow at 60 °C, which is in agreement with the previously reported studies at lower temperatures below 70 °C [175]. When the reaction temperature increased from 60 to 80 °C the lignin removal was increased. However, as the reaction temperature further increased from 80 to 95 °C a reduction in lignin removal was observed. This is because at higher temperatures (>80 °C) the suspension becomes viscous jelly, which might cause incomplete lignin decomposition.

Likewise, Figure 3-2 (c) shows the influence of NaOH concentration on lignin decomposition when the NaOH concentration changed from 2% to 8%, and time and temperature were kept at constant values of 90 min and 80 °C, respectively. At 2% NaOH concentration, the percentage of lignin removal was found to be slightly lower (58.63%). This could be because the alkali was not efficient in decomposing the lignin and other impurities from the fiber. Increasing NaOH levels from 2% to 5% led to increased lignin extraction. High alkalinity promotes the deterioration of lignin and the breakdown of hemicelluloses [176, 177]. However, with a higher concentration (greater than 6.5%) of NaOH, a slight decrease in the lignin removal was observed.

The variations in process parameters also affect the yield of alkali-treated TS fiber. In all conditions yield of fiber decreases with an increase in the process parameters which implies the decomposition of the macromolecules present in the straw. From Figure 3-2 (a), when the time of the reaction was increased from 30 min to 90 min, the alkali-treated fiber yield decreased. However, a further increase in treatment time to 150 min had a negligible effect on fiber yield. Likewise, from Figure 3-2 (b), a profound effect was observed as the temperature further increased from 80 °C to 95 °C where the yield decreased severely. This might be due to the cellulose was also decomposed at this treatment temperature. The increase in NaOH concentration from 2 to 6.5 (wt. %) also decreased alkali-treated fiber yield, as shown in Figure 3-2 (c), confirming the removal of non-cellulosic components from the raw TS fiber. However, a further rise in NaOH concentration had a negligible effect on cellulose yield.

There is an inverse relationship between cellulose yield and lignin removal up to a certain point, as observed in Figure 3.2. However, beyond this point, both lignin removal efficiency and yield decrease. This effect is particularly observed during higher temperature processing (>80°C). At higher temperatures, the solution becomes viscous after some time of reaction, which might reduce the contact between the lignin and the alkali. This in turn causes incomplete lignin decomposition as discussed above. However, at this reaction temperature, the cellulose structure weakens and breaks down into smaller molecules, such as sugars [178]. This reduces the overall yield of cellulose, even though some lignin is successfully removed

In conclusion, the delignification process requires balancing lignin removal with minimizing cellulose degradation. Finding the optimal temperature for a specific biomass and process is

crucial to achieve a good balance. From the responses, effective lignin decomposition (i.e. higher percentage of lignin removal) without affecting the cellulose of TS fibers was obtained in 90 min, 80 °C, and 5% of treatment time, temperature, and NaOH concentration, respectively. Further optimization study using RSM could be conducted to observe the synergistic effect between process pretreatments on the delignification efficiency of the alkali pretreatment on *Teff* straw.

3.3.3. Thermogravimetry Analysis

The characterization of cellulose is important for determining its appropriate applications. The thermal stability of cellulose samples is one of the parameters to be considered to evaluate their applicability in new formulations that require high-temperature processing, such as new composite materials. Furthermore, the thermal stability of cellulose depends on various factors, such as crystallinity, and intra/intermolecular hydrogen bonding. Those factors in turn depend upon the starting materials and processing techniques. Fundamental information regarding the thermal stability of the fibers is obtained from Thermogravimetry analysis. In this study, the TGA and DTA data of each sample (raw TS, alkali treated, and cellulose fiber) were used to determine the starting (T_{on}) temperature and the maximum degradation temperatures (T_{max}) of the samples. Figure 3-3 shows the obtained TGA and DTG curves of the raw, alkali-treated fiber and the bleached cellulose fibers from TS. The details of major thermal degradation data and the corresponding percentage of weight losses are tabulated in Table 3-3.

The thermal degradation of raw fiber shows several stages, indicating the presence of different components that decompose at different temperatures. All samples experienced a slight weight reduction between 45 and 130 °C due to the removal of moisture. As illustrated in Table 3-3, the treated fibers absorbed less moisture compared to the untreated original material. This suggests that hydrophilic substances like hemicellulose and lignin were successfully removed during the treatment process. The degradation of raw TS observed in the temperature range of 220 to 300 °C could be due to the thermal decomposition of hemicelluloses and some portions of lignin. This stage of degradation is not seen on the alkali-treated and bleached fiber. However, because of the existence of phenyl groups, the decomposition temperature of lignin occurs in a wide range below 200 °C and up to 700 °C [179].

Table 3-3 Onset temperature (T_{on}), maximum decomposition temperature (T_{max}), and corresponding percentage of weight losses of the raw, alkali treated, and bleached fiber

Sample	First thermal degradation range (°C)	WL (%)	T_{on} (°C)	T_{max} (°C)	WL_{max}, (%)
Raw TS	45-110	5.8	230	356	46.1
Alkali treated	50-130	5.2	274	371	46.2
Bleached	60-120	4.8	255	365.5	65.1

Table 3-3 reveals that raw, alkali-treated, and pure cellulose fibers primarily degrade between 260-375°C, 285-390°C, and 290-395°C, respectively. The manufactured fiber demonstrated stability up to 255°C. This thermal resilience makes cellulose suitable for various industrial uses, particularly in the plastics industry, where processing often exceeds 200°C [180]. Furthermore, the onset temperature, i.e., the temperature at which cellulose starts to degrade, for untreated TS fiber, was found to be at around 230 °C. However, the onset temperatures of the produced bleached fibers were significantly higher than that of the untreated TS fiber as shown in Table 3-3. This is a result of the removal of non-cellulosic components which degrade at lower temperatures.

Similarly, the DTG curve shows a decomposition peak for the untreated TS at 320 °C, which is the decomposition temperature for hemicellulose (Appendix A3). This peak disappeared as expected after the alkali and bleaching treatments which imply the elimination of hemicellulose from TS. Nevertheless, as presented in Table 3-3, the T_{max} of the bleached cellulose fiber is slightly lower than the alkali-treated fiber which implies the bleached cellulose fiber has lower thermal stability compared to the alkali-treated fibers. This could be due to repeated chemical treatments in the bleaching process, and the removal of the residual lignin from alkali-treated fiber after bleaching.

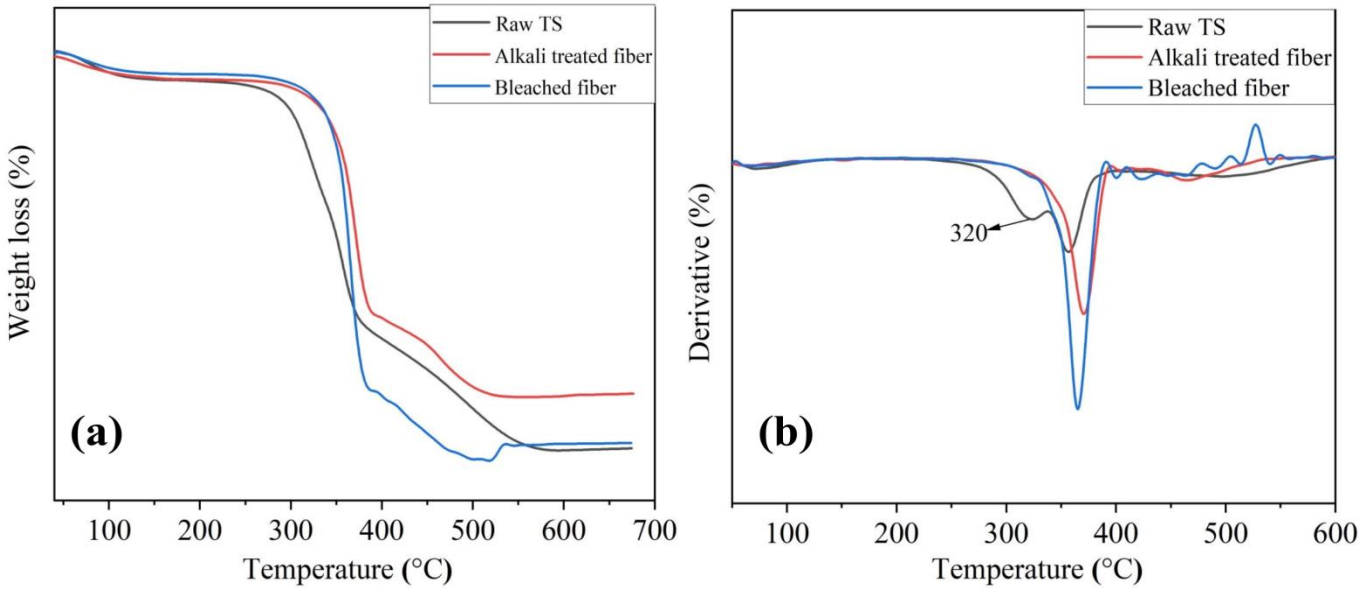

Fig. 3-3 TGA and DTG curve of TS fibers before and after treatments

3.3.4. X-ray Diffraction Analysis

Figure 3-4 shows the X-ray spectra for the raw, alkali-treated, and cellulose fibrils. All samples showed consistent crystalline structures with primary diffraction peaks at 16°, 22°, and 34° degrees. These peaks indicate a typical cellulose I crystal arrangement, corresponding to crystallographic planes of 110, 200, and 040, respectively. The miller indices were assigned to the diffraction peaks according to the recent theoretical calculations as reported in the literature (Appendix A4) [181, 182]. The intensity level at 18° is due to the amorphous component. Moreover, similar X-ray diffraction patterns for all samples demonstrated that the alkali bleaching treatment kept unchanged the crystal polymorphism of isolated cellulose.

The crystallinity index (CrI) is a parameter that measures proportion of crystalline material within a sample. The CrI value for all prepared samples was calculated using the Segal formula in Eq. (3-3), and the results are showed in Table 3-4. XRD analysis revealed a gradual enhancement in crystallinity index (CrI) following alkali and bleaching processes. In addition to this, the A diffraction peak appearing at 22° has become sharper after the treatments, which shows an increase in the crystallinity of the bleached fiber. Although the crystal structures were not altered, the CrI varied significantly among the samples due to the chemical treatment process.

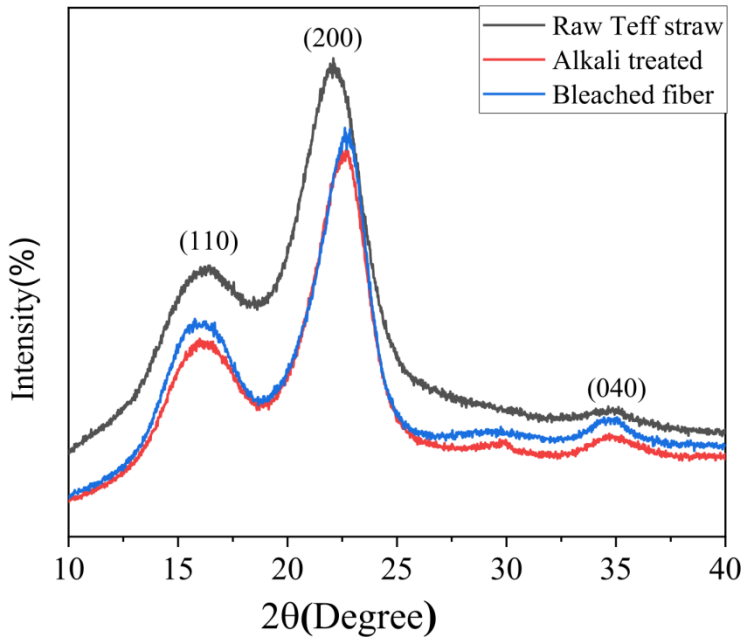

Fig. 3-4 XRD patterns for the treated and untreated TS fibers

The significant increase in CrI is caused by the extensive removal of lignin and hemicellulose, which were previously bound to the cellulose. Raw lignocellulosic material is a mix of ordered (crystalline) and disordered (amorphous) regions. In contrast, cellulose, due to its structure formed by tightly bonded glucose chains, has a highly organized, crystalline, thread-like appearance [183]. The increased crystallinity observed in the bleached sample compared to the raw material suggests that the non-cellulose substances, such as hemicellulose and lignin, which were primarily located in the disordered parts of the raw material, have been effectively removed during the bleaching process [184].

Table 3-4 Crystallinity index values of raw, alkali treated, and bleached fibers

Samples	**Crystallinity index (%)**
Raw	50.58
Alkali treated	65.48
Bleached	65.51

3.3.5. Morphology Change Analysis

The morphology of *Teff* straw fibers was examined using a scanning electron microscope both before and after processing. From Figure 3-5, there is an obvious difference between the morphologies and size of the raw, alkali-treated, and bleached TS fibers. The raw TS fibers have a rigid and smooth surface with an average diameter of 135 μm due to the lignin and hemicellulose where they shield and bind to harden and strengthen the plant cell wall (Figure 3-5a). However, the morphology of the raw TS was changed where the cell walls partially collapsed after the alkali treatment, as shown in Figure 3-5b. Moreover, the average diameter of the fiber bundles after the alkali treatment was 11 μm, which was much lower than that of the diameter of original TS fibers. This change in morphology and decrease in the diameter of the fiber indicates that NaOH can dissolve the lignin and disrupt the initial fiber structure, which causes the disaggregation of micro-fibrils from their neighboring fibers [185].

After a further bleaching treatment, the fibers are broken down in both their radial and axial directions, leading to an individualized and more uniform fiber distribution. The histogram of the size distribution for the obtained bleached fibers is presented in Figure 3- 6. The diameter of 80% of the bleached fibers falls within the 2 to 6 micrometer range centered around 4.5 micrometers. Furthermore, the final cellulose fibers showed round, fine, and long characteristics as seen in Figure 3-5c.

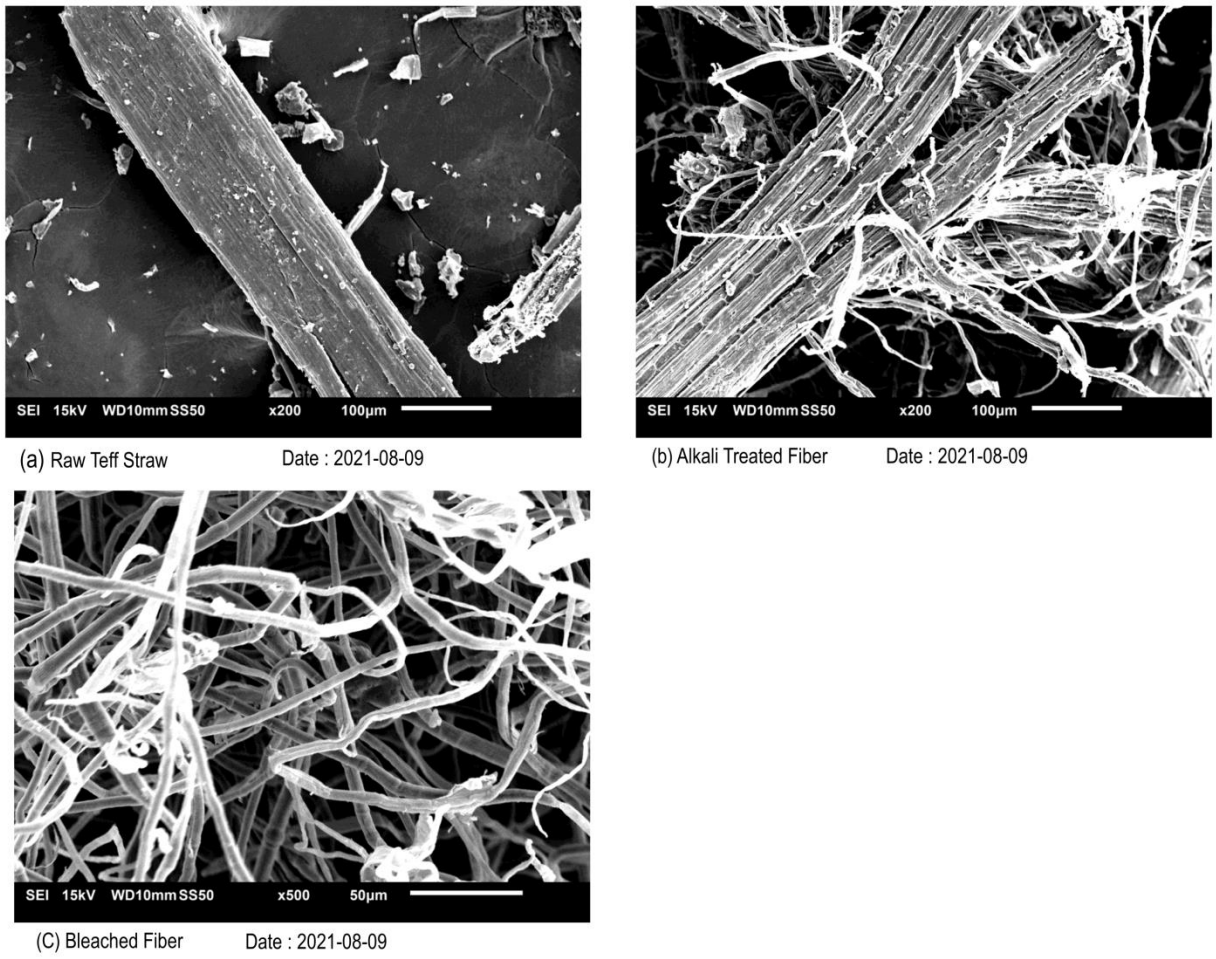

Fig. 3-5 SEM images of the raw and treated *Teff* Straw fibers

Therefore, this significant decrease in the diameter and change of *Teff* straw fiber indicates that with alkali hydrogen peroxide treatment the entire components that bind the fibers were removed, thus enabling the bundles of fibers to separate into individual fibers. The findings were consistent with the chemical and X-ray analyses, indicating the successful removal of hemicellulose and lignin binding the cellulose fibers.

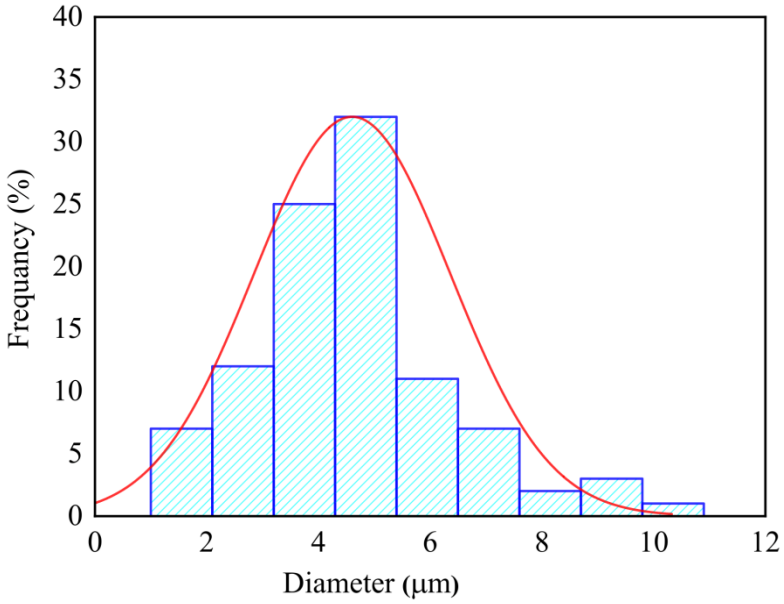

Fig. 3- 6 Size distribution analyses of bleached cellulose fibers

3.4. Conclusions

In this research, cellulose was successfully prepared from TS using alkali and bleaching treatments. Chemical examination confirmed that the bleached fiber contained a higher proportion of cellulose and a lower proportion of non-cellulose components. Furthermore, among the alkali treatment parameters, the temperature has a significant effect on fiber yield. In all samples, the XRD curves show that the crystal lattice of cellulose I was maintained while the crystallinity of TS fibers was increased from 50.58 to 65.51% after the chemical treatments. Additionally, from the TGA curve, the thermal stability of the yielded cellulose was found to be higher than that of untreated TS fiber. However, compared to the alkali-treated fiber, the thermal stability of the bleached fibers showed a slight decrease due to the repeated bleaching treatments as well as the higher lignin content on the alkali-treated fiber. Furthermore, microscopic examination of the isolated cellulose revealed distinct, elongated structures resembling rods, with an average diameter of 4.5 micrometers. Consequently, the successful extraction and analysis of cellulose from *Teff* straw in this study highlight its potential as a raw material for producing cellulose-based biofillers for polymer composites.

CHAPTER 4: TRANSITION METAL SALTS ASSISTED DILUTE ACID HYDROLYSIS FOR SYNTHESIS OF MICROCRYSTALLINE CELLULOSE FROM *TEFF STRAW*

Based on the published paper:

Assefa, E.G., Kiflie, Z. & Demsash, H.D. Transition metal salt assisted dilute acid hydrolysis for synthesis of microcrystalline cellulose from Teff Straw. Cellulose 30, 6289–6301 (2023). https://doi.org/10.1007/s10570-023-05270-0

Abstract

The application of agricultural residues for value-added products has the potential to contribute to a cleaner environment. This research aimed to examine microcrystalline cellulose extracted from *Teff* straw in a multi-step method that included alkaline treatment, alkaline hydrogen peroxide bleaching, and catalyzed dilute acid hydrolysis. FT-IR, SEM, XRD, and TGA were used to characterize changes in the chemical and physical properties of samples. FT-IR results indicated the elimination of non-cellulosic components, while the X-ray diffraction showed a significant increase in crystallinity during pretreatment and the subsequent catalyzed acid hydrolysis. The crystallinity index values for the prepared microcrystalline celluloses (Cr(III), Fe(III)Cl, and Fe(III) catalyzed MCCs) were 73.34 %, 67.58 % and 66.69 % respectively. Additionally, from the TGA analysis, the obtained MCCs showed T_{on} and T_{max} values of (285, 359), (273, 340), and (275, 335) °C for the Cr(III), Fe(III)Cl, and Fe(III) catalyzed MCCs, respectively. The results imply that $Cr(NO_3)_3$ catalyzed dilute acid hydrolysis produces MCC with the highest crystallinity and best thermal stability. The results of this study showed that TS could be used as a new source to obtain MCC. Furthermore, the preparation method used in this study could also be a preferential method over the conventional mineral acid hydrolysis.

Keywords: *Teff* straw; Pretreatment; MCC isolation; Characterization.

4.1. Introduction

Microcrystalline cellulose is a pure, white, odorless powder with a crystalline structure. It is created by breaking down the non-crystalline part of cellulose into smaller units [94]. The important characteristics of MCC make it a very promising material as a bio-filler for polymer composite materials. Recent scientific and technological research has motivated on the exploitation of agricultural residues for the extraction of MCC. Agricultural residues such as cotton stalk waste [17], tea waste [93], sugarcane bagasse [186], rice husk [96], were previously exploited for the preparation of microcrystalline cellulose.

As reported in chapter 3 , TS has a chemical composition of approximately 40, 29, and 18 wt. % of cellulose, hemicellulose, and lignin, respectively [187], showing higher cellulose content than those of corn stover (36.5), rice straw (32), wheat straw (29-35), and banana waste (13.2) [188, 189], and lower than sugarcane bagasse fibers (45) [20]. Thus, TS could be investigated as a viable alternative cellulosic material for microcrystalline cellulose production. The preparation of MCC from cellulose is mainly performed through acid hydrolysis. It produces MCC with high crystallinity index as the amorphous phase of cellulose is readily hydrolyzed when exposed to the mineral acid.

Many previous studies indicated that concentrated mineral acids have been used for the preparation of MCC from various biomass sources. Hachaichi et al.[91] extracted MCC from Palm fibers using 64 wt. % of sulphuric acid solution at 45 °C for 30 min. Asif et al.[94] also isolated MCC from Lagenaria siceraria fruit pedicles with 40% H_2SO_4 at 95 °C for 40–50 min. The acid hydrolysis method is a simple and rapid process for microcrystalline cellulose production; nevertheless, the procedure is normally associated with several restrictions, such as corrosion of equipment, the need for a large amount of water, the difficulty of acid recovery, and over-degradation of cellulose. In certain instances, scientists have utilized acid hydrolysis alongside other methods to facilitate the disintegration of cellulose. Ismail et al. [190] prepared MCC using steam-assisted acid hydrolysis from palm empty fruit bunch fiber.

Transition metal salt catalysts have been widely and effectively employed in various types of chemical reactions. They are Lewis acids and have received use as acid homogenous catalysts for the cellulose hydrolysis. Studies have shown that the metal ion catalyst speeds up the breakdown

of cellulose. It does this by making the reaction easier to initiate through a reduction in activation energy, thereby improving the overall efficiency of the process [87]. Moreover, the use of metal salts enhances the breakdown of cellulose in biomass by selectively attacking the C-O-C and C-H linkages [88]. Furthermore, the metal salts are less corrosive, show less severity conditions, and can be recovered through ultrafiltration process as compared to the strong mineral acids.

Based on literature studies, iron and chrome-based catalysts were found to contain Lewis acid sites and can perform the hydrolysis of cellulose efficiently. Lu's group has prepared nanocellulose through ultrasonication-assisted $FeCl_3$-catalyzed hydrolysis from bamboo pulp [191]. Their research findings indicate that Fe^{3+} can selectively diffuse into the amorphous regions of cellulose and promote the cleavage of glycosidic linkages of cellulose chains into smaller dimensions. Catalysts made from chromium-based metal salts have also proven exceptionally successful at breaking down the cellulose structure by severing the glycosidic bonds and disrupting the hydrogen bonding network [24, 26, 192]. Furthermore, the valence state of the transition metal ion plays a significant role in hydrolysis efficiency [193]. A greater valence state results in increased hydrogen ion generation, which plays a crucial role in accelerating the acid hydrolysis reaction in the presence of metal ions. Chen's research group studied the effect of $Fe(NO_3)_3$-, $Co(NO_3)_2$- and $Ni(NO_3)_2$-metal salts, and the results showed that crystallinity index of the prepared nanocellulose hydrolyzed with the trivalent Fe^{3+} catalyst was higher than cellulose treated by the divalent Co^{2+} and Ni^2 catalyst under same hydrolysis condition [194].

Hence in this study, iron and chrome-based metal salt with trivalent ions (Chromium (III) nitrate [$Cr(NO_3)_3$]), Iron (III) chloride [$FeCl_3$], and Iron (III) nitrate [$Fe(NO_3)_3$]) were selected as catalysts to depolymerize a pretreated *Teff* straw fiber into microcrystalline celluloses. On the other hand, during sulphuric acid hydrolysis, negative surface charges are generated on the surface hydroxyl groups of cellulose crystals which provide more stable suspensions. Hence, the presence of the acidic medium (H_2SO_4) could have a synergistic effect during the transition metal ions-catalyzed acid hydrolysis process.

Since *Teff* is cultivated on a large scale in Ethiopia, the successful preparation of MCC from this plentiful source could provide valuable crystalline cellulose material with the possibility to be used as green filler in bio-composite applications. To date, no published studies have been

reported on the preparation of microcrystalline cellulose from TS by acid hydrolysis with transition metal salt catalysts.

Thus, the objective of this study were to extract and analyze microcrystalline cellulose from *Teff* straw via transition metal salts catalyzed dilute acid hydrolysis. The effects of three trivalent transition metals salts, Chromium (III) nitrate [$Cr(NO_3)_3$]), Iron (III) chloride [$FeCl_3$], and Iron (III) nitrate [$Fe(NO_3)_3$] used as catalysts were investigated. Furthermore, changes in crystallinity, morphology, particle size and thermal properties of the obtained MCC were studied.

4.2. Materials and Methods

4.2.1. Materials

The chemical reagents used were Sulfuric acid (H_2SO_4, 98% purity), Sodium hydroxide (NaOH, 98%), Hydrogen peroxide (H_2O_2, 30%), Glacial acetic acid, Nitric acid (HNO_3, 69%), Perchloric acid ($HClO_4$, 70%), Ethanol, Chromium (III) nitrate ($Cr(NO_3)_3$, 99.5%), Iron(III) chloride ($FeCl_3$, 97%), and Iron (III) nitrate ($Fe(NO_3)_3$, 98%). All chemical reagents were of analytical grades.

4.2.2. Experimental Methods

4.2.2.1. *Pretreatment*

The pretreatment of TS was conducted mainly through a three-step process – namely hot water, alkali, and bleaching treatments, as discussed in the previous work [187]. Firstly, TS was collected from a local farm, cleaned thoroughly, sun-dried for 72 h, and milled. It was then boiled in distilled water (liquor ratio of 1:50 g/mL) at 70 °C for 2 h under constant stirring. The sample thus treated was filtered and washed with cold distilled water to remove water-soluble extractives, and left overnight for drying in a hot air oven at 60 °C. This sample was labeled as hot water-treated TS and stored in an airtight plastic bag to prevent fungal development.

The hot water-treated TS (5 g) was then treated with 150 mL of sodium hydroxide solution (5 wt. %) at 90 °C for 1.5 h under strong stirring to remove lignin and hemicelluloses from TS. The resulting sample was cooled to room temperature and filtered to separate the liquid fraction from the solid one. Following filtration, the solid material was washed using distilled water and oven-dried at 60 °C. Subsequently, bleaching treatment was done by adding the obtained alkali treated

and dried fiber in a preheated mixture of H_2O_2 (20 wt. %) and NaOH (5 wt. %) at 65 °C under continuous stirring for 1.5 h. At the end of the reaction, the sample was filtered and washed with distilled water several times until the pH became neutral. This bleaching treatment was repeated two times. Finally, the residue was dried in an oven at 60 °C until a constant weight was reached and pulverized into powder resulting in pure white colored cellulose fibers. In these alkali and bleaching treatments, the fibers to liquor ratios were kept at 1:30 (g/mL).

4.2.2.2. *Synthesis of Microcrystalline cellulose (MCC) by metal salts assisted dilute acid hydrolysis*

Microcrystalline cellulose was prepared from the pretreated TS fiber by three transition metal salt catalysts assisted dilute acid hydrolysis process. 15% sulfuric acid and 0.6 M of each catalyst (Cr $(NO_3)_3$, $FeCl_3$, and Fe $(NO_3)_3$) were mixed separately at a ratio of 1:1 (v/v), to obtain three types of dilute acid solutions. Then, 5 g of pretreated TS sample was added to the prepared mixed acid solution at solid cellulose to liquor ratio of 1:40 g/mL. The hydrolysis was performed in an atlas reactor at 60 °C for 1.5 h to hydrolyze the amorphous domains of the obtained cellulose fibers. Following the completion of the hydrolysis, the suspension was diluted with excess (100 ml) cold distilled water to stop the reaction. This suspension was then filtered and washed using distilled water repeatedly until neutral pH was achieved. Finally, the sample was dried at 50 °C in a vacuum oven to constant weight and pulverized to powder using a high-speed universal disintegrator (FW100, China). Figure 4-1 shows the process flow diagram for the isolation of microcrystalline cellulose from TS. The raw, pretreated and the obtained products are labeled as Raw - TS, Pretreated - TS, Cr (III) - MCC, Fe(III)Cl - MCC, and Fe(III) – MCC, respectively where the obtained MCC are labeled depending on the type of catalyst used during the extraction.

The yield (%) of microcrystalline cellulose was estimated gravimetrically based on its dry weight before and after the MCC synthesis according to Eq. (4-1) below:

$$yield_{MCCs}(\%) = \frac{M_{MCCs}}{M_{\text{Pr}etreated\ TS}} * 100 \qquad (4-1)$$

Where M_{MCCs} is the dry mass of the obtained microcrystalline celluloses, and $M_{Pretreated\ TS}$ is the dry mass of the pre-treated *Teff* straw residue.

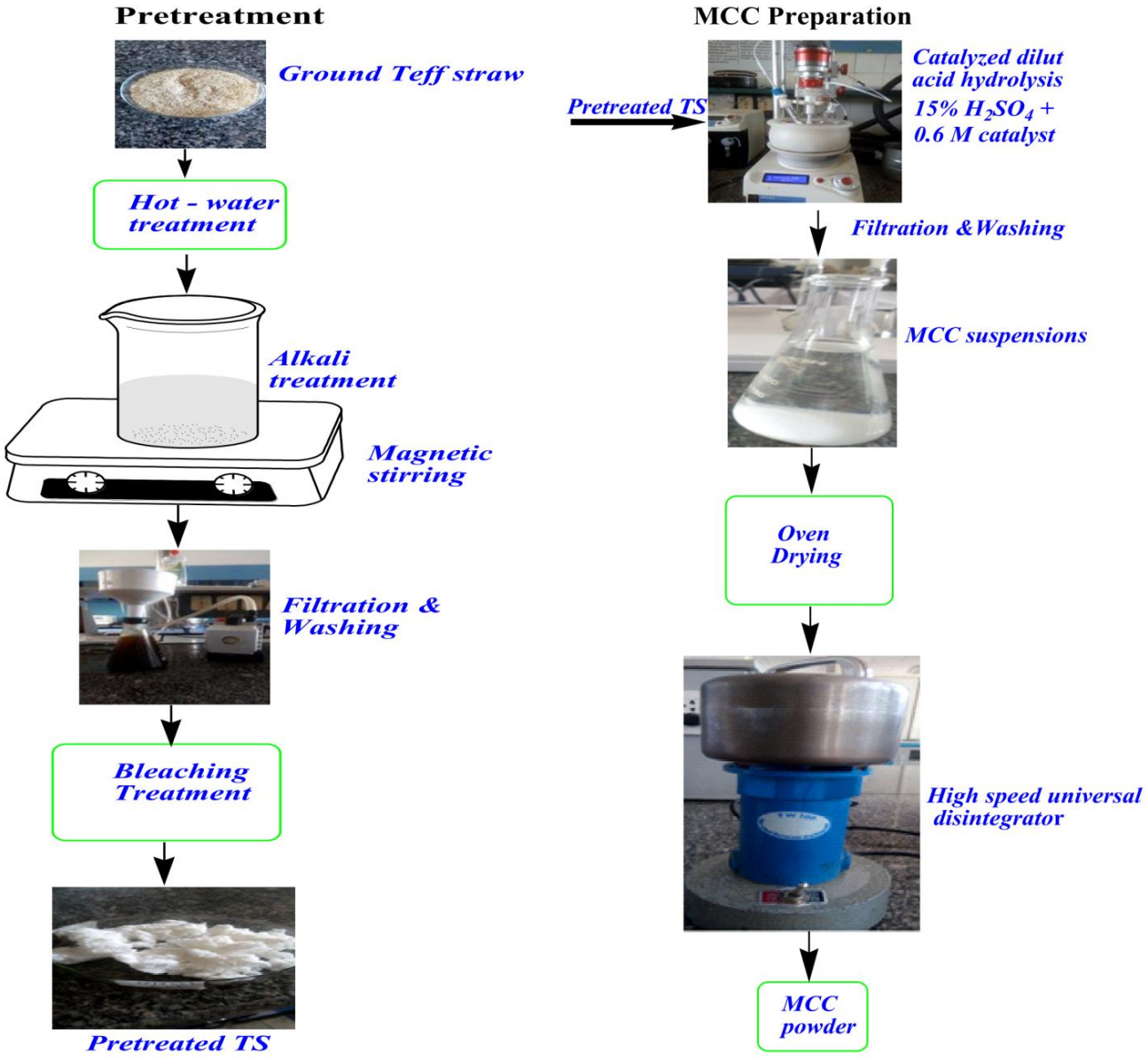

Fig. 4-1 Schematic representation for the isolation of MCC fiber from TS via catalyzed dilute acid hydrolysis

4.2.2.3. *Composition Analysis*

The detail of the chemical composition determination of the raw and pretreated TS fiber was presented in the previous work [187]. The amount of extractives was calculated by water/alcohol

extraction method using the NREL/TP-510-42619 method [165]. Whereas, inorganic material (ash) amount was determined by placing a measured sample in a furnace at 575 °C based on the NREL/TP-510-42622 procedure [164]. For lignin content determination, a two-step acid hydrolysis based on NREL/TP-510-42618, method was used [166]. Similarly, cellulose content was determined by hydrolyzing with a mixture of nitric acid and ethanol according to the Kurschner-Hoffer gravimetrical method [167]. Finally, the hemicellulose percentage of TS (% w/w) was determined indirectly by subtracting the combined weight percentages of extractives, lignin, cellulose, and ash from the total weight.

4.2.2.4. *Microcrystalline cellulose characterization*

The types of chemical groups in the samples were determined using Fourier Transform Infrared Spectroscopy (FT-IR, JASCO FT/IR- 6600) analysis. The spectra were recorded between 500 and 4000 cm^{-1}rs with a precision of 4 cm^{-1}. The X-ray diffraction profiles of the different samples were obtained using an X-ray diffractometer (D2 phaser, Bruker, Germany) with CuKα radiation (λ = 0.15406 nm), and operated at 30 kV and 10 mA. The samples were analyzed using X-ray diffraction at room temperature within an angle range of 10 to 40 °, gradually increasing the angle at a steady pace of 1°/min. The resulting data was used to determine the crystallinity of the samples following a standardized method outlined by Segal and colleagues [169].

$$CrI\left(\%\right)=\frac{I_{200}-I_{am}}{I_{200}}*100 \qquad (4-2)$$

Where *CrI* is the relative degree of crystallinity, I_{200} represents to the highest peak intensity at the lattice diffraction (200) of the crystalline regions and I_{am} is the minimum value between planar reflections (200) and (110), which refers to reflection intensity of the amorphous parts of the samples.

The average crystallite size (D) of the microcrystalline cellulose fibers was estimated using Scherer equation [195].

$$D=\frac{\kappa\lambda}{\beta cos\theta} \qquad (4-3)$$

Where κ is a Scherrer constant (0.89), λ= is the x-ray wavelength of the radiation which is constant (λ = 0.15406 nm), β = full width at half-max of the XRD peak, and θ is diffraction angle in radians.

Thermogravimetric analysis of the raw TS, pretreated TS fiber, and the microcrystalline cellulose prepared by three different catalysts was examined using a thermal analyzer (HCT-1, BJHENVEN, China) to determine the thermal decomposition of fibers in the temperature range of 20-700 °C at a constant heating rate of 20 °C/ min under a nitrogen environment. The surface morphologies were analyzed using scanning electron microscope (JEOL JSM-IT 100, Japan).

The AAS used for the analysis of the metals was PG Instruments (AA500 spectrophotometer, England) equipped with deuterium lamps and hollow cathode lamps with air-acetylene flame. The wavelength was set at 357.9 and 248.3 nm for chrome (Cr (III)) and iron (Fe (III)) concentration determination, respectively. Such technique of elemental analysis requires aqueous samples. Thus, solid samples were converted into solutions. Nitric– perchloric acid sample digestion method was used for the dissolution of MCCs samples as described elsewhere [196].

Briefly, 0.5 grams of samples were weighed and mixed with 5 ml of concentrated HNO_3 in a 125 ml Erlenmeyer flask. The mixture was boiled on a hot plate for 40 min. After cooling, 2.5 ml of 70% $HClO_4$ was added and the mixture was boiled until dense white fumes appeared. After cooling and filtration, the solution was transferred quantitatively into a 50 mL volumetric flask for analysis.

4.3. Results and Discussion

4.3.1. Chemical Compositions Analysis

In a previous study [187], the chemical compositions of the raw TS was investigated and the results showed that the raw fibers contained 40 % cellulose, 29 % hemicellulose, and 18 wt.% lignin. However, the chemical composition of raw TS was changed after the chemical treatments. The cellulose amount raised from 40 to 68.5 wt. % while, hemicellulose and lignin contents were reduced to 21 and 7 wt. %, respectively after the alkali treatment. The significant decrease in lignin content from the raw TS was due to the disruption and breaking of hydrogen bonds through NaOH treatments. To further eliminate the residual lignin, the NaOH-treated samples were subjected to a hydrogen peroxide treatment at alkaline conditions where the celluloses content was further increased to 85.5 wt. % with lignin and hemicellulose contents of 2.5 and 12 wt. %, respectively. Furthermore, the obtained pretreated fiber was pure white suggesting the elimination of most of the non-cellulosic components from the TS (Figure 4-1).

4.3.2. FTIR Analysis

Figure 4-2 presents the FTIR spectra of the raw TS, pretreated fibers, and microcrystalline cellulose isolated by catalyzed diluted acid hydrolysis. The figure clearly shows that all samples exhibit similar peaks at 3410, 2900, 1430, 1382, and 890 cm^{-1} which are related to the cellulose I characteristic absorption peaks. As reported elsewhere [197], the peak at around 3400 cm^{-1} is characteristic of the O-H stretching intermolecular hydrogen bonds; while the peak at 2900 cm^{-1} corresponds to the C-H symmetrical stretching group present in the carbohydrates of cellulose. Likewise, the typical spectral bands observed at 1430, and 897 cm^{-1} are attributed to the symmetric bending of CH_2 and β-glycosidic linkages between glucose units of cellulose, respectively. In addition, the vibration peak detected at 1382 cm^{-1} in all samples has been associated with the C–H bending in the cellulose. Furthermore, a peak at around 1644 cm^{-1} which is attributed to the O–H bending due to water adsorbed in the fibers is observed in all samples. The fact that the cellulose I characteristic peaks remain in the MCCs indicates that the pretreatment and the hydrolysis processes have not changed the main chemical structure of cellulose [182].

However, in the FTIR spectra of the raw TS fiber, there appear some peaks that are not observed in the spectra of the pretreated fiber and synthesized MCCs. These include the peak at 1730 cm^{-1} which correspond to C-O stretching vibration for the acetyl and ester linkages in lignin and hemicellulose, and the peaks at 1502 and 1250 cm^{-1} which are attributed to the C=C stretching vibrations of the aromatic rings and C–O out-of-plane stretching due to the aryl group in lignin, respectively [198]. Presumably, the disappearance of these absorption peaks in the FTIR spectra of pretreated fiber and synthesized MCCs is related to the successful removal of lignin and hemicellulose as a result of the pretreatment and catalyzed dilute acid hydrolysis processes. This observation is in agreement with similar investigations reported in the literature [195].

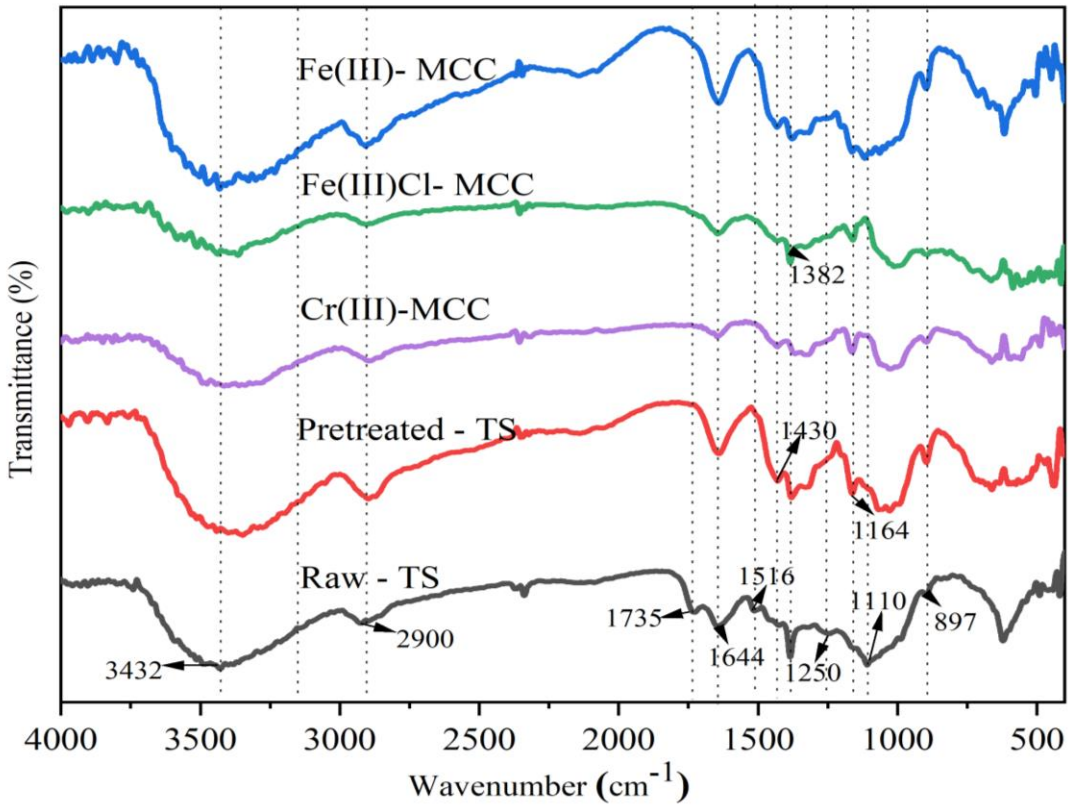

Fig. 4-2 FTIR spectrum of (a) *Teff* Straw, (b) chemically purified cellulose, and (c) the obtained MCCs

Furthermore, a peak at 1110 cm^{-1}, which is associated with the C–O-C stretching of hemicellulose, is observed in the FTIR spectra of the raw TS indicating the presence of hemicellulose. However, this peak gradually disappeared in the isolated MCC spectra, suggesting

that hemicellulose was successfully removed because of hydrolysis. On the contrary, the peaks at 1164 and 897 cm^{-1} which are attributed with the C-O-C stretching of cellulose and C–H deformation of glycosidic linkages between glucose units in cellulose [199], have increased in intensity after the pretreatment and catalyzed dilute acid hydrolysis of TS.

Overall, The FTIR spectra of our samples match the typical patterns found in other lignocellulosic materials as described in previous studies.

4.3.3. Thermogravimetry Analysis (TGA)

Understanding how well microcrystalline cellulose withstands heat is crucial for deciding if it can be used to strengthen bio-composites. The thermal degradation characteristics of the untreated TS, pretreated fiber and the prepared microcrystals are presented in Figure 4-3. The degradation onset temperature (T_{on}), the maximum degradation temperature (T_{max}), and the maximum weight loss (WL_{max}) for raw, pretreated TS, and obtained MCCs are summarized in Table 4-1.

Figure 4-3 illustrated an initial small mass loss in the temperature range of 45–120 °C which may be due to the evaporation and removal of bound water and loss of extractives existing in the fibers. This is in agreement with the FTIR analyses results which indicate the presence of absorbed water in the fibers. Furthermore, when examining weight loss in this specific area across various samples, the MCC samples consistently experienced less weight reduction compared to the untreated raw TS. This suggests that the MCCs contained slightly less moisture than the raw TS fibers. This difference might be attributed to the addition of sulfate groups to the MCCs' outer layer during the acid treatment process.

The second degradation occurs between 250 and 320 °C, primarily due to the thermal breakdown of hemicellulose and a portion of lignin. The presence of acetyl groups might have made hemicellulose more susceptible to thermal degradation than cellulose. The thermal decomposition peak for hemicellulose which is shown on the DTG graph of the raw TS has disappeared, as expected, in the prepared MCCs.

Table 4-1 Onset temperature (T_{on}), maximum decomposition temperature (T_{max}), and corresponding percentage of weight losses of the raw, pretreated fiber, and obtained MCCs

Sample	**Code**	**First thermal degradation range (°C)**	**WL (%)**	**T_{on} (°C)**	**DTG T_{max} (°C)**	**WL_{max} (%)**
Raw fiber	Raw – TS	45-110	5.8	230	356	46.1
Pretreated TS	Pretreated – TS	60-120	4.8	255	365.5	65.1
$Cr(NO_3)_3$ treated	Cr(III) – MCC	56-106	5.01	285	359	73.52
$FeCl_3$ treated	Fe(III)Cl – MCC	50-110	3.89	273	340	67.45
$Fe(NO_3)_3$ treated	Fe(III) - MCC	56-107	4.76	275	335	72.27

The final and most substantial phase of decomposition occurs between 300 and 390 °C. This is attributed to the breakdown of cellulose into its individual sugar components. From the TGA analysis, the T_{on} values of TS, Cr(III) - MCC, Fe(III)Cl - MCC, and Fe(III) - MCC were 230, 285, 273, and 275 °C, respectively (Table 4-1). The observed increase in the T_{on} of MCCs might be a result of the elimination of hemicellulose and lignin components which were present in the raw TS. The hemicellulose and lignin components had low thermal degradation temperatures, and the degradation of one of these components could initiate the thermal degradation of the surrounding cellulose fibers [200].

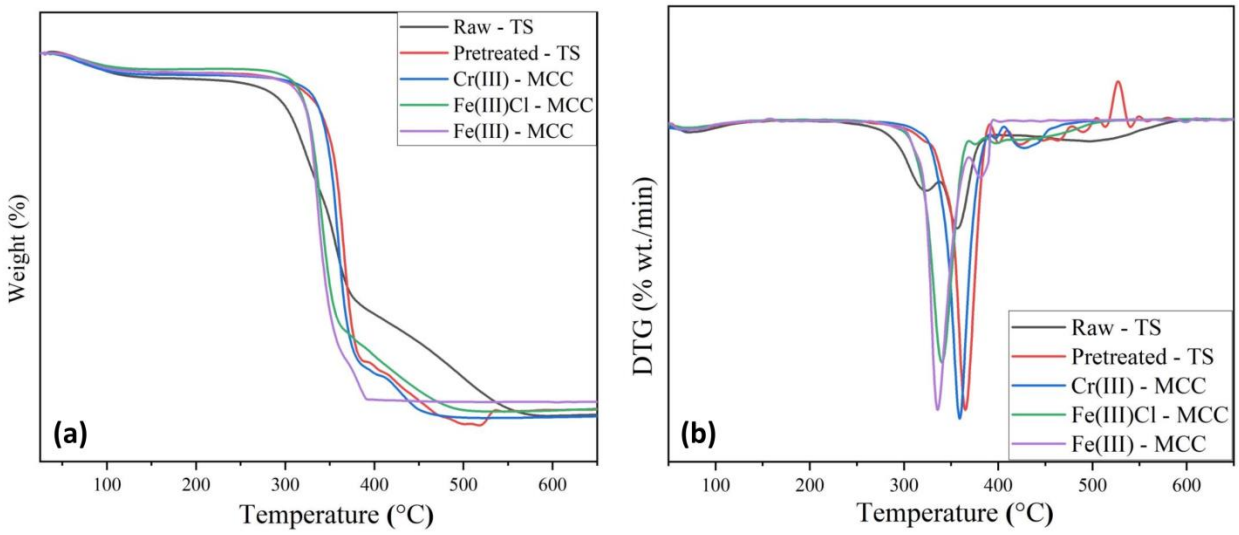

Fig. 4-3 TGA and DTG curve of raw TS fibers, pretreated TS fiber and the prepared MCCs

The higher T_{on} values of the MCCs show the higher thermal stability of these fibers. However, it is worth to note that the Cr $(NO_3)_3$ catalyzed and extracted MCC has exhibited the highest T_{on} value of 285 °C, which is 55 °C higher than that of the raw TS.

Furthermore, in the same high temperature degradation range, differences in maximum degradation temperatures (T_{max}) are observed among the different samples. In this regard, the pretreated cellulose fiber shows a higher maximum degradation temperature (T_{max}) than the MCCs (Table 4-1). This might be related to the smaller particle sizes of the MCCs (increase in specific surface area) which have facilitated the thermal degradation to occur at lower temperatures [201, 202]. Fe $(NO_3)_3$ - treated microcrystalline cellulose exhibited the lowest T_{max} value of 335.0 °C, which was 21.0 °C lower than that of raw TS.

Overall, the higher thermal stability (higher T_{on} and T_{max} values) of the isolated MCC could be attributed to the higher crystallinity of the obtained MCC as well as to the removal of hemicellulose and lignin from these fibers [27, 203]. These results are highly consistent with the information provided by XRD and FTIR spectroscopic techniques. Therefore, from the TGA, it can be concluded that MCCs prepared from TS by using transmission metal salts assisted dilute sulfuric acid hydrolysis exhibit higher thermal stability. The high processing temperatures typically required for thermoplastics (above 200 °C) make the stability of these MCCs crucial for their industrial applications [201].

4.3.4. X-Ray Diffraction Analyses (XRD)

The crystalline structure of cellulose is a result of its molecules being held closely together by powerful hydrogen bonds and weaker Van der Waals forces [50]. This property makes it different from other components in the lignocellulosic biomass. Moreover, the crystallinity of the extracted microcrystalline cellulose has a direct influence on the strength of biocomposite materials with MCC as fillers [204]. However, since the crystallinity and the size of the crystallites of MCC could be affected during the MCC isolation processes, X-ray Diffraction analyses were conducted to observe the crystalline behavior of the three MCCs obtained from TS.

Figure 4-4 shows the X-ray diffraction patterns for the samples studied. The XRD patterns in this figure reveal that all samples exhibit the three distinct peaks of cellulose at 2θ values of 16.3°, 22.4°, and 34.5°, confirming that the cellulose-I allomorph is well-maintained after the dilute acid hydrolysis process [199, 205].

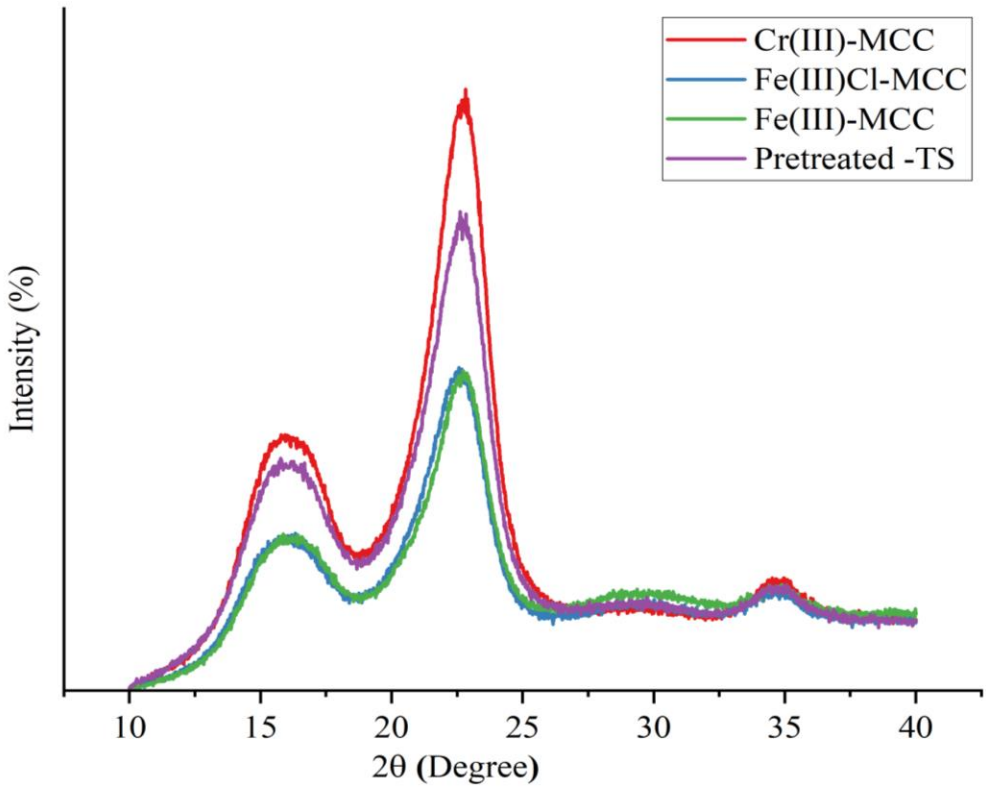

Fig. 4-4 XRD diffraction patterns of pretreated TS fibers, and the prepared microcrystalline celluloses

Further information can also be obtained from the CrI and the average crystallite sizes as presented in Table 4-2. As can be observed from this table, all treated samples (PTS, Cr(III)–MCC, Fe(III)Cl-MCC and Fe(III)-MCC) show significant increases in the CrI values with respect to raw TS. As CrI measures the proportion of crystalline substance in a sample, the results suggest that the MCCs contain a higher percentage of crystalline material. Similar findings have been reported elsewhere [195]. Table 4-2 also shows that the MCCs have higher yield, and larger crystallite sizes as compared to the raw TS.

Table 4-2 Crystallinity index values and Crystallite size of raw TS, pretreated TS fiber, and obtained MCCs

Sample	**Code**	**Yield (%)**	**Crystallinity index (%)**	**Crystallite size (D=nm)**
Raw TS	Raw-TS	------	50.58	1.03
Pretreated TS	Pretreated – TS	------	65.51	2.99
$Cr(NO_3)_3$ treated	Cr(III) – MCC	84	73.69	3.14
$FeCl_3$ treated	Fe(III)Cl - MCC	82	67.58	2.72
$Fe(NO_3)_3$ treated	Fe(III) - MCC	76	66.69	2.83

This was primarily resulted from the elimination of lignin and hemicellulose, alignment of the crystalline domains into more ordered conformation, and subsequent release of individual crystallites in the MCC samples [24, 192]. Among the prepared microcrystalline celluloses, Cr (III)-MCC sample shows higher crystallinity (Table 4-2) as compared to Fe (III)Cl - MCC and Fe(III) - MCC samples which suggests Cr (III) ion was more effective for selective hydrolysis of the amorphous region of the fiber. In addition to the CrI, the crystallite size is also supportive for the description of crystallinity of the yielded microcrystalline celluloses. From Table 4-2, the crystal size of the isolated microcrystalline celluloses, Cr(III) - MCC, Fe(III)Cl – MCC, and Fe(III) - MCC calculated by Scherer equation (eq. 4-3) was found to be 3.14, 2.72, and 2.83 nm, respectively. Comparable results for MCCs isolated from coconut husk fiber and rice husk have been documented in previous research [206].

4.3.5. Morphological Investigation

Figure 4-5 shows SEM images of the raw pulverized TS (a), the alkali treated fiber (b), the pretreated fiber following the elimination of lignin and hemicellulose (c) and finally, the microcrystalline cellulose isolated by transition metal salts catalyzed dilute acid hydrolysis of the pretreated fiber (d, e, and f). SEM analysis revealed substantial alterations in shape and size following the treatment. The morphology of the raw TS fiber (Figure 4-5 (a)) had a regularly arranged, homogenous structure, and bound closely together because of the binding materials around the cellulose fibrils such as hemicellulose, lignin, and other none cellulosic components which help in the formation of compact structure [207].

Furthermore, the raw TS fiber's surface, as depicted in Figure 4-5(a), appeared smooth because of the wax and oil coating. After subsequent alkali and bleaching treatments, defibrillation of the raw TS fibers occurred whereby the diameter of the resulting fibrils significantly decreasing because of the removal of the binding materials. Thus, the bleaching process makes it suitable for the subsequent acid hydrolysis process to produce MCC.

Additionally, as can be observed in Figure 4-5(c), the resulting pretreated fiber was long in length. This is due to the fact that natural cellulose fibers are composed of multiple, tiny microfibers bundled together. With further acid hydrolysis treatment, the transition metal, and the hydronium ions generated during the hydrolysis had broken down the fibers into smaller pieces and further reduction of its diameter. Figures 5(d), (e), and (f) shows a SEM image of the MCC fibers (Cr (III) - MCC, Fe (III) – MCC, and Fe(III)Cl - MCC), respectively. Additionally, the average diameter for TS, and microcrystalline celluloses (Cr (III) - MCC, Fe (III) – MCC, and Fe(III)Cl – MCC) measured using the ImageJ software was 135.7, 3.67, 5.08, and 4.97 μm, respectively proving that the average diameter of fibers was tremendously reduced throughout the chemical processes.

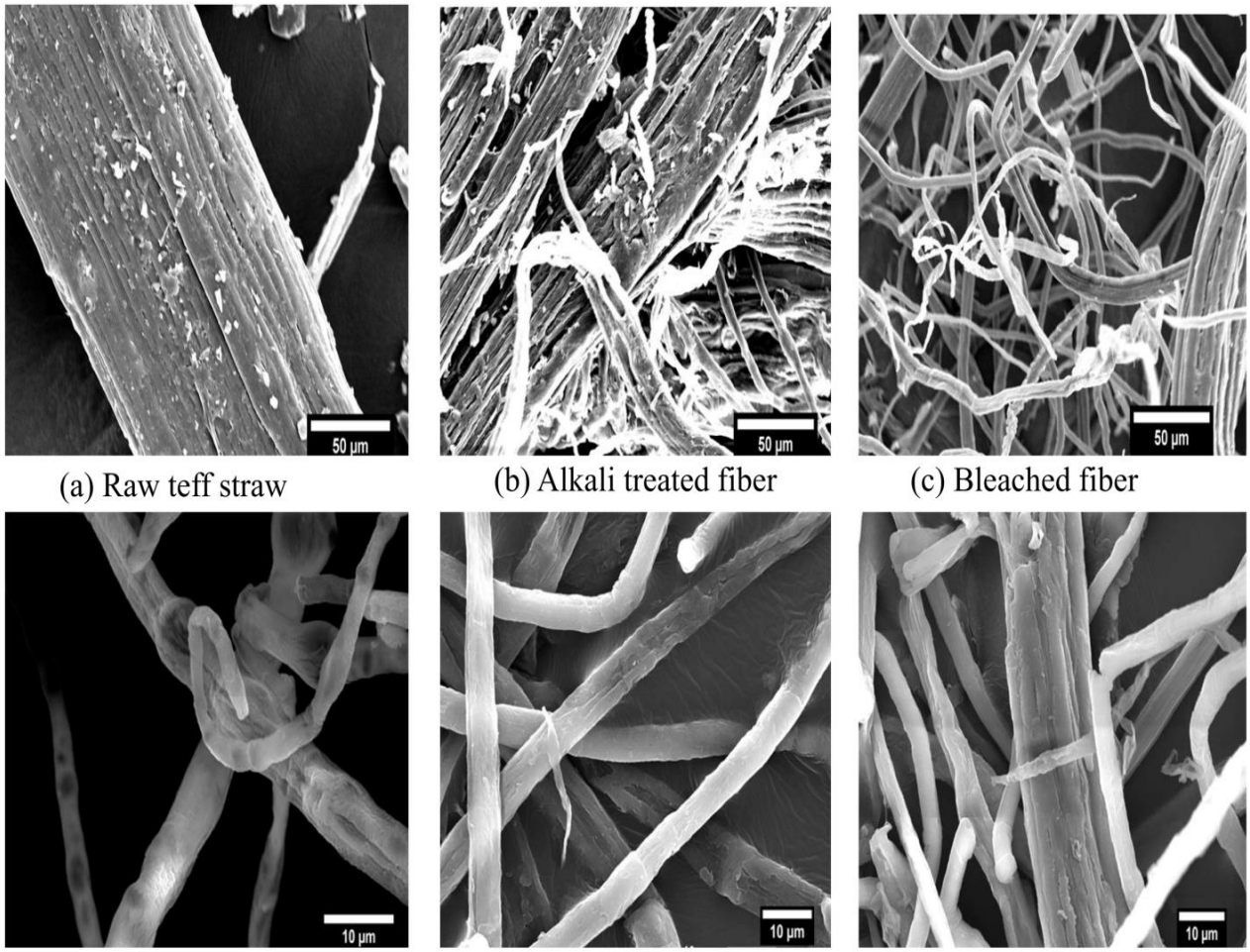

[1]

Fig. 4-5 SEM morphologies of the raw TS fibers, pretreated TS fibers, and prepared microcrystalline celluloses

[1] The obtained MCCs are labeled depending on the type of catalyst used during the extraction process:

- Cr(III) – MCC: MCC obtained after treating pretreated teff straw fibers using Cr(NO3)3 catalyzed dilute acid hydrolysis.
- Fe(III)Cl – MCC: MCC obtained after treating pretreated teff straw fibers using FeCl3 dilute acid hydrolysis.
- Fe(III) - MCC: MCC obtained after treating pretreated teff straw fibers using Fe(NO3)3 dilute acid hydrolysis.

4.3.6. Atomic Absorption Spectrometer (AAS) Analysis

Atomic absorption spectroscopy (AAS) analysis was applied to investigate the presence of chrome (Cr (III)) and iron (Fe (III)) ions in the prepared MCCs. Before the determination of chromium and iron in the real sample, four series of standard chromium and iron solutions in different concentrations were prepared. After determining the absorbance for all the standard solutions, a calibration curve was constructed (Appendix B1). The absorbance of the prepared samples was then compared against the calibration to obtain the corresponding concentrations. The levels of metal ions in each MCC samples were presented in Table 4-3 below.

Table 4-3 Elemental analysis for the prepared MCC samples using AAS

Samples	**Code**	**Metal ion**	**Concentration (ppm)**
$Cr(NO_3)_3$ treated	Cr(III) – MCC	Cr(III)	0.348
$FeCl_3$ treated	Fe(III)Cl - MCC	Fe(III)	1.144
$Fe(NO_3)_3$ treated	Fe(III) - MCC	Fe(III)	0.865

The prepared MCCs are intended to be used as a biofiller in the creation of bio-composites for packaging purposes. European Union(EU) and United States(USA) sets out a maximum limit of 100 ppm for heavy metals or their compounds in packaging or a packaging component [208, 209]. This implies that the results of this study (Table 4-3) were much lower than the maximum permissible limit set by the EU and USA. In conclusion, the metal ion contamination in the synthesized MCCs was significantly reduced through efficient washing post-hydrolysis.

4.4. Conclusions

Microcrystalline cellulose was successfully prepared from an abundant and low-cost Ethiopian *Teff* straw via alkali and bleaching pretreatments followed by transition metal salts catalyzed dilute acid hydrolysis. Each transition metal catalyst showed different effects on the crystallinity, crystallite size, surface morphology, and thermal stability of the obtained microcrystalline cellulose. Microscopic observation showed the influence of chemical processes on the surface of the TS. The XRD and TGA analyses respectively showed that the MCCs have higher crystallinity and thermal stability, respectively. Among the prepared MCCs, the Cr(III) ions synthesized MCC rendered relatively the highest crystallinity and thermal stability, reflecting its better hydrolysis selectivity as compared to Fe(III)Cl and Fe(III) - metal ions. Furthermore, all MCCs exhibited degradation temperatures higher than typical processing temperatures of polymeric materials, making them suitable for the preparation of polymer-based bio-composite materials. Thus, it can be said that the method followed in this work has been successful in extracting MCCs from TS and the obtained MCCs can be used as green and sustainable fillers in bio-composite materials preparation.

CHAPTER 5: EFFECT OF *TEFF* STRAW (*ERAGROSTIS TEF*) BASED MICROCRYSTALLINE CELLULOSE ON ENHANCEMENT OF THERMO-MECHANICAL AND MICROSTRUCTURAL PROPERTIES OF PVA BIO-DEGRADABLE POLYMERS

Based on the published paper:

Assefa, E. G., Kiflie, Z., Demsash, H. D., & Habtu, N. G. (2024). Effect of Teff Straw (Eragrostis Tef) Based Microcrystalline Cellulose on Enhancement of Thermo-Mechanical and Microstructural Properties of PVA Bio-Degradable Polymers. Waste and Biomass Valorization, 1-12. https://doi.org/10.1007/s12649-024-02553-w

Abstract

This study investigated the potential of microcrystalline cellulose fibers, extracted from *Teff* straw using a chemical treatment with metal catalysts, as reinforcement for polyvinyl alcohol films. The effects of MCC type (derived from different metal catalysts) and loading (0, 2, 5, and 8 wt. %) on the physico-mechanical properties (including thermal stability) of PVA films, were investigated. The incorporation of MCCs significantly improved the films' mechanical strength. Compared to neat PVA, the tensile strength increased by up to 49%, 71%, and 67% when incorporating Cr(III)-MCC, Fe(III)Cl-MCC, and Fe(III)-MCC, respectively, at a 5% loading level. The thermal stability of the PVA/MCC composites also improved, with a higher onset degradation temperature compared to neat PVA. For instance, The T_{on} for the neat PVA, Cr(III)-MCC, Fe(III)Cl-MCC, and Fe(III)-MCC-based PVA films were 295, 305, 308, and 303 °C at a level of 5% MCC content, respectively. Scanning electron microscopy (SEM) analysis revealed good dispersion of MCC fibers within the PVA matrix, indicating strong interaction between the materials. Overall, TS MCCs show promise as low-cost, bio-based reinforcement for producing biodegradable films with enhanced mechanical properties and thermal stability, making them suitable for various applications like food packaging.

Keywords: *Teff straw*; microcrystalline cellulose; biodegradable films; polyvinyl alcohol; characterization

5.1. Introduction

The environmental concerns associated with polymeric waste management have led to academic research into the development of green composites for applications that currently use synthetic polymers. Although biodegradable polymers address environmental concerns, they have drawbacks in terms of their performance, such as difficulty in withstanding heat, barrier properties, and mechanical strength. Many approaches with different reinforcing fillers have been considered to improve the physical characteristics of biopolymers. For instance, adding bio-fillers to polylactic acid (PLA) not only makes the resulting material fully biodegradable but also substantially enhances its physical and thermal properties [210, 211]. Gbadeyan et al.[210] investigated the use of bio-nano calcium carbonate as a filler to reinforce a PLA biopolymer matrix. Here it is reported that the obtained PLA with nano-$CaCO_3$ showed enhanced properties than pure PLA films.

Polyvinyl alcohol is a semi-crystalline and non-toxic polymer that is a good candidate for the production of green composites. Furthermore, PVA shows excellent film-forming properties due to the presence of hydroxyl groups. However, it has limitations such as low mechanical properties and poor thermal stability. To use PVA in the packaging industry, these must be significantly enhanced without damaging its valuable properties. A wide range of reinforcing filler materials, including cellulose, clay, graphene oxide, carbon nanoparticles, and polypropylene fibers, have been demonstrated to effectively improve the mechanical and thermal properties of PVA [212–216]. Recently, Gbadeyan et al. [217] optimized the concentration of PVA, cellulose nanocrystals (CNC), and snail shell nanoparticles (SSN) for the development of enhanced PVA-based bio-plastic films.

Researchers are exploring the potential of agricultural residues by transforming them into valuable products, particularly biodegradable composites. Tan et al. [131] prepared PVA composite films reinforced with oil palm cellulose fiber. Tan and colleagues found that combining cellulose with PVA to create films resulted in materials that are stronger, better at preventing moisture loss, more heat resistant, and less transparent than films made solely from PVA. Santi et al. [123] used commercial microcrystalline cellulose and found that the PVA/MCC composite exhibited a good stress–strain behavior. They also noticed a close correlation between

MCC content on tensile, thermal, and degradation properties. Likewise, according to Spagnol and colleagues [126] , the addition of cellulose nanocrystals enhanced the tensile strength of PVA by as much as 33% and its elastic modulus by up to 140%. The extent of these improvements varied based on the nanocrystals' chemical composition and concentration. The characteristics of MCC-reinforced PVA composites can change depending on the source of the MCC and the isolation method used.

As mentioned earlier, in Ethiopia, the agricultural sector produces millions of tons of agricultural residues each year. *Teff* straw, in particular, is abundant, affordable, and a readily available agricultural residue. MCC was successfully isolated and characterized from TS using a chlorine-free bleaching process and transmission metal salts catalyzed dilute acid hydrolysis [187, 218]. MCCs derived from *Teff* Straw exhibit strong crystalline structure and resistance to heat, making them ideal for producing composite films. To the best of our knowledge, no investigations have been carried out on the thermal stability and mechanical strength of *Teff* straw MCC based PVA composite films. Thus, an overarching goal of this study is to develop a composite film of PVA reinforced with MCC obtained from *Teff* straw via transmission metal salts catalyzed dilute acid hydrolysis method.

The PVA/MCC composite films were prepared by solution casting technique. The solution casting technique is a very easy and inexpensive method to develop films. Moreover, this method helps to control thickness uniformity, dispersion of additives, and obtain maximum optical purity. Previously different researchers investigated varying MCC content from different raw materials and the highest tensile strength of the composite obtained was at 7.5% MCC [90], 1% MCC [132], and 2.5% cellulose fiber [131]. Those results showed that at lower MCC content, the mechanical and thermal properties of MCC-PVA composites improved successfully. Hence, in this study 2, 5 and 8 wt. % MCC content (relative to PVA dry wt.) were used to prepare the PVA/MCC biodegradable composite film. Moreover, PVA film without MCC was prepared for control.

Subsequently, the physical and chemical characteristics of the *Teff* straw PVA/MCC composite films were examined. In particular, the researchers focused on how the amount and type of MCC affected the composite’s mechanical properties. This was assessed by measuring the composite’s tensile strength, stiffness, and flexibility.

5.2. Materials and Methods

5.2.1. Materials and chemicals

Sodium hydroxide (NaOH, 98%) and hydrogen peroxide (H_2O_2, 30%) from Uni-chem Chemical Reagents were used to pretreat the raw TS. Sulfuric acid (H_2SO_4, 98%), also from Uni-chem Chemical Reagents, was used during the MCC preparation process. Chromium (III) nitrate ($Cr(NO_3)_3$, 99.5%, Uni-chem Chemical Reagents), iron (III) chloride ($FeCl_3$, 97%, Alpha-Chemika, India), and iron (III) nitrate ($Fe(NO_3)_3$, 98%, Research-Lab Fine Chemical Industries, India) served as catalysts during the MCC preparation. Poly (vinyl alcohol) with a purity exceeding 95% was purchased from a chemical supplier in Addis Ababa, Ethiopia, for use as the polymer matrix.

5.2.2. Experimental Methods

5.2.2.1. *Pretreatment of Teff straw*

The pretreatment and isolation of microcrystalline cellulose from TS was carried out as described in the previous works [187, 218]. *Teff* straw was washed thoroughly and then sun dried. The dried TS was ground and screened. The portion between 250 µm and 850 µm sieve size was then used for the next experiment. Initially, the cleaned and milled TS was treated with hot water under stirring at a liquor ratio of 1:50 g/mL and 70 °C for 120 min to remove the water soluble extractives. The resulting slurry was filtered and washed with distilled water followed by drying in the oven at 60 °C. Alkaline treatment of the hot water treated TS fibers was performed using a 5 wt. % NaOH solution at 80 °C for 90 min under continuous stirring to remove lignin. The resulting fibers were then filtered, washed, and dried in an air circulating oven at 60 °C to constant weight.

The dried fibers were further processed by an environmentally friendly bleaching method. This involved, mixing the fibers with a hot solution containing hydrogen peroxide (20 wt. %) and sodium hydroxide (5 wt. %) to eliminate hemicellulose and leftover lignin. This process was conducted at a constant temperature of 65 °C for 90 min while continually stirring. The resulting material was then filtered, washed, and oven at 60 °C. To achieve the desired cellulose fibrils, this bleaching process was repeated twice under the same conditions.

5.2.2.2. *Preparation of TS microcrystalline cellulose*

Cellulose fibers treated with alkali and bleach to produce cellulose fibrils, were then immersed in three different acid solutions to create microcrystalline cellulose. The acid solutions were made by combining a dilute sulfuric acid solution (15% by weight) with one of three transition metal salt catalysts (0.6 M of each catalyst Cr $(NO_3)_3$, $FeCl_3$, and Fe $(NO_3)_3$) in equal ratio of 1:1 (v/v). The hydrolysis was performed at 60 °C for 90 min under constant stirring to hydrolyze the amorphous domains of the obtained cellulose fibers. Following the hydrolysis reaction, 100 mL of cold distilled water was added to stop the reaction. The MCC suspension was repeatedly rinsed with pure water until it reached a neutral acidity level. Afterward, the rinsed material was dried thoroughly in a vacuum oven at a temperature of 50 °C. Once completely dry, it was pulverized into a fine powder using a a high-speed universal disintegrator (FW100, China).

5.2.2.3. *Preparation of PVA/MCC film*

After successfully isolating MCC from *Teff* straw, its ability to act as a reinforcing agent in PVA polymer matrices was further explored. The solution casting method was used in this study as shown in Figure 5-1. Different amounts of MCC were added to a 5% PVA solution to form biocomposite with various MCC compositions. Due to hydrogen bonding between cellulose chains in fibers, agglomeration or entanglement of fibers can occur in the polymer matrix. To reduce this interaction between hydroxyl groups, the microcrystalline cellulose was maintained as a 1 wt. % solid content suspension in water.

The 5 wt. % PVA solution was prepared firstly by soaking in distilled water [5 g in 100 mL] for 60 min to improve their solubility, followed by heating the solution at 80 ° C for 30 min under constant stirring. Previously prepared aqueous MCC water suspension(1 wt. % solid content) were then added to the 5 wt.% PVA solution at 2, 5, and 8 wt.% of MCC loadings. The resulted mixture is then further stirred mechanically for another 90 min. stirred continuously until the solution mixture became a homogeneous viscous appearance. Before casting, the resultant viscous mixture was cooled at room temperature until trapped air bubbles were removed. The final mixed solution was then cast into a polypropylene Petri dish and further kept at ambient temperature until films were made.

The obtained films were then dried at 50 ° C for 240 min to ensure complete evaporation of water and then removed from the Petri dish and were kept in the desiccators. The composite films were coded as PVA/ Cr(III) - MCC, PVA/ Fe(III) Cl - MCC, PVA/ Fe(III) - MCC depending on the type of catalyst used to prepare the MCCs.

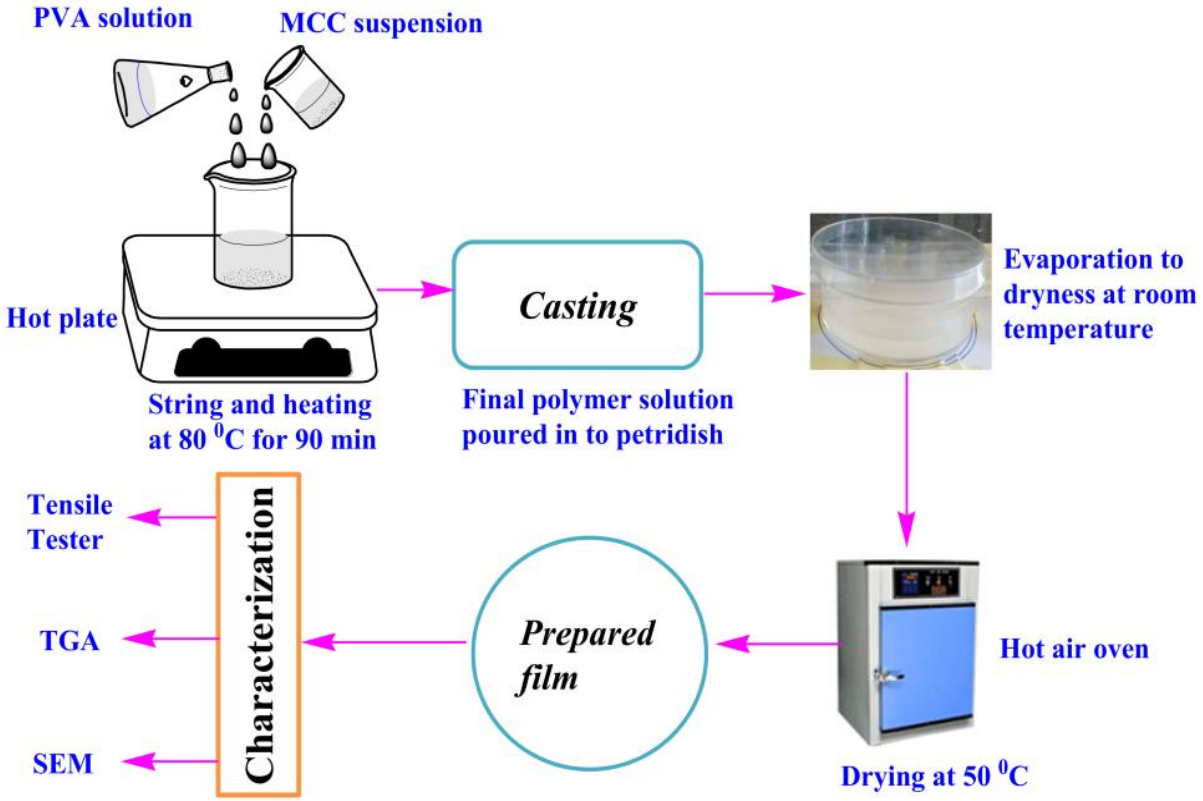

Fig. 5-1 PVA-MCC bio composite films preparation by using solution casting method

5.2.2.4. *Characterizations*

A hand-held micrometer was used to measure the thickness of composite film samples. Each film sample was measured at ten random positions and the mean values of thickness were used in the calculations for the mechanical properties. The structural interactions within PVA/MCC composite films were examined using Fourier Transform Infrared (FTIR) spectroscopy. A PerkinElmer Spectrum FT-IR Spectrometer (PerkinElmer Inc., Waltham, MA, USA) was used to collect spectra from directly loaded film samples. Measurements were performed across a wavenumber range of 4000-450 cm^{-1}. The resulting spectra were analyzed to understand the

influence of *Teff* straw-based MCC filler on the PVA matrix. This analysis focused on identifying changes in peak intensity and position caused by the MCC incorporation.

The thermal stability of the film samples (both control (pure PVA) and composite) were examined using Thermal Gravimetric Analyzer (HCT-1, BJHENVEN, China). For this, the samples were heated in the temperature range of 25 to 700 °C, at a heating rate of 20 °C min^{-1} under a nitrogen atmosphere. Temperature at onset of degradation (T_{on}), maximum degradation temperature (T_{max}), and percentage residual weight (RW) after complete degradation, were considered as representative parameters to evaluate possible thermal differences in the composites under investigation.

Mechanical properties of the composite films were investigated using MesdanLab strength tester equipped with a 5 kN cell load. Sample preparations and test methods were in accordance with the ASTM D882 standard method. The measurements were conducted at room temperature for at least five samples from each composite film. The morphologies of neat PVA and different PVA/MCC based composites samples were investigated using a scanning electron microscope at an accelerating voltage of 1 kV.

5.3. Results and Discussion

5.3.1. Films appearance and thickness variation

Figure 5-2 shows the photographs of PVA/MCC composite films. Generally, films without MCC (control film) displayed a clear appearance as compared to other prepared films. However, as the content of MCC increased, the films became less flexible, their softness decreased, and they became rough.

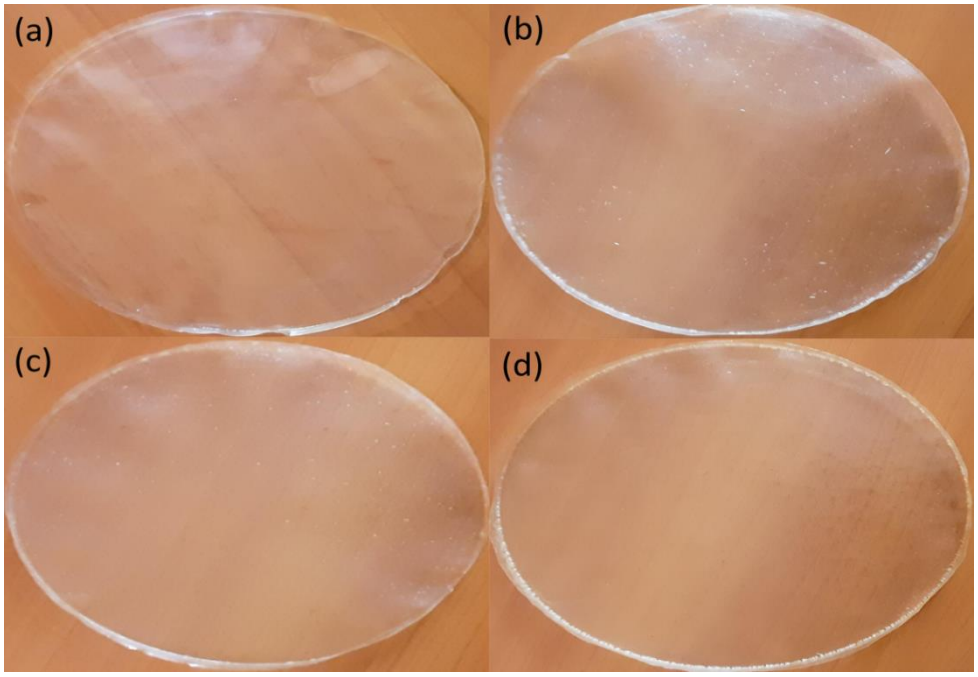

Fig. 5-2 Physical appearance of (a) neat PVA; (b) PVA/5% Cr(III) - MCC; (c) PVA /5% Fe(III)Cl - MCC; and (d) PVA /5% Fe(III) – MCC

Furthermore, Table 5-1 shows the thicknesses of PVA/MCC composite films. MCC addition resulted in slight increase of the film thicknesses compared to that of the neat PVA film (0.24 mm) with the highest thickness corresponding to the PVA/MCC composite films with 8 % MCC content. This increase in film thickness might be attributed to the increased chain-to-chain interactions that occur upon MCC addition, leading to the formation of higher-performance films (increased tensile strength, and enhanced toughness).

Table 5-1 Thickness variation for TS MCC reinforced PVA composite films with different amounts of MCCs

Sample Name	**Thickness (mm)**			
	0%	**2%**	**5%**	**8%**
PVA	0.239 ±0.004	-	-	-
PVA/ Cr(III) – MCC	-	0.267 ±0.011	0.284 ±0.011	0.313 ±0.011
PVA/ Fe(III)Cl - MCC	-	0.2588 ±0.017	0.311 ±0.01	0.342 ±0.015
PVA/ Fe(III) - MCC	-	0.2586 ±0.006	0.277 ±0.011	0.352 ±0.01

5.3.2. FT-IR analysis

Figure 5-3 presents the FT-IR spectra of pure PVA and PVA/MCC films containing 5% Cr(III)–MCC, Fe(III)Cl–MCC, and Fe(III)–MCC. These spectra were obtained to investigate potential chemical interactions between PVA and MCC during processing. For neat PVA, the broad band around 3320 cm^{-1} attributed to the stretching vibrations of O-H bonds arising from both intramolecular and intermolecular hydrogen bonds within the PVA structure. Additionally, the peaks at 2855 cm^{-1} and 2920 cm^{-1} are attributed to the symmetric and antisymmetric stretching vibrations of C-H bonds in the PVA's alkyl groups. The spectrum also reveals a peak at approximately 1720 cm^{-1}, confirming the presence of a C=O stretching vibration characteristic of acetate groups within the PVA. Additionally, peaks observed at 1097 cm^{-1} and 1425 cm^{-1} correspond to C-O-C stretching and CH_2 group bending vibrations, respectively. The observed functional groups, as evidenced by the major peaks in the PVA spectrum, are consistent with previous literature reports [90, 124, 219].

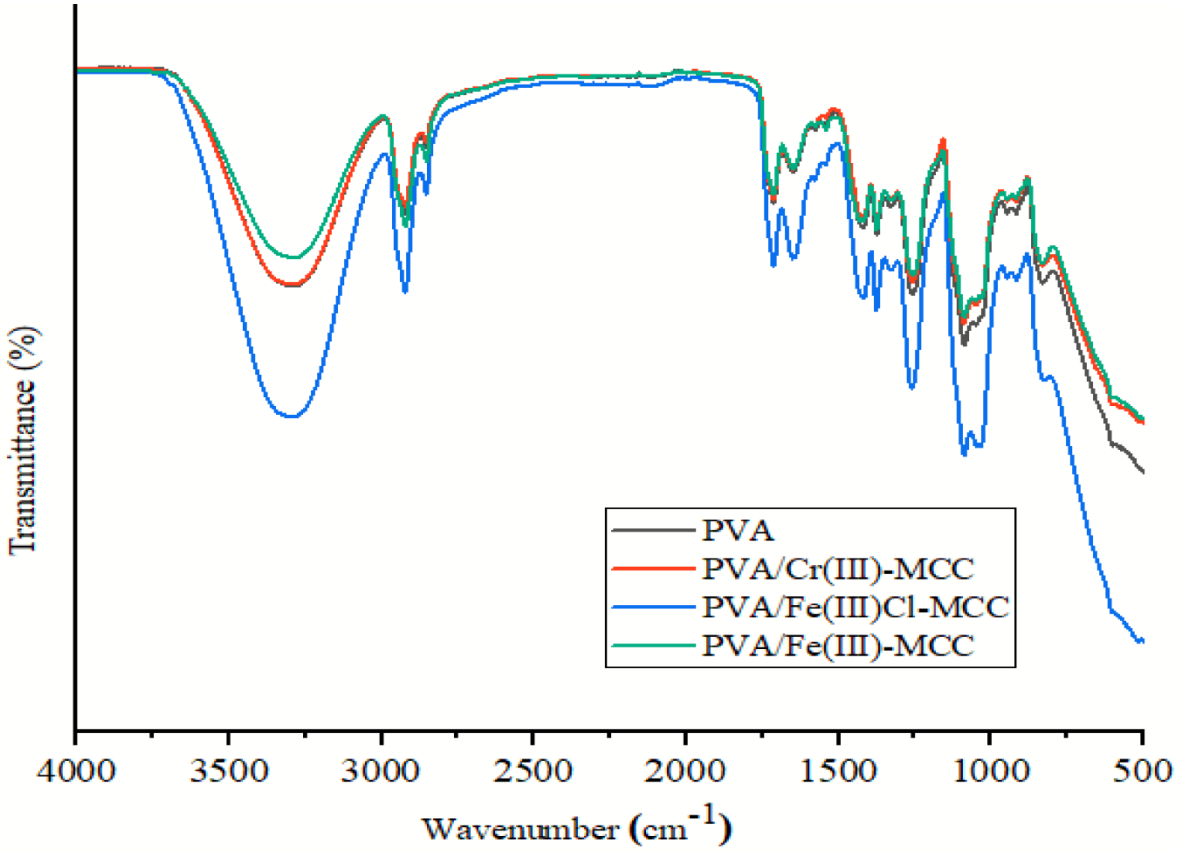

Fig.5-3 FTIR spectra of pure PVA and PVA composite films containing 5wt. % MCCs

The infrared spectra of all composite films closely resembled the neat PVA film, indicating minimal changes in the film's functional groups due to the low (5 wt.%) MCC content and the presence of similar functional groups in both materials [220, 221]. However, a shift can be observed in the spectra after incorporating MCC into PVA.

Figure 5-3 show, a change in the O-H stretching vibration band from 3320 cm^{-1} in neat PVA to 3290 cm^{-1} in PVA-MCC films. This shift suggests a possible disruption of hydrogen bonds within the neat PVA film and the potential formation of new hydrogen bonds between PVA's OH groups and MCCs [132]. The infrared spectra of composite films also show a slight shift in the C=O stretching vibration peak compared to neat PVA. The neat PVA peak at 1720 cm^{-1} shifts to a lower wavenumber (1708 cm^{-1}) in PVA-MCC. Similarly, the characteristic peak of pure PVA at 839 cm^{-1} moves to a lower frequency (828 cm^{-1}) in PVA-MCC, indicating changes in the PVA's crystalline domains. Finally, the broad peak at around 1100 - 980 cm^{-1} in the PVA-MCC spectrum appears to resolve into two distinct peaks at 1090 and 1030 cm^{-1}. Conversely, the neat PVA spectrum retains a single broad peak at 1096 cm^{-1} in this region [222]. These observations support the possibility of new intra- or intermolecular hydrogen bonds forming, along with conformational changes within PVA-MCC composite films.

5.3.3. Mechanical properties of pure PVA and PVA composite films

5.3.3.1. *Tensile strength and Young's modulus*

A series of biodegradable composite films were prepared by reinforcing PVA with varying amounts of MCC fibers extracted from TS. The mechanical properties of the composite films were then characterized by tensile tests.

Figure 5-4 illustrates the mechanical analysis of the tensile strength (MPa) and Young's modulus (MPa) of these composite films at different MCC contents. This study revealed a significant increase in both tensile strength and Young's modulus of PVA films with the incorporation of the prepared MCCs. Pure PVA exhibited a tensile strength of 35.83 MPa and a Young's modulus of 12 MPa. As Figure 5-4 (a–b) illustrate, incorporating just 2% of Cr(III)-MCC, Fe(III)Cl-MCC, and Fe(III)-MCC led to respective improvements of 90%, 89%, and 59.5% in tensile strength, and 276%, 225%, and 244% in Young's modulus compared to the pure PVA film. These results indicate that the addition of *Teff* straw MCC effectively improves the mechanical properties of

PVA films. This enhancement likely results from both the excellent mechanical properties of MCC and its good chemical compatibility with PVA. Furthermore, the increase in tensile modulus and strength is attributed to improved adhesion between MCCs and the polymer matrix, leading to more effective strain transfer at the interface. This finding aligns with the work of Khan et al. [223] and Erden et al. [224].

Moreover, Figure 5-4 reveals that MCCs obtained using different catalysts (Cr(III)-MCC, Fe(III)Cl-MCC, and Fe(III)-MCC) showed different reinforcement effects for the PVA composite films. As shown in Figure 5-4 (a), the tensile strength of Cr(III)-MCC-based PVA composites improved by 90% at 2% MCC content. Further addition of Cr(III)-MCC to the PVA matrix improved the tensile strength by 38% and 24% with the addition of 5% and 8% Cr(III)-MCC content, respectively.

On the other hand, the tensile strength of Fe(III)Cl-MCC-based PVA composites increased from 35.8 to 70.8 MPa as the Fe(III)Cl-MCC content increased from 0 to 5% (w/w), representing 97.5% enhancement. However, the tensile strength of the composites decreased with increasing Fe(III)Cl-MCC content beyond 5%. These results indicate that the addition of Fe(III)Cl-MCC to PVA can effectively improve the tensile strength of the composite films up to a 5% Fe(III)Cl-MCC content. Beyond this point, the tensile strength decreases which may be due to the agglomeration of the MCC particles.

In contrast, the tensile strength of Fe(III)-MCC-based PVA composites showed small improvement (59.5%) at lower Fe(III)-MCC content (2%) . However, the improvement reached 89.4% relative to pure PVA at 8% Fe(III)-MCC content. These results show that the addition of Fe(III)-MCC to PVA can effectively improve the tensile strength of the composite films but at higher Fe(III)-MCC content.

The trend of Young's modulus for the composites was similar to that of the tensile strength. As shown in Figure 5-4(b), the Young's modulus of the composites increased with increasing MCC content up to certain point, and then decreased. This is likely due to the same factors that affect tensile strength, namely the agglomeration of MCC particles at higher MCC contents.

In summary, the reinforcement effect of the prepared MCCs on PVA composite films depends on the type and content of MCC used. Cr (III)-MCC is mostly effective for improving the tensile strength of PVA composite films at lower content, while Fe(III)-MCC is the most effective at higher MCC content. Of all the composites, the 5 wt. % Fe(III)Cl–MCC-based PVA composite had the highest increase in tensile strength and Young's modulus. This improvement may be linked to a stronger bond between the additive and the polymer, as well as an even distribution of the additive throughout the polymer material. Additionally, from this experimental investigation, Cr(III)-MCC was found to be most effective in enhancing the tensile strength of PVA composite films at a lower content of 2%. Consequently, future research should explore even lower concentrations (<2% of Cr(III)-MCC) to further optimize the composite properties.

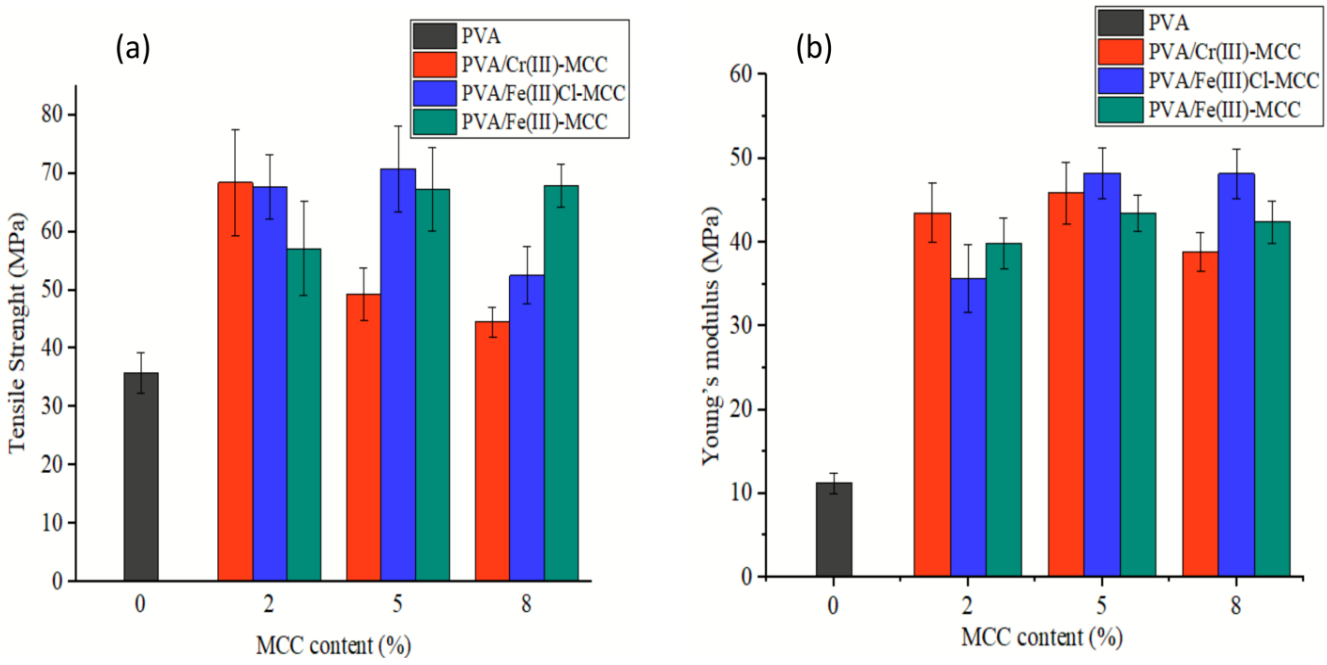

Fig. 5-4 Tensile property of neat PVA and *Teff* straw MCC reinforced PVA-based composite films: (a) Tensile strength (MPa), (b) Young's modulus (MPa)

5.3.3.2. *Percent of elongation at break*

Table 5-2 shows the decrease in elongation at break of *Teff* straw MCCs reinforced PVA composite films with the addition of MCC. This behavior is common in composites with stiff lignocellulosic fillers, like MCC [225]. The presence of MCC restricts the mobility of PVA molecules due to strong interfacial interactions, ultimately leading to reduced ductility [226].

Additionally, MCC agglomeration during film formation could further contribute to the decrease in elongation at break. For example, Chin et al. [90] found that the elongation at break of the composite decreased because the highly crystalline and rigid MCC-RS restricted the mobility of the soft chains in the polyvinyl alcohol matrix. Santi et al. [123] also found that the addition of MCC filler reduced the high deformability of PVA films, resulting in an increasingly brittle behavior of the composite. Studies have shown that films tend to become brittle when reinforcement particles are added [227]. This is also the case for cellulose fibers reinforced biodegradable composite films [126, 223].

Table 5-2 Elongation at break for *Teff* straw MCC reinforced PVA composite films with different amounts of MCCs

	Elongation at break at different MCC contents (%)			
Sample name	**0 %**	**2 %**	**5 %**	**8 %**
PVA	129.12 ±24.52	-	-	-
PVA/ Cr(III)–MCC	-	13.3 ±4.38	8.89 ±0.4	9.24 ±1.31
PVA/ Fe(III)Cl–MCC	-	12.36 ±1.31	10.32 ±3.63	9.96 ±1.27
PVA/ Fe(III)-MCC	-	15.24 ±5.24	9.24 ±0.78	12.963.69

5.3.4. Thermogravimetry analysis

To investigate the thermal degradation behavior, Thermogravimetry (TGA) and Derivative Thermogravimetry (DTG) analyses were conducted on neat PVA and MCC-reinforced PVA composite films. All the films analyzed demonstrated a consistent three-phase breakdown when heated between 50 and 700 °C (see Figure 5-5a). Initially (50-200°C), the films lost 4 to 9% of their weight due to the evaporation of absorbed water. Subsequently (200-450°C), a more significant weight loss of 64-71.5% occurred (Table 5-3), likely caused by the breakdown of PVA molecules into smaller units through water removal, forming a polyene structure [228]. The final weight reduction (450-500°C) is believed to result from the decomposition of the remaining polyene components into volatile substances like aromatic hydrocarbons [220].

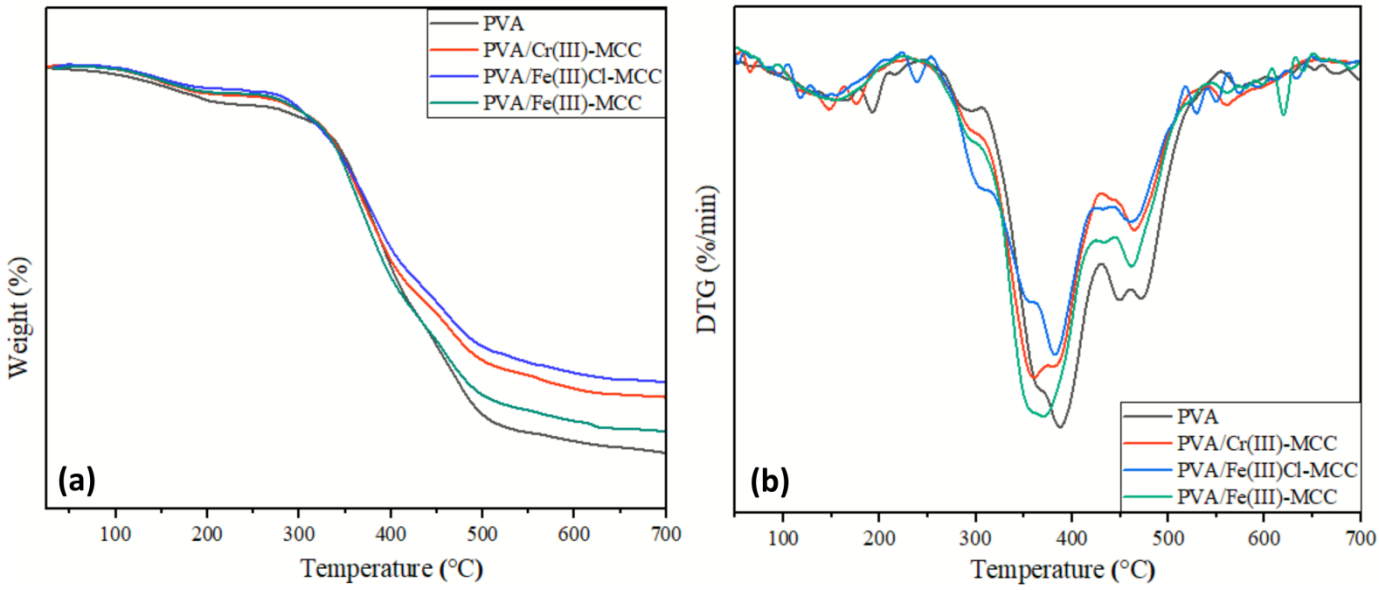

Fig. 5-5 Thermogravimetric analysis results of neat PVA and 5% *Teff* straw MCCs reinforced PVA composite films (a) TGA curves (b) DTG curves

The onset temperature (T_{on}), the maximum temperature (T_{max}), and the residual weight (RW) were obtained and summarized in Table 5-3. All PVA-MCC composites started to degrade at higher temperatures than those of neat PVA. The addition of MCC to PVA induced a progressive increase in degradation temperature compared to neat PVA. This is due to the formation of hydrogen bonds between MCC fibers and PVA matrix bonds as confirmed by FTIR analysis. The formation of hydrogen bonds restricts the movement of the polymer chains within the composite films, creating a denser structure. This denser structure helps to prevent the PVA from breaking down. This observation is in line with the results reported in literature [128, 225, 229]. Therefore, the incorporation of MCC into the PVA matrix has led to the enhanced thermal stability of the films. Moreover, the improvement in the thermal stability of PVA composite films varies with the types of catalysts used to prepare the MCCs even for the same MCC composition (Table 5-3).

The DTG curves (Figure 5-5b) also show that during the second degradation process, the T_{max} of neat PVA film (387.6 °C) was slightly higher than those of the PVA composite films containing lower MCC contents (see also Table 5-3). This is likely because the presence of MCCs reduces the polymer matrix's free volume. The free volume of a polymer matrix is the empty space between the polymer chains, allowing them to move. MCC molecules occupy some of this space, reducing the free volume and inhibiting the mobility of the polymer chains, potentially leading to

a decreased T_{max} [132, 230, 231]. The higher thermal conductivity of MCC could be another cause of the decreased T_{max} of PAV/MCC composites [226]. This is because it facilitates heat transfer within the composite, which can enhance the thermal degradation of PVA after its addition. However, when the MCC content is increased to 8%, the T_{max} value shows an increase relative to pure PVA.

The residual weight was approximately 25% and above for all composites containing TS MCCs. Pure PVA, however, exhibited a lower RW (~20%). These variations in RW could be related to the interfacial interactions between components and the presence of sulfate groups on the surface of MCC, which act as dehydration catalysts and facilitate char residue formation [220, 229, 230].

Table 5-3 Thermal degradation parameters of neat PVA and MCC-reinforced PVA composite films obtained from the TGA/DTG analysis

Sample name	**T_{on} (°C)**	**T_{max} (°C)**	**Maximum Weight losses (%)**	**Residual weight (RW (%))**
PVA	295	386.26	71.31	20.23
PVA/ 2 wt.% Cr(III) – MCC	304	383.65	70.56	25.38
PVA/ 2 wt.% Fe(III)Cl - MCC	308	381.33	69.45	26.33
PVA/ 2 wt.% Fe(III) - MCC	303	384.88	71.41	24.57
PVA/ 5 wt.% Cr(III) – MCC	305	380.02	67.32	24.87
PVA/ 5 wt.% Fe(III)Cl - MCC	308	382.6	68.76	25.16
PVA/ 5 wt.% Fe(III) - MCC	303	370.0	69.01	24.54
PVA/ 8 wt.% Cr(III) – MCC	306	390.1	67.01	25.43
PVA/ 8 wt.% Fe(III)Cl - MCC	310	391.3	67.11	26.72
PVA/ 8 wt.% Fe(III) - MCC	306	387.6	64.16	27.40

Overall, this study demonstrates that adding *Teff* straw MCC to PVA enhances the thermal stability of the resulting films. The higher onset temperature (T_{on}) of the MCC-PVA composite is well-suited for biomaterial applications.

5.3.5. Surface morphology of PVA and PVA /MCC composite films

Scanning electron microscopy was used to investigate the surface topography of MCC-PVA composite films. SEM can provide information about the presence of voids, the presence of aggregates, and the distribution of the reinforcing phase within the polymer matrix.

Figure 5-6 shows FESEM micrographs of the surface of *Teff* straw MCC reinforced PVA composite films at 5% MCC content and neat PVA. The pure PVA has a smooth and homogeneous surface. However, the incorporation of MCCs changed the surface morphology and structure of the PVA composite films. The formation of hydrogen bonds between the PVA chain and free MCC hydroxyl groups, as confirmed with FTIR analysis, caused significant changes in morphology. For all PVA composite films, SEM images show good dispersion of MCCs within the PVA matrix, and the surfaces of the MCC fibers are seen to be covered with PVA polymer. However, comparing the surfaces of PVA/ Cr(III)-MCC , PVA/ Fe(III)Cl-MCC, and PVA/ Fe(III)-MCC films, different distributions of MCCs are observed across the surfaces.

The PVA/ Fe(III)Cl-MCC film exhibits a relatively even distribution of MCCs throughout the PVA matrix. Additionally, its surface appears smooth and homogeneous without visible aggregates. These observations could suggest good compatibility between Fe(III)Cl-MCC and PVA. The uniform distribution of the Fe(III)Cl-MCC in the PVA matrix is likely to improve the mechanical strength of the film.

On the other hand, compared to the PVA/ Fe(III)Cl-MCC film, the PVA/ Cr(III)-MCC and PVA/ Fe(III)-MCC films exhibit slightly uneven distributions of MCCs, with the MCC fibers appearing somewhat clustered in specific areas. This non-uniform dispersion could potentially impact the films' mechanical properties.

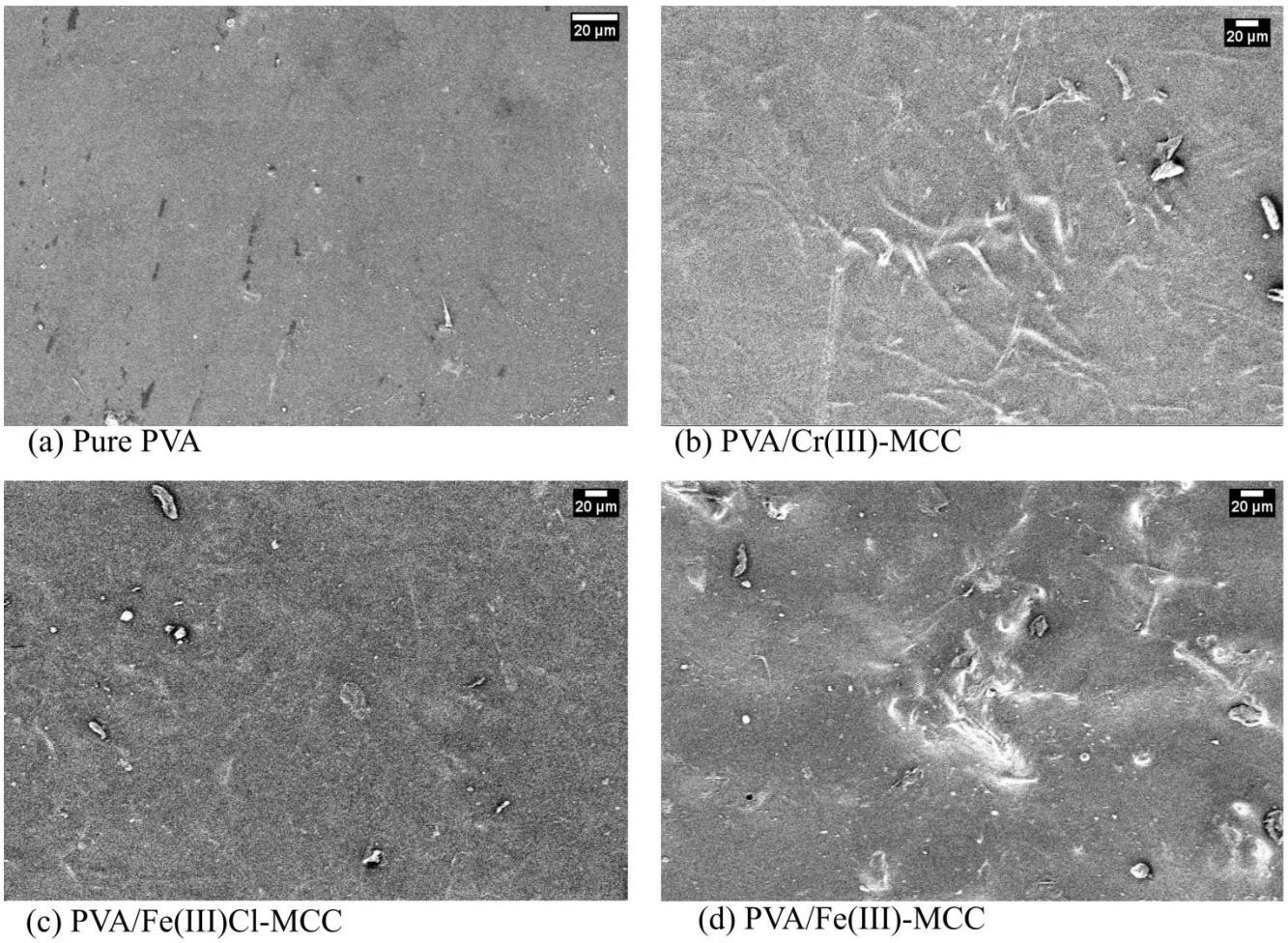

(a) Pure PVA (b) PVA/Cr(III)-MCC

(c) PVA/Fe(III)Cl-MCC (d) PVA/Fe(III)-MCC

Fig. 5-6 SEM micrographs of PVA and 5% *Teff* straw MCCs reinforced PVA composite films

The study found that the enhanced mechanical and thermal properties of PVA/MCC composite films can be attributed to changes in the material's surface structure caused by the inclusion of MCC. The uniform distribution of MCC in the PVA matrix is expected to improve the mechanical properties of the film, while the poor compatibility between MCC and PVA is likely to reduce the mechanical properties of the film. Further investigation might be necessary to optimize the dispersion process for the prepared films, as recent studies demonstrate that ultrasonication techniques can effectively improve the dispersion of microcrystalline cellulose particles within a PVA matrix [232].

5.4. Conclusions

This study achieved successful preparation of PVA-MCC green composite films through solution casting. FTIR spectra of the MCC-PVA composite films displayed a shift in peak positions, suggesting the formation of intra- and intermolecular hydrogen bonds between the hydroxyl groups (OH) of MCC and PVA.

The PVA/MCC composites also exhibited higher mechanical properties, i.e., tensile strength and Young's modulus, as compared to the neat PVA. Increasing the percentage composition of MCCs in the PVA composite films led to different reinforcement effects compared to the neat PVA matrix. These effects also depended on the type of catalyst used to prepare the MCCs (Cr(III)-MCC, Fe(III)Cl-MCC, and Fe(III)-MCC). The addition of Cr(III)-MCC to PVA composites significantly enhanced their mechanical properties at low concentrations. However, for Fe(III)Cl-MCC-based composites, the tensile strength increased only up to 5% Fe(III)Cl-MCC content. Beyond this point, the tensile strength decreased probably due to the agglomeration of the MCC particles. Conversely, Fe(III)-MCC composites showed a slight improvement at low MCC content, with a more significant increase compared to pure PVA at higher Fe(III)-MCC content. Notably, PVA with 5 wt. % Fe(III)Cl-MCC exhibited the best performance, reaching a tensile strength of 30.6 MPa and a Young's modulus of 2.26 GPa.

The TGA results demonstrate the improved thermal stability of PVA/MCC films. All PVA/ MCC composites started to degrade at higher temperatures compared to neat PVA. Additionally, the residual weight of composites was around 25% and above, while pure PVA exhibited a lower value (~20%). Microscopic analysis revealed acceptable dispersion of MCCs within the PVA matrix for all samples, with the PVA coating the MCC fiber surfaces. Notably, the Fe(III)Cl-PVA/MCC film exhibits a more even distribution of MCCs compared to other composites prepared. This uniform distribution of Fe(III)Cl-MCC within the PVA matrix is expected to enhance the film's mechanical properties.

The results of this study demonstrate that the prepared MCCs from *Teff* straw can be a potential additive to enhance the properties of PVA composites. Furthermore, the improved thermal stability of the PVA/MCC composites suggests that they could be used in applications where high-temperature processing is required.

CHAPTER 6: GENERAL CONCLUSIONS AND FUTURE WORKS

6.1. General Conclusions

This dissertation presents the synthesis and characterization of microcrystalline cellulose derived from *Teff* straw, along with an evaluation of its effectiveness as reinforcement for polyvinyl alcohol. While sulfuric acid hydrolysis has historically been the common method for MCC production, its limitations prompted the exploration of an alternative approach. This work utilizes a multi-step process involving alkali and bleaching pretreatments to obtain cellulose-rich fibers, followed by transition metal salts catalyzed dilute acid hydrolysis for controlled MCC production.

Chemical composition analysis confirmed the effectiveness of the pretreatments in removing non-cellulosic components like lignin and hemicellulose. Compared to untreated TS fibers, the treated fibers exhibited significantly higher cellulose content and lower levels of non-cellulosic components. The influence of process variables like temperature, time, and NaOH concentration on the effectiveness of the alkali treatment was also investigated. The results revealed that these variables significantly impacted the degree of lignin removal and the yield of cellulose fibers. X-ray diffraction analysis confirmed that the pretreatments successfully preserved the cellulose I crystalline structure present in the TS. Furthermore, the crystallinity of the cellulose fibers increased significantly after pretreatment, demonstrating an improvement in their structural order. Thermogravimetry analysis revealed that the isolated cellulose exhibited higher thermal stability compared to untreated TS fibers. The successful isolation of cellulose from TS with significantly higher cellulose content, crystallinity, and thermal stability paves the way for its potential utilization in the production of high-quality microcrystalline cellulose. This sustainable and readily available resource offers an eco-friendly alternative to traditional sources of cellulose, contributing to the development of more sustainable and bio-based materials.

This study also explores the transformation of alkali hydrogen peroxide-extracted *Teff* straw cellulose into microcrystalline cellulose using a novel approach. MCC were prepared from the pretreated TS fiber by three transition metal salt catalysts assisted dilute acid hydrolysis process. Each transition metal catalyst showed different effects on the crystallinity, crystallite size, surface morphology, and thermal stability of the obtained microcrystalline cellulose. The XRD and TGA

analyses respectively showed that the MCCs have higher crystallinity and thermal stability, respectively. Among the prepared MCCs, the Cr(III) ions synthesized MCC rendered relatively the highest crystallinity and thermal stability, reflecting its better hydrolysis selectivity as compared to Fe(III)Cl and Fe(III) - metal ions. Furthermore, all MCCs exhibited degradation temperatures higher than typical processing temperatures of polymeric materials, making them suitable for the preparation of polymer-based composite materials. This method could further reduce the consumption of acids without compromising the thermal stability, dispersibility, crystallinity and production yield of MCC.

The synthesized MCC effectively reinforced polyvinyl alcohol matrices, increasing tensile strength and Young's modulus while reducing elongation at break. The influence of MCC type and content varied, likely due to differences in particle interactions and potential agglomeration. Notably, Fe(III)Cl-MCC at 5 wt. % achieved significant reinforcement, highlighting the crucial role of catalyst selection and processing conditions. Furthermore, MCC incorporation enhanced thermal stability of PVA films, indicating broader potential applications.

Overall, this study highlights the potential of *Teff* straw MCCs as a viable and sustainable reinforcement for PVA composites, opening doors for the development of new and improved materials with diverse applications.

6.2. Future works

This study has made a significant contribution to the production of microcrystalline cellulose from *Teff* straw with enhanced physico-chemical properties, however further work may be required to further investigate process parameters of the alkali pretreatment, and dilute acid hydrolysis.

Experimental work was performed to observe the influence of process variables (temperature, time, and NaOH concentration) on the responses (the lignin removal and fiber yield) based on a single factor effect during the alkali treatment of *Teff* straw. The variation of these parameters has shown their effect on the percentage of lignin removal and fiber yield. Further optimization study using RSM could be conducted to observe the synergistic effect between process pretreatments on the delignification efficiency of the alkali pretreatment on TS.

Also in future work, the dilute acid hydrolysis needs to be optimized for pretreated TS to get maximum crystallinity index and yield of MCC. Four independent parameters including reaction temperature, reaction time, acid concentration (H_2SO_4) and concentration of transition metal salts could generally optimize. Effects of interaction between the parameters could be examined using the response surface method (CCD; Design Expert software package).

For optimal reinforcement with constant filler loading, enhancing microcrystalline cellulose dispersion within the polyvinyl alcohol matrix is crucial. Ultrasonication has emerged as an effective technique to achieve superior dispersion leading to enhanced filler-matrix interaction, and improved tensile strength. Thus, ultrasonication is strongly recommended for incorporating MCC into the PVA matrix. This approach optimizes reinforcement efficiency while maintaining filler content, resulting in superior mechanical properties.

Due to constraints in funding, time, and resources, additional experiments to determine the modulus and density of microcrystalline cellulose (MCC) were not conducted. Characterizing these properties of the MCC obtained from TS is recommended for future research. Characterizing co-products of this study, such as the extracted lignin, is also recommended for future research.

Furthermore, tensile testing revealed that Cr(III)-MCC significantly improved the tensile strength of PVA composite films at a low concentration of 2%. To further optimize composite properties, exploring even lower concentrations of Cr(III)-MCC (<2%) is suggested for future studies.

REFERENCES

1. Trache, D., Hussin, M. H., Chuin, C. T. H., Sabar, S., Fazita, M. N., Taiwo, O. F., ... & Haafiz MM (2016) Microcrystalline cellulose: Isolation, characterization and bio-composites application—A review. International Journal of Biological Macromolecules, 93, 789-804. https://doi.org/10.1016/j.ijbiomac.2016.09.056

2. Dat, T. T., Khanh, T. T., & Trinh H V. (2023) Synthesis of microcrystalline cellulose from sugarcane bagasse and its incorporation into Polyvinyl Alcohol (PVA) matrix to test the composites mechanical properties. Materials Research Express, 10(3), 035101.

3. Qiu K, Netravali AN (2012) Fabrication and characterization of biodegradable composites based on microfibrillated cellulose and polyvinyl alcohol. Compos Sci Technol 72:1588–1594. https://doi.org/10.1016/j.compscitech.2012.06.010

4. Ali, N. A., Huseen, S. I., & Jaffer HI (2017) . Barrier, mechanical and thermal of polyvinyl alchol/microcrystalline cellouse composites in packaging application. composites, 5(6), 7. https://doi.org/10.11648/j.ajpa.20170504.11

5. Ashfaq, J., Channa, I. A., Memon, A. G., Chandio, I. A., Chandio, A. D., Shar, M. A., ... & Devanesan S (2023) . Enhancement of Thermal and Gas Barrier Properties of Graphene-Based Nanocomposite Films. ACS omega, 8(44), 41054-41063. https://doi.org/10.1021/acsomega.3c02885

6. Abdullah, Z. W., Dong, Y., Han, N., & Liu S (2019) (2019) . Water and gas barrier properties of polyvinyl alcohol (PVA)/starch (ST)/glycerol (GL)/halloysite nanotube (HNT) bionanocomposite films: Experimental characterisation and modelling approach. Composites Part B: Engineering, 174, 107033. Compos Part B 107033. https://doi.org/10.1016/j.compositesb.2019.107033

7. Sau, S., Pandit, S., & Kundu S (2021) (2021) . Crosslinked poly (vinyl alcohol): structural, optical and mechanical properties. Surfaces and Interfaces, 25, 101198. Surfaces and Interfaces 25:101198. https://doi.org/10.1016/j.surfin.2021.101198

8. Sharma, P., Agrawal, P. K., Singh, V. K., Chauhan, S., & Bhaskar J (2023) . A

comprehensive review on properties of polyvinyl alcohol (PVA) crosslinked with carboxylic acid. J. Mater. Environ. Sci., 14 (10), 1236, 1252. 14:1236–1252

9. Xiang, A., Lv, C., & Zhou H (2020) Changes in crystallization behaviors of poly (vinyl alcohol) induced by water content. Journal of Vinyl and Additive Technology, 26(4), 613-622. https://doi.org/10.1002/vnl.21775

10. Trache, D., Tarchoun, A. F., Derradji, M., Hamidon, T. S., Masruchin, N., Brosse, N., & Hussin MH (2020) Nanocellulose: from fundamentals to advanced applications. Frontiers in chemistry, 8, 392.

11. Tanpichai, S., Biswas, S. K., Witayakran, S., & Yano H (2019) . Water hyacinth: a sustainable lignin-poor cellulose source for the production of cellulose nanofibers. ACS Sustainable Chemistry & Engineering, 7(23), 18884-18893. https://doi.org/10.1021/acssuschemeng.9b04095

12. Mohamad, N. A. N., & Jai J (2022) Response surface methodology for optimization of cellulose extraction from banana stem using NaOH-EDTA for pulp and papermaking. Heliyon, 8(3). 8:. https://doi.org/10.1016/j.heliyon.2022.e09114

13. Gichuki, J., Kareru, P. G., Gachanja, A. N., & Ngamau C (2022) Characteristics of microcrystalline cellulose from coir fibers. Journal of Natural Fibers, 19(3), 915-930. https://doi.org/10.1080/15440478.2020.1764441

14. Tadele E, Hibistu T (2022) Spatial production distribution, economic viability and value chain features of teff in Ethiopia: Systematic review: Cogent Economics and Finance. 10:. https://doi.org/10.1080/23322039.2021.2020484

15. Adeosun, S. O., Lawal, G. I., Balogun, S. A., & Akpan EI (2012) Review of green polymer nanocomposites. Journal of Minerals and Materials Characterization and Engineering.Vol. 11, No.4, pp.483-514, 2012

16. Miao C, Hamad WY (2013) Cellulose reinforced polymer composites and nanocomposites: A critical review. Cellulose 20:2221–2262. https://doi.org/10.1007/s10570-013-0007-3

17. Li M, He B, Zhao L (2019) Isolation and characterization of microcrystalline cellulose from Cotton Stalk Waste. BioResources 14:3231–3246. https://doi.org/10.15376/biores.14.2.3231-3246

18. Moshood TD, Nawanir G, Mahmud F, et al (2022) Biodegradable plastic applications towards sustainability : A recent innovations in the green product. Clean Eng Technol 6:100404. https://doi.org/10.1016/j.clet.2022.100404

19. Moshood TD, Nawanir G, Mahmud F, et al (2025) Current Research in Green and Sustainable Chemistry Sustainability of biodegradable plastics : New problem or solution to solve the global plastic pollution ? 5:. https://doi.org/10.1016/j.crgsc.2022.100273

20. de Oliveira, F. B., Bras, J., Pimenta, M. T. B., da Silva Curvelo, A. A., & Belgacem MN (2016) . Production of cellulose nanocrystals from sugarcane bagasse fibers and pith. Industrial Crops and Products, 93, 48-57. https://doi.org/10.1016/j.indcrop.2016.04.064

21. Kumar A, Negi YS, Choudhary V, Bhardwaj NK (2013) Characterization of Cellulose Nanocrystals Produced by Acid-Hydrolysis from Sugarcane Bagasse as Agro-Waste. Journal of Materials Physics and Chemistry.Vol. 2, No. 1, 1-8. https://doi.org/10.12691/jmpc-2-1-1

22. Mohomane, S. M., Motloung, S. V., Koao, L. F., & Motaung TE . Effects of acid hydrolysis on the extraction of cellulose nanocrystals (CNCs): A review. Cellulose Chemistry and Technology, 56(7-8), 691-703.

23. Shankaran DR (2018) . Cellulose nanocrystals for health care applications. In Applications of nanomaterials (pp. 415-459). Woodhead Publishing. Elsevier Ltd.

24. Chen YouWei, C. Y., Lee HweiVoon, L. H., & Sharifah Bee AH (2016) Preparation of nanostructured cellulose via Cr(III)- and Mn(II)-transition metal salt catalyzed acid hydrolysis approach. BioResources 11(3), 7224-7241. https://doi.org/10.15376/biores.11.3.7224-7241

25. Wei CY (2017) Isolation and characterization of nanocrystalline cellulose from oil palm biomass via transition metal salt catalyzed hydrolysis process (Master thesis, University of

Malaya (Malaysia)).

26. Chen, Y. W., Tan, T. H., Lee, H. V., & Abd Hamid SB (2017) Easy fabrication of highly thermal-stable cellulose nanocrystals using Cr (NO3)3 catalytic hydrolysis system: a feasibility study from macro-to nano-dimensions. Materials, 10(1), 42. https://doi.org/10.3390/ma10010042

27. Alemdar, A., & Sain M (2008) Isolation and characterization of nanofibers from agricultural residues–Wheat straw and soy hulls. Bioresource technology, 99(6), 1664-1671. https://doi.org/10.1016/j.biortech.2007.04.029

28. Dinand, E., Chanzy, H., & Vignon MR (1996) Parenchymal cell cellulose from sugar beet pulp: preparation and properties. Cellulose, 3, 183-188.

29. Chufo, A., Yuan, H., Zou, D., Pang, Y., & Li X (2015) Biomethane production and physicochemical characterization of anaerobically digested teff (Eragrostis tef) straw pretreated by sodium hydroxide. Bioresource Technology, 181, 214-219. https://doi.org/10.1016/j.biortech.2015.01.054

30. Bageru, A. B., & Srivastava VC (2017) . Preparation and characterisation of biosilica from teff (eragrostis tef) straw by thermal method. Materials Letters, 206, 13-17. Mater Lett 206:13–17. https://doi.org/10.1016/j.matlet.2017.06.100

31. Wassie AB, Srivastava VC (2017) Synthesis and Characterization of Nano-Silica from Teff Straw. Journal of Nano Research ISSN: 1661-9897, Vol. 46, pp 64-72. https://doi.org/10.4028/www.scientific.net/JNanoR.46.64

32. Wassie AB, Srivastava VC (2016) Teff straw characterization and utilization for chromium removal from wastewater : Kinetics , isotherm and thermodynamic modelling. Journal of Environmental Chemical Engineering 4 (2016) 1117–1125. https://doi.org/10.1016/j.jece.2016.01.019

33. Ghanbarzadeh, B., & Almasi H (2013) Biodegradable polymers. Biodegradation-life of science, 141-185.

34. Kian LK, Saba N, Jawaid M, Sultan MTH (2019) A review on processing techniques of bast fibers nanocellulose and its polylactic acid (PLA) nanocomposites. International Journal of Biological Macromolecules 121 1314–1328. https://doi.org/10.1016/j.ijbiomac.2018.09.040

35. Haafiz, M. M., Hassan, A., Arjmandi, R., Marliana, M. M., & Fazita MN (2016) Exploring the potentials of nanocellulose whiskers derived from oil palm empty fruit bunch on the development of polylactid acid based green nanocomposites. Polymers and Polymer Composites, 24(9), 729-734. https://doi.org/10.1177/096739111602400908

36. Samir, A., Ashour, F. H., Hakim, A. A., & Bassyouni M (2022) . Recent advances in biodegradable polymers for sustainable applications. Npj Materials Degradation, 6(1), 68. https://doi.org/10.1038/s41529-022-00277-7

37. Murthy N, Wilson S, Sy JC, Petit PH (2012) Biodegradation of Polymers

38. Nayak PL (1999) (2007) . Biodegradable polymers: opportunities and challenges. 37–41

39. Alaswad, S. O., Mahmoud, A. S., & Arunachalam P (2022) (2022) . Recent advances in biodegradable polymers and their biological applications: a brief review. Polymers, 14(22), 4924.

40. Yue, S., Zhang, T., Wang, S., Han, D., Huang, S., Xiao, M., & Meng Y (2024) . Recent Progress of Biodegradable Polymer Package Materials: Nanotechnology Improving Both Oxygen and Water Vapor Barrier Performance. Nanomaterials, 14(4), 338.

41. Rigved Nagarkar, Jatin Patel (2019) Polyvinyl Alcohol: A Comprehensive Study. Acta Scientific Pharmaceutical Sciences 3.4 (2019): 34-44.

42. Asad, M., Saba, N., Asiri, A. M., Jawaid, M., Indarti, E., & Wanrosli WD (2018) "Preparation and characterization of nanocomposite films from oil palm pulp nanocellulose/poly (Vinyl alcohol) by casting method". Carbohydrate polymers, 191, 103-111. https://doi.org/10.1016/j.carbpol.2018.03.015

43. Gaaz, T. S., Sulong, A. B., Akhtar, M. N., Kadhum, A. A. H., Mohamad, A. B., & Al-

Amiery AA (2015) Properties and applications of polyvinyl alcohol, halloysite nanotubes and their nanocomposites. Molecules, 20(12), 22833-22847. https://doi.org/10.3390/molecules201219884

44. Ben Halima N (2016) Poly(vinyl alcohol): Review of its promising applications and insights into biodegradation. RSC Advances. 6:39823–39832. https://doi.org/10.1039/c6ra05742j

45. Abo, B. O., Gao, M., Wang, Y., Wu, C., Ma, H., & Wang Q (2019) Lignocellulosic biomass for bioethanol: an overview on pretreatment, hydrolysis and fermentation processes. Reviews on environmental health, 34(1), 57-68. https://doi.org/10.1515/reveh-2018-0054

46. Naraian, R., & Gautam RL (2018) Penicillium enzymes for the saccharification of lignocellulosic feedstocks. In New and future developments in microbial biotechnology and bioengineering (pp. 121-136). Elsevier. Elsevier B.V.

47. Henning Jørgensen JBK and CF (2007) Enzymatic conversion of lignocellulose into fermentable sugars: challenges and opportunities. Biofuels, Bioproducts and Biorefining, Wiley InterScience. https://doi.org/10.1002/bbb

48. Chen, H., & Chen H (2014) Chemical composition and structure of natural lignocellulose. Biotechnology of lignocellulose: Theory and practice, 25-71.

49. Jung SJ, Kim SH, Chung IM (2015) Comparison of lignin, cellulose, and hemicellulose contents for biofuels utilization among 4 types of lignocellulosic crops. Biomass and Bioenergy 83:322–327. https://doi.org/10.1016/j.biombioe.2015.10.007

50. Zhang YHP, Lynd LR (2004) Toward an aggregated understanding of enzymatic hydrolysis of cellulose: Noncomplexed cellulase systems. Biotechnol Bioeng 88:797–824. https://doi.org/10.1002/bit.20282

51. Matsuzaki K (1965) Microcrystalline Cellulose. Industrial and Engineering Chemistry, Vol 54. 285–289. https://doi.org/10.1295/kobunshi.14.285

52. Mukherjee, T., Sani, M., Kao, N., Gupta, R. K., Quazi, N., & Bhattacharya S (2013) . Improved dispersion of cellulose microcrystals in polylactic acid (PLA) based composites applying surface acetylation. Chemical Engineering Science, 101, 655-662. https://doi.org/10.1016/j.ces.2013.07.032

53. Marras, S. I., Zuburtikudis, I., & Panayiotou C (2010) . Solution casting versus melt compounding: effect of fabrication route on the structure and thermal behavior of poly (l-lactic acid) clay nanocomposites. Journal of materials science, 45, 6474-6480. 6474–6480. https://doi.org/10.1007/s10853-010-4735-6

54. Mohamad Haafiz MK, Eichhorn SJ, Hassan A, Jawaid M (2013) Isolation and characterization of microcrystalline cellulose from oil palm biomass residue. Carbohydr Polym 93:628–634. https://doi.org/10.1016/j.carbpol.2013.01.035

55. Chen, H., Liu, J., Chang, X., Chen, D., Xue, Y., Liu, P., ... & Han S (2017) A review on the pretreatment of lignocellulose for high-value chemicals. Fuel Processing Technology, 160, 196-206. https://doi.org/10.1016/j.fuproc.2016.12.007

56. Li Y-Y, Wang B, Ma M-G, Wang B (2018) The Influence of Pre-treatment Time and Sulfuric Acid on Cellulose Nanocrystals. BioResources 13:3585–3602. https://doi.org/10.15376/biores.13.2.3585-3602

57. Dahadha S, Amin Z, Bazyar Lakeh AA, Elbeshbishy E (2017) Evaluation of Different Pretreatment Processes of Lignocellulosic Biomass for Enhanced Biomethane Production. Energy and Fuels 31:10335–10347. https://doi.org/10.1021/acs.energyfuels.7b02045

58. Karimi, K., Shafiei, M., & Kumar R (2013) Progress in physical and chemical pretreatment of lignocellulosic biomass. In Biofuel technologies: recent developments (pp. 53-96). Berlin, Heidelberg: Springer Berlin Heidelberg.

59. Rajendran, K., Drielak, E., Sudarshan Varma, V., Muthusamy, S., & Kumar G (2018) Updates on the pretreatment of lignocellulosic feedstocks for bioenergy production–a review. Biomass conversion and biorefinery, 8, 471-483. https://doi.org/10.1007/s13399-017-0269-3

60. Ji, X. J., Huang, H., Nie, Z. K., Qu, L., Xu, Q., & Tsao GT (2012) Fuels and chemicals from hemicellulose sugars. Biotechnology in China III: biofuels and bioenergy, 199-224. https://doi.org/10.1007/10

61. Kumar, A. K., & Sharma S (2017) Recent updates on different methods of pretreatment of lignocellulosic feedstocks: A review. Bioresources and Bioprocessing, 4, 7. https://doi.org/10.1186/s40643-017-0137-9

62. Mood, S. H., Golfeshan, A. H., Tabatabaei, M., Jouzani, G. S., Najafi, G. H., Gholami, M., & Ardjmand M. (2013) Lignocellulosic biomass to bioethanol, a comprehensive review with a focus on pretreatment. Renewable and sustainable energy reviews, 27, 77-93. https://doi.org/10.1016/j.rser.2013.06.033

63. Cherian, B. M., Leão, A. L., de Souza, S. F., Costa, L. M. M., de Olyveira, G. M., Kottaisamy, M., ... & Thomas S (2011) . Cellulose nanocomposites with nanofibres isolated from pineapple leaf fibers for medical applications. Carbohydrate Polymers, 86(4), 1790-1798. https://doi.org/10.1016/j.carbpol.2011.07.009

64. Sun Y, Cheng J (2002) Hydrolysis of lignocellulosic materials for ethanol production: A review. Bioresour Technol 83:1–11. https://doi.org/10.1016/S0960-8524(01)00212-7

65. Sun S, Sun S, Cao X, Sun R (2016) The role of pretreatment in improving the enzymatic hydrolysis of lignocellulosic materials. Bioresour Technol 199:49–58. https://doi.org/10.1016/j.biortech.2015.08.061

66. Behera S, Arora R, Nandhagopal N, Kumar S (2014) Importance of chemical pretreatment for bioconversion of lignocellulosic biomass. Renew Sustain Energy Rev 36:91–106. https://doi.org/10.1016/j.rser.2014.04.047

67. Song K, Zhu X, Zhu W, Li X (2019) Preparation and characterization of cellulose nanocrystal extracted from Calotropis procera biomass. Bioresour Bioprocess 6:. https://doi.org/10.1186/s40643-019-0279-z

68. Rosa, M. D. F., Medeiros, E., Malmonge, J. A., Gregorski, K. S., Wood, D. F., Mattoso, L. H. C., ... & Imam SH (2010) . Cellulose nanowhiskers from coconut husk fibers: Effect of

preparation conditions on their thermal and morphological behavior. Carbohydrate polymers, 81(1), 83-92. https://doi.org/10.1016/j.carbpol.2010.01.059

69. Yue, Y., Han, J., Han, G., Aita, G. M., & Wu Q (2015) . Cellulose fibers isolated from energycane bagasse using alkaline and sodium chlorite treatments: Structural, chemical and thermal properties. Industrial Crops and Products, 76, 355-363. https://doi.org/10.1016/j.indcrop.2015.07.006

70. Hafemann, E., Battisti, R., Bresolin, D., Marangoni, C., & Machado RAF (2020) . Enhancing chlorine-free purification routes of rice husk biomass waste to obtain cellulose nanocrystals. Waste and Biomass Valorization, 11, 6595-6611. https://doi.org/10.1007/s12649-020-00937-2

71. Naz, S., Ahmad, N., Akhtar, J., Ahmad, N. M., Ali, A., & Zia M (2016) . Management of citrus waste by switching in the production of nanocellulose. IET nanobiotechnology, 10(6), 395-399. https://doi.org/10.1049/iet-nbt.2015.0116

72. Huang, X., De Hoop, C. F., Li, F., Xie, J., Hse, C. Y., Qi, J., ... & Chen Y (2017) . Dilute alkali and hydrogen peroxide treatment of microwave liquefied rape straw residue for the extraction of cellulose nanocrystals. Journal of Nanomaterials, 2017. https://doi.org/10.1155/2017/4049061

73. Xu, C., Zhu, S., Xing, C., Li, D., Zhu, N., & Zhou H (2015) . Isolation and properties of cellulose nanofibrils from coconut palm petioles by different mechanical process. PLoS One, 10(4), e0122123. https://doi.org/10.1371/journal.pone.0122123

74. Gu J, Hsieh Y Lo (2017) Alkaline cellulose nanofibrils from streamlined alkali treated rice straw. ACS Sustain Chem Eng 5:1730–1737. https://doi.org/10.1021/acssuschemeng.6b02495

75. Abraham, E., Deepa, B., Pothan, L. A., Jacob, M., Thomas, S., Cvelbar, U., & Anandjiwala R (2011) . Extraction of nanocellulose fibrils from lignocellulosic fibres: A novel approach. Carbohydrate Polymers, 86(4), 1468-1475. https://doi.org/10.1016/j.carbpol.2011.06.034

76. Aurelia C, Murdiati A, . S, Ningrum A (2019) Effect of Sodium Hydroxide and Sodium Hypochlorite on the Physicochemical Characteristics of Jack Bean Skin (Canavalia ensiformis). Pakistan Journal of Nutrition, ISSN 1680-5194, 18: 193-200. https://doi.org/10.3923/pjn.2019.193.200

77. Fareez, I. M., Ibrahim, N. A., Wan Yaacob, W. M. H., Mamat Razali, N. A., Jasni, A. H., & Abdul Aziz F (2018) . Characteristics of cellulose extracted from Josapine pineapple leaf fibre after alkali treatment followed by extensive bleaching. Cellulose, 25, 4407-4421. https://doi.org/10.1007/s10570-018-1878-0

78. Chen, W., Yu, H., Liu, Y., Chen, P., Zhang, M., & Hai Y (2011) . Individualization of cellulose nanofibers from wood using high-intensity ultrasonication combined with chemical pretreatments. Carbohydrate polymers, 83(4), 1804-1811. https://doi.org/10.1016/j.carbpol.2010.10.040

79. Khalil, H. A., Davoudpour, Y., Islam, M. N., Mustapha, A., Sudesh, K., Dungani, R., & Jawaid M (2014) . Production and modification of nanofibrillated cellulose using various mechanical processes: a review. Carbohydrate polymers, 99, 649-665. https://doi.org/10.1016/j.carbpol.2013.08.069

80. Harmsen, P. F., Huijgen, W., Bermudez, L., & Bakker R (2010) Literature review of physical and chemical pretreatment processes for lignocellulosic biomass (No. 1184). Wageningen UR-Food & Biobased Research.

81. Siqueira, G., Abdillahi, H., Bras, J., & Dufresne A (2010) High reinforcing capability cellulose nanocrystals extracted from Syngonanthus nitens (Capim Dourado). Cellulose, 17, 289-298. 289–298. https://doi.org/10.1007/s10570-009-9384-z

82. Lupidi, G., Pastore, G., Marcantoni, E., & Gabrielli S (2023) . Recent developments in chemical derivatization of microcrystalline cellulose (MCC): Pre-treatments, functionalization, and applications. Molecules, 28(5), 2009.

83. Jacquet, N., Vanderghem, C., Danthine, S., Quiévy, N., Blecker, C., Devaux, J., & Paquot M (2012) . Influence of steam explosion on physicochemical properties and hydrolysis rate

of pure cellulose fibers. Bioresource Technology, 121, 221-227. https://doi.org/10.1016/j.biortech.2012.06.073

84. Jahan, M. S., Saeed, A., He, Z., & Ni Y (2011) Jute as raw material for the preparation of microcrystalline cellulose. Cellulose, 18, 451-459. https://doi.org/10.1007/s10570-010-9481-z

85. Thulluri, C., Goluguri, B. R., Konakalla, R., Shetty, P. R., & Addepally U (2013) . The effect of assorted pretreatments on cellulose of selected vegetable waste and enzymatic hydrolysis. Biomass and Bioenergy, 49, 205-213. https://doi.org/10.1016/j.biombioe.2012.12.022

86. Wang W, Yuan TQ, Cui BK (2013) Fungal treatment followed by FeCl3 treatment to enhance enzymatic hydrolysis of poplar wood for high sugar yields. Biotechnol Lett 35:2061–2067. https://doi.org/10.1007/s10529-013-1306-3

87. Zhang, Y., Li, Q., Su, J., Lin, Y., Huang, Z., Lu, Y., ... & Zhu Y (2015) . A green and efficient technology for the degradation of cellulosic materials: structure changes and enhanced enzymatic hydrolysis of natural cellulose pretreated by synergistic interaction of mechanical activation and metal salt. Bioresource Technology,. https://doi.org/10.1016/j.biortech.2014.11.085

88. Wei, H., Donohoe, B. S., Vinzant, T. B., Ciesielski, P. N., Wang, W., Gedvilas, L. M., ... & Tucker MP (2011) Elucidating the role of ferrous ion cocatalyst in enhancing dilute acid pretreatment of lignocellulosic biomass. Biotechnology for biofuels, 4, 1-16. 1–16

89. Siró, I., & Plackett D (2010) Microfibrillated cellulose and new nanocomposite materials : a review . Cellulose, 17, 459-494. https://doi.org/10.1007/s10570-010-9405-y

90. Chin KM, Ting SS, Lin OH, Owi WT (2017) Extraction of microcrystalline cellulose from rice straw and its effect on polyvinyl alcohol biocomposites film. AIP Conf Proc 1865:. https://doi.org/10.1063/1.4993348

91. Hachaichi, A., Kouini, B., Kian, L. K., Asim, M., & Jawaid M (2021) Extraction and characterization of microcrystalline cellulose from date palm fibers using successive

chemical treatments. Journal of Polymers and the Environment, 29, 1990-1999. https://doi.org/10.1007/s10924-020-02012-2

92. Tarchoun, A. F., Trache, D., Klapötke, T. M., Derradji, M., & Bessa W (2019) . Ecofriendly isolation and characterization of microcrystalline cellulose from giant reed using various acidic media. Cellulose, 26, 7635-7651. https://doi.org/10.1007/s10570-019-02672-x

93. Zhao, T., Chen, Z., Lin, X., Ren, Z., Li, B., & Zhang Y (2018) . Preparation and characterization of microcrystalline cellulose (MCC) from tea waste. Carbohydrate polymers, 184, 164-170. https://doi.org/10.1016/j.carbpol.2017.12.024

94. Asif, M., Ahmed, D., Ahmad, N., Qamar, M. T., Alruwaili, N. K., & Bukhari SNA (2022) . Extraction and characterization of microcrystalline cellulose from Lagenaria siceraria fruit pedicles. Polymers, 14(9), 1867. https://doi.org/10.3390/polym14091867

95. Ejikeme PM (2008) Investigation of the physicochemical properties of microcrystalline cellulose from agricultural wastes I: Orange mesocarp. Cellulose 15:141–147. https://doi.org/10.1007/s10570-007-9147-7

96. Ohwoavworhua, F. O., Mitchell, J. W., & Okhamafe AO (2019) Rice husk as a sustainable source of microcrystalline cellulose: pharmacopoeial, crystalline and spectroscopic characteristics. Drug Discov, 13, 79-87. 13:

97. Suesat J, Suwanruji P (2011) Preparation and properties of microcrystalline cellulose from corn residues. Adv Mater Res 332–334:1781–1784. https://doi.org/10.4028/www.scientific.net/AMR.332-334.1781

98. Tolessa A (2023) Bioenergy potential from crop residue biomass resources in Ethiopia. Heliyon 9:e13572. https://doi.org/10.1016/j.heliyon.2023.e13572

99. Taffesse, A. S., Dorosh, P., & Asrat S (2012). (2013) Crop production in Ethiopia: Regional patterns and trends. Food and agriculture in Ethiopia: Progress and policy challenges, 74, 53.

100. Crymes AR (2015) The International Footprint of Teff: Resurgence of an Ancient Ethiopian Grain. Arts & Sciences, Master thesis at Washington University

101. Jack R. Harlan JMJ de W and ABLS (1779) Origins of African Plant Domestication. ASA Review of Books, Vol. 5 (1979), pp. 120-123: Cambridge University Press

102. Ketema S (1997) Tef. Eragrostis tef (Zucc.) Trotter. Promoting the conservation and use of underutilized and neglected crops. Institute of Plant Genetics and Crop Plant Research, Gatersleben/International Plant Genetic Resources Institute, Rome, Italy, ISBN 92-9043-304-3

103. Lazăr, S., Dobrotă, D., Breaz, R. E., & Racz SG . Eco-Design of Polymer Matrix Composite Parts: A Review. Polymers, 15(17), 3634.

104. Maurya, A. K., de Souza, F. M., Dawsey, T., & Gupta RK (2024) . Biodegradable polymers and composites: recent development and challenges. Polymer Composites, 45(4), 2896-2918. https://doi.org/10.1002/pc.28023

105. Biglari, N., & Zare EN (2024) . Conjugated polymer-based composite scaffolds for tissue engineering and regenerative medicine. Alexandria Engineering Journal, 87, 277-299. https://doi.org/10.1016/j.aej.2023.12.041

106. Kong, I., Tshai, K. Y., & Hoque ME (2015) . Manufacturing of natural fibre-reinforced polymer composites by solvent casting method. Manufacturing of natural fibre reinforced polymer composites, 331-349. https://doi.org/10.1007/978-3-319-07944-8

107. Karimah, A., Ridho, M. R., Munawar, S. S., Adi, D. S., Damayanti, R., Subiyanto, B., ... & Fudholi A (2021) . A review on natural fibers for development of eco-friendly bio-composite: characteristics, and utilizations. Journal of materials research and technology, 13, 2442-2458. https://doi.org/10.1016/j.jmrt.2021.06.014

108. Djafari Petroudy, S. R., Chabot, B., Loranger, E., Naebe, M., Shojaeiarani, J., Gharehkhani, S., ... & Thomas S (2021) . Recent advances in cellulose nanofibers preparation through energy-efficient approaches: A review. Energies, 14(20), 6792.

109. Magalhães, S., Fernandes, C., Pedrosa, J. F., Alves, L., Medronho, B., Ferreira, P. J., & Rasteiro MDG (2023) . Eco-friendly methods for extraction and modification of cellulose: an overview. Polymers, 15(14), 3138.

110. Bharimalla, A. K., Deshmukh, S. P., Patil, P. G., & Vigneshwaran N (2015) . Energy efficient manufacturing of nanocellulose by chemo-and bio-mechanical processes: a review. World Journal of Nano Science and Engineering, 5(4), 204-212. 204–212

111. Venkatarajan, S., & Athijayamani AJMTP (2020) . An overview on natural cellulose fiber reinforced polymer composites. Materials Today: Proceedings, 37, 3620-3624. Mater Today Proc. https://doi.org/10.1016/j.matpr.2020.09.773

112. Wang, Z., Yao, Z., Zhou, J., He, M., Jiang, Q., Li, A., ... & Zhang D (2019) . Improvement of polylactic acid film properties through the addition of cellulose nanocrystals isolated from waste cotton cloth. International journal of biological macromolecules, 129, 878-886. https://doi.org/10.1016/j.ijbiomac.2019.02.021

113. Qian S, Zhang H, Yao W, Sheng K (2018) Effects of bamboo cellulose nanowhisker content on the morphology, crystallization, mechanical, and thermal properties of PLA matrix biocomposites. Compos Part B Eng 133:203–209. https://doi.org/10.1016/j.compositesb.2017.09.040

114. Kurihara, T., & Isogai A (2014) Properties of poly (acrylamide)/TEMPO-oxidized cellulose nanofibril composite films. Cellulose, 21, 291-299. https://doi.org/https://doi.org/10.1021/acssuschemeng.8b00551

115. Lo Re, G., Spinella, S., Boujemaoui, A., Vilaseca, F., Larsson, P. T., Adås, F., & Berglund LA (2018) Poly (ε-caprolactone) biocomposites based on acetylated cellulose fibers and wet compounding for improved mechanical performance. ACS sustainable chemistry & engineering, 6(5), 6753-6760.

116. Vu, D. H., Mahboubi, A., Ferreira, J. A., Taherzadeh, M. J., & Åkesson D (2022) . Polyhydroxybutyrate-Natural Fiber Reinforcement Biocomposite Production and Their Biological Recyclability through Anaerobic Digestion. Energies, 15(23), 8934.

https://doi.org/10.3390/en15238934

117. Ibrahim, M. M., Moustafa, H., Rahman, E. N. A. E., Mehanny, S., Hemida, M. H., & El-Kashif E (2020) . Reinforcement of starch based biodegradable composite using Nile rose residues. Journal of Materials Research and Technology, 9(3), 6160-6171. https://doi.org/10.1016/j.jmrt.2020.04.018

118. Usman A, Hussain Z, Riaz A, Khan AN (2016) Enhanced mechanical , thermal and antimicrobial properties of poly (vinyl alcohol)/ graphene oxide / starch / silver nanocomposites films. Carbohydr Polym 153:592–599. https://doi.org/10.1016/j.carbpol.2016.08.026

119. Wang, L. P., Wang, Y. P., & Zhang FA (2005) Preparation and characterization of Ni2+-montmorillonite/polyvinyl alcohol water-soluble nanocomposite film. Polymers and Polymer Composites, 13(8), 839-846. https://doi.org/https://doi.org/10.1021/acssuschemeng.8b00551

120. Mousa M, Dong Y (2018) Strong Poly(Vinyl Alcohol) (PVA)/Bamboo Charcoal (BC) Nanocomposite Films with Particle Size Effect. ACS Sustain Chem Eng 6:467–479. https://doi.org/10.1021/acssuschemeng.7b02750

121. Solikhin A, Murayama K (2018) Enhanced properties of poly(vinyl alcohol) composite films filled with microfibrillated cellulose isolated from continuous steam explosion. Int J Plast Technol 22:122–136. https://doi.org/10.1007/s12588-018-9208-9

122. Chakraborty A, Sain M (2005) Cellulose microfibrils : A novel method of preparation using high shear refining and cryocrushing. Holzforschung, Vol. 59, pp. 102–107, 2005. https://doi.org/10.1515/HF.2005.016

123. Santi R, Cigada A, Del Curto B, Farè S (2019) Modulable properties of PVA/cellulose fiber composites. J Appl Biomater Funct Mater 17:. https://doi.org/10.1177/2280800019831224

124. Hasan, M. Z., Arafat, Y., Bashar, M. M., Niloy, M. N. N., Islam, M. I., Khandaker, S., & Chowdhury AS (2022) . Poly-(vinyl alcohol) composite films reinforced with carboxylated

functional microcrystalline cellulose from jute fiber. Composites and Advanced Materials, 31, 26349833221103888. https://doi.org/10.1177/26349833221103888

125. Wang Z, Qiao X, Sun K (2018) Rice straw cellulose nanofibrils reinforced poly(vinyl alcohol) composite films. Carbohydr Polym 197:442–450. https://doi.org/10.1016/j.carbpol.2018.06.025

126. Spagnol, C., Fragal, E. H., Witt, M. A., Follmann, H. D., Silva, R., & Rubira AF (2018) . Mechanically improved polyvinyl alcohol-composite films using modified cellulose nanowhiskers as nano-reinforcement. Carbohydrate polymers, 191, 25-34. https://doi.org/10.1016/j.carbpol.2018.03.001

127. Li, W., Wu, Q., Zhao, X., Huang, Z., Cao, J., Li, J., & Liu S (2014) . Enhanced thermal and mechanical properties of PVA composites formed with filamentous nanocellulose fibrils. Carbohydrate Polymers, 113, 403-410. https://doi.org/10.1016/j.carbpol.2014.07.031

128. Wang Z, Qiao X, Sun K (2018) Rice straw cellulose nanofibrils reinforced poly(vinyl alcohol) composite films. Carbohydr Polym 197:442–450. https://doi.org/10.1016/j.carbpol.2018.06.025

129. Mandal A, Chakrabarty D (2014) Studies on the mechanical , thermal , morphological and barrier properties of nanocomposites based on poly (vinyl alcohol) and nanocellulose from sugarcane bagasse. Journal of Industrial and Engineering Chemistry 20, 462–473. https://doi.org/10.1016/j.jiec.2013.05.003

130. Cho M, Park B (2011) Tensile and thermal properties of nanocellulose-reinforced poly(vinyl alcohol) nanocomposites. Journal of Industrial and Engineering Chemistry 17 (2011) 36–40. https://doi.org/10.1016/j.jiec.2010.10.006

131. Tan, J. Y., Tey, W. Y., Panpranot, J., Lim, S., & Lee KM (2022) . Valorization of oil palm empty fruit bunch for cellulose fibers: a reinforcement material in polyvinyl alcohol biocomposites for its application as detergent capsules. Sustainability, 14(18), 11446. https://doi.org/10.3390/su141811446

132. Naduparambath, S., Sreejith, M. P., Shaniba, V., Balan, A. K., Jinitha, T. V., &

Purushothaman E (2018) . Poly (vinyl alcohol) green composites reinforced with microcrystalline cellulose through sonication. Materials Today: Proceedings, 5(8), 16411-16417. https://doi.org/10.1016/j.matpr.2018.05.139

133. Bos, H.L., Van Den Oever, M.J.A. & Peters OCJJ (2002) Tensile and compressive properties of flax fibers. Journal of Materials Science 37 (2002) 1683– 1692. https://doi.org/10.1023/A:1014925621252

134. Azizi Samir MAS, Alloin F, Dufresne A (2005) Review of recent research into cellulosic whiskers, their properties and their application in nanocomposite field. Biomacromolecules 6:612–626. https://doi.org/10.1021/bm0493685

135. Rwawiire, S., Tomkova, B., Militky, J., Jabbar, A., & Kale BM (2015) Rwawiire, S., Tomkova, B., Militky, J., Jabbar, A., & Kale, B. M. (2015). Development of a biocomposite based on green epoxy polymer and natural cellulose fabric (bark cloth) for automotive instrument panel applications. Composites Part B: Engineering, 81. https://doi.org/10.1016/j.compositesb.2015.06.021

136. Oishi Y, Nakaya M, Matsui E, Hotta A (2015) Structural and mechanical properties of cellulose composites made of isolated cellulose nanofibers and poly(vinyl alcohol). Compos Part A Appl Sci Manuf 73:72–79. https://doi.org/10.1016/j.compositesa.2015.02.026

137. Mischnick P, Momcilovic D (2010) Chemical Structure Analysis of Starch and Cellulose Derivatives. In: Advances in Carbohydrate Chemistry and Biochemistry. Academic Press, pp 117–210

138. Galiwango, E., Rahman, N. S. A., Al-Marzouqi, A. H., Abu-Omar, M. M., & Khaleel AA (2019) . Isolation and characterization of cellulose and α-cellulose from date palm biomass waste. Heliyon, 5(12). https://doi.org/10.1016/j.heliyon.2019.e02937

139. Kargarzadeh, H., Ioelovich, M., Ahmad, I., Thomas, S., & Dufresne A (2017). Methods for extraction of nanocellulose from various sources. Handbook of nanocellulose and cellulose nanocomposites, 1, 1-49.

140. Waliszewska, B., Mleczek, M., Zborowska, M., Goliński, P., Rutkowski, P., & Szentner K (2019) . Changes in the chemical composition and the structure of cellulose and lignin in elm wood exposed to various forms of arsenic. Cellulose, 26, 6303-6315. https://doi.org/10.1007/s10570-019-02511-z

141. Deepa, B., Abraham, E., Cordeiro, N., Mozetic, M., Mathew, A. P., Oksman, K., ... & Pothan LA (2015) . Utilization of various lignocellulosic biomass for the production of nanocellulose: a comparative study. Cellulose, 22, 1075-1090. https://doi.org/10.1007/s10570-015-0554-x

142. Kalyani DC, Fakin T, Horn SJ, Tschentscher R (2017) Valorisation of woody biomass by combining enzymatic saccharification and pyrolysis. Green Chem 19:3302–3312. https://doi.org/10.1039/c7gc00936d

143. Belay, G., Tefera, H., Tadesse, B., Metaferia, G., Jarra, D., & Tadesse T (2005) . Participatory variety selection in the Ethiopian cereal tef (Eragrostis tef). Experimental Agriculture, 42(1), 91-101. https://doi.org/10.1017/S0014479705003108

144. Beyan, S. M., Ambio, T. A., Sundramurthy, V. P., Gomadurai, C., & Getahun AA (2022) . Adsorption phenomenon for removal of Pb (II) via teff straw based activated carbon prepared by microwave-assisted pyrolysis: process modelling, statistical optimisation, isotherm, kinetics, and thermodynamic studies. International Journal of Environment. https://doi.org/10.1080/03067319.2022.2026942

145. Amibo TA, Beyan SM, Damite TM (2022) Production and Optimization of Bio-Based Silica Nanoparticle from Teff Straw (Eragrostis tef) Using RSM-Based Modeling, Characterization Aspects, and Adsorption Efficacy of Methyl Orange Dye. J Chem 2022:. https://doi.org/10.1155/2022/9770520

146. Amibo TA, Beyan SM, Damite TM (2021) Novel Lanthanum Doped Magnetic Teff Straw Biochar Nanocomposite and Optimization Its Efficacy of Defluoridation of Groundwater Using RSM: A Case Study of Hawassa City, Ethiopia. Adv Mater Sci Eng 2021:. https://doi.org/10.1155/2021/9444577

147. Beyan SM, Prabhu SV, Ambio TA, Gomadurai C (2022) A Statistical Modeling and Optimization for Cr(VI) Adsorption from Aqueous Media via Teff Straw-Based Activated Carbon: Isotherm, Kinetics, and Thermodynamic Studies. Adsorpt Sci Technol 2022:. https://doi.org/10.1155/2022/7998069

148. Gabriel, T., Belete, A., Syrowatka, F., Neubert, R. H., & Gebre-Mariam T (2020) . Extraction and characterization of celluloses from various plant byproducts. International journal of biological macromolecules, 158, 1248-1258. https://doi.org/10.1016/j.ijbiomac.2020.04.264

149. Henriksson M, Henriksson G, Berglund LA, Lindström T (2007) An environmentally friendly method for enzyme-assisted preparation of microfibrillated cellulose (MFC) nanofibers. Eur Polym J 43:3434–3441. https://doi.org/10.1016/j.eurpolymj.2007.05.038

150. Razali, N. A. M., Mohd Sohaimi, R., Othman, R. N. I. R., Abdullah, N., Demon, S. Z. N., Jasmani, L., ... & Halim NA (2022) . Comparative study on extraction of cellulose fiber from rice straw waste from chemo-mechanical and pulping method. Polymers, 14(3), 387. https://doi.org/10.3390/polym14030387

151. Qingzheng Cheng, 1* Siqun Wang 1 Qingyou Han2 (2010) Novel Process for Isolating Fibrils from Cellulose Fibers by High-Intensity Ultrasonication. II. Fibril Characterization. Journal of Applied Polymer Science, Vol. 115, 2756–2762 (2010), Wiley Periodicals, Inc. https://doi.org/10.1002/app

152. Moniruzzaman M, Ono T (2013) Separation and characterization of cellulose fibers from cypress wood treated with ionic liquid prior to laccase treatment. Bioresour Technol 127:132–137. https://doi.org/10.1016/j.biortech.2012.09.113

153. Yashim, M. M., Mohammad, M., Asim, N., Fudholi, A., & Abd Kadir NH (2021) . Characterisation of microfibrils cellulose isolated from oil palm frond using high-intensity ultrasonication. In IOP Conference Series: Materials Science and Engineering (Vol. 1176, No. 1, p. 012004). IOP Publishing. https://doi.org/10.1088/1757-899x/1176/1/012004

154. Rehman N, Alam S, Mian I, Ullah H (2019) Environmental friendly method for the

extraction of cellulose from Triflolium resopinatum and its characterization. Bulletin of the Chemical Society of Ethiopia,2019, 33(1), 61-68. ISSN 1011-3924. https://doi.org/10.4314/bcse.v33i1.6

155. Sukri, S.S.M., Rahman, R.A., Illias, R.M. and Yaakob H (2014) Optimization of alkaline pretreatment conditions of oil palm fronds in improving the lignocelluloses contents for reducing sugar production. Romanian Biotechnological Letters, Vol. 19, No. 1, 2014 9006

156. Abolore, R. S., Jaiswal, S., & Jaiswal AK (2024) . Green and sustainable pretreatment methods for cellulose extraction from lignocellulosic biomass and its applications: a review. Carbohydrate Polymer Technologies and Applications, 100396. Carbohydr Polym Technol Appl 7:100396. https://doi.org/10.1016/j.carpta.2023.100396

157. Mehdi Jonoobi, Jalaludin Harun, Alireza Shakeri, Manjusri Misra and KO (2009) . Chemical composition, crystallinity and thermal degradation of bleached and unbleached kenaf bast (Hibiscus cannabinus) pulp and nanofiber. BioResources, 4(2), 626-639.

158. Chen, Y., Stevens, M. A., Zhu, Y., Holmes, J., & Xu H (2013) . Understanding of alkaline pretreatment parameters for corn stover enzymatic saccharification. Biotechnology for biofuels, 6, 1-10. https://doi.org/10.1201/b18437

159. Qasim, U., Jamil, F., Al-Muhtaseb, A. A. H., Rafiq, S., Ali, M., Khan Niazi, M. B., ... & Saqib S (2020) . Isolation of cellulose from wheat straw using alkaline hydrogen peroxide and acidified sodium chlorite treatments: comparison of yield and properties. Advances in Polymer Technology, 2020, 1-7. https://doi.org/10.1155/2020/9765950

160. Dutra, E. D., Santos, F. A., Alencar, B. R. A., Reis, A. L. S., de Souza, R. D. F. R., Aquino, K. A. D. S., ... & Menezes RSC (2017) . Alkaline hydrogen peroxide pretreatment of lignocellulosic biomass: status and perspectives. Biomass Conversion and Biorefinery, 8, 225-234. https://doi.org/10.1007/s13399-017-0277-3

161. de Morais Teixeira, E., Bondancia, T. J., Teodoro, K. B. R., Corrêa, A. C., Marconcini, J. M., & Mattoso LHC (2011) . Sugarcane bagasse whiskers: extraction and characterizations. Industrial Crops and Products, 33(1), 63-66. https://doi.org/10.1016/j.indcrop.2010.08.009

162. Ng, H. M., Sin, L. T., Tee, T. T., Bee, S. T., Hui, D., Low, C. Y., & Rahmat AR (2015) . Extraction of cellulose nanocrystals from plant sources for application as reinforcing agent in polymers. Composites Part B: Engineering, 75, 176-200. https://doi.org/10.1016/j.compositesb.2015.01.008

163. Sun XF, Sun RC, Fowler P, Baird MS (2004) Isolation and characterisation of cellulose obtained by a two-stage treatment with organosolv and cyanamide activated hydrogen peroxide from wheat straw. Carbohydr Polym 55:379–391. https://doi.org/10.1016/j.carbpol.2003.10.004

164. Sluiter, A., Hames, B., Ruiz, R., Scarlata, C., Sluiter, J., & Templeton D (2005) . Determination of ash in biomass. Laboratory analytical procedure (LAP). National Renewable Energy Laboratory, NREL/TP-510-42622 .

165. Sluiter, A., Ruiz, R., Scarlata, C., Sluiter, J., & Templeton DJLAP (2005) . Determination of extractives in biomass. Laboratory analytical procedure (LAP),National Renewable Energy Laboratory, NREL/TP-510-42619.

166. Sluiter, A., Hames, B., Ruiz, R., Scarlata, C., Sluiter, J., Templeton, D., & Crocker DLAP (2008) . Determination of structural carbohydrates and lignin in biomass. Laboratory analytical procedure,National Renewable Energy Laboratory, NREL/TP-510-42618.

167. Kürschner K. HA (1931) quantitative cellulose bestimmung. Chemiker Zeitung. 1931, 55: 161-163. Zeitschrift für Pflanzenernährung, Düngung, Bodenkd 88:1–13

168. Ouensanga A (1989) Variation of fiber composition in sugar cane stalks. Wood fiber Sci J Soc Wood Sci Technol 21:105–111

169. Segal L, Creely JJ, Martin AE, Conrad CM (1959) An Empirical Method for Estimating the Degree of Crystallinity of Native Cellulose Using the X-Ray Diffractometer. Text Res J 29:786–794. https://doi.org/10.1177/004051755902901003

170. Gabriel T, Wondu K, Dilebo J (2021) Valorization of khat (Catha edulis) waste for the production of cellulose fibers and nanocrystals. PLoS One 16:1–20. https://doi.org/10.1371/journal.pone.0246794

171. Reddy JP, Rhim JW (2018) Extraction and Characterization of Cellulose Microfibers from Agricultural Wastes of Onion and Garlic. J Nat Fibers 15:465–473. https://doi.org/10.1080/15440478.2014.945227

172. Paixão, S. M., Ladeira, S. A., Silva, T. P., Arez, B. F., Roseiro, J. C., Martins, M. L. L., & Alves L (2016) . Sugarcane bagasse delignification with potassium hydroxide for enhanced enzymatic hydrolysis. RSC advances, 6(2), 1042-1052. https://doi.org/10.1039/c5ra14908h

173. Fengel D, Shao X (1984) A chemical and ultrastructural study of the Bamboo species Phyllostachys makinoi Hay. Wood Science and Technology, Springer-Verlag, 18:103-112. Wood Sci Technol. https://doi.org/10.1007/BF00350469

174. Reddy, K. O., Maheswari, C. U., Dhlamini, M. S., Mothudi, B. M., Kommula, V. P., Zhang, J., ... & Rajulu A V. (2018) . Extraction and characterization of cellulose single fibers from native african napier grass. Carbohydrate Polymers, 188, 85-91. https://doi.org/10.1016/j.carbpol.2018.01.110

175. Vardhini KJV, Murugan R, Selvi CT, Surjit R (2016) Optimisation of alkali treatment of banana fibres on lignin removal. Indian J Fibre Text Res 41:156–160

176. Sun XF, Sun RC, Tomkinson J, Baird MS (2004) Degradation of wheat straw lignin and hemicellulosic polymers by a totally chlorine-free method. Polym Degrad Stab 83:47–57. https://doi.org/10.1016/S0141-3910(03)00205-2

177. Lee SH, Doherty T V., Linhardt RJ, Dordick JS (2009) Ionic liquid-mediated selective extraction of lignin from wood leading to enhanced enzymatic cellulose hydrolysis. Biotechnol Bioeng 102:1368–1376. https://doi.org/10.1002/bit.22179

178. Li Qun, L. Q., Wang AiJiao, W. A., Ding WenHui, D. W., & Zhang YuJia ZY (2017) . Influencing factors for alkaline degradation of cellulose.

179. Deepa, B., Abraham, E., Cordeiro, N., Mozetic, M., Mathew, A. P., Oksman, K., ... & Pothan LA (2015) . Utilization of various lignocellulosic biomass for the production of nanocellulose: a comparative study. Cellulose, 22, 1075-1090. https://doi.org/10.1007/s10570-015-0554-x

180. Cheng, M., Qin, Z., Chen, Y., Hu, S., Ren, Z., & Zhu M (2017) . Efficient extraction of cellulose nanocrystals through hydrochloric acid hydrolysis catalyzed by inorganic chlorides under hydrothermal conditions. ACS Sustainable Chemistry & Engineering, 5(6), 4656-4664. https://doi.org/10.1021/acssuschemeng.6b03194

181. Parikin, M. Dani, B. Sugeng, N. D. Purnamasari SA dan SGS (2017) "Bragg formula aritmetic evaluation on crystal structure of high temperature structural steel type f1, a2 and a2-aps". Center for Science and Technology of Advanced Materials, Indonesia .

182. French AD (2014) Idealized powder diffraction patterns for cellulose polymorphs. Cellulose 21:885–896. https://doi.org/10.1007/s10570-013-0030-4

183. Darby Harris, Vincent Bulone, Shi-You Ding and SDD (2010) Tools for cellulose analysis in plant cell walls. Plant Physiol 153:420–426. https://doi.org/10.1104/pp.110.154203

184. Li, Rongji, Jianming Fei, Yurong Cai, Yufeng Li, Jianqin Feng and JY (2009) . Cellulose whiskers extracted from mulberry: A novel biomass production. Carbohydrate polymers, 76(1), 94-99. https://doi.org/10.1016/j.carbpol.2008.09.034

185. Rezende, C. A., De Lima, M. A., Maziero, P., deAzevedo, E. R., Garcia, W., & Polikarpov I (2011) . Chemical and morphological characterization of sugarcane bagasse submitted to a delignification process for enhanced enzymatic digestibility. Biotechnology for biofuels, 4, 1-19. https://doi.org/10.1186/1754-6834-4-54

186. Katakojwala R, Mohan SV (2020) Microcrystalline cellulose production from sugarcane bagasse: Sustainable process development and life cycle assessment. J Clean Prod 249:119342. https://doi.org/10.1016/j.jclepro.2019.119342

187. Assefa, E. G., Kiflie, Z., & Demsash HD (2022) Valorization of abundantly available ethiopian teff (eragrostis tef) straw for the isolation of cellulose fibrils by alkaline hydrogen peroxide treatment method. Journal of Polymers and the Environment, 31(3), 900-912. https://doi.org/10.1007/s10924-022-02646-4

188. Yang, S., Zhang, Y., Yue, W., Wang, W., Wang, Y. Y., Yuan, T. Q., & Sun RC (2016) . Valorization of lignin and cellulose in acid-steam-exploded corn stover by a moderate

alkaline ethanol post-treatment based on an integrated biorefinery concept. Biotechnology for biofuels, 9, 1-14. https://doi.org/10.1186/s13068-016-0656-1

189. Kapoor M, Panwar D, Kaira GS (2016) Bioprocesses for Enzyme Production Using Agro-Industrial Wastes: Technical Challenges and Commercialization Potential. Elsevier Inc.

190. Ismail, F., Othman, N. E. A., Wahab, N. A., Hamid, F. A., & Aziz AA (2021) . Preparation of microcrystalline cellulose from oil palm empty fruit bunch fibre using steam-assisted acid hydrolysis. Journal of Advanced Research in Fluid Mechanics and Thermal Sciences, 81(1), 88-98. https://doi.org/10.37934/arfmts.81.1.8898

191. Lu, Q., Tang, L., Lin, F., Wang, S., Chen, Y., Chen, X., & Huang B((2014) . Preparation and characterization of cellulose nanocrystals via ultrasonication-assisted FeCl 3-catalyzed hydrolysis. Cellulose, 21, 3497-3506. https://doi.org/10.1007/s10570-014-0376-2

192. Chen YW, Lee HV, Abd Hamid SB (2017) Investigation of optimal conditions for production of highly crystalline nanocellulose with increased yield via novel Cr(III)-catalyzed hydrolysis: Response surface methodology. Carbohydr Polym 178:57–68. https://doi.org/10.1016/j.carbpol.2017.09.029

193. Jinbao, L., Melvin, T., John, D., & Yun J (2013) . Effects and Mechanism of Metal Chloride Salts on Pretreatment and Enzymatic Digestibility of Corn Stover. Industrial and Engineering Chemistry Research. 52:1775–1782. https://doi.org/10.1021/ie3019609

194. Chen YW, Lee HV, Abd Hamid SB (2016) Preparation and characterization of cellulose crystallites via Fe(III)-, Co(II)- and Ni(II)-assisted dilute sulfuric acid catalyzed hydrolysis process. J Nano Res 41:96–109. https://doi.org/10.4028/www.scientific.net/JNanoR.41.96

195. Kumar A, Negi YS, Choudhary V, Bhardwaj NK (2013) Characterization of Cellulose Nanocrystals Produced by Acid-Hydrolysis from Sugarcane Bagasse as Agro-Waste. Journal of Materials Physics and Chemistry.Vol. 2, No. 1, 1-8. https://doi.org/10.12691/jmpc-2-1-1

196. Uddin, A. H., Khalid, R. S., Alaama, M., Abdualkader, A. M., Kasmuri, A., & Abbas SA (2016) . Comparative study of three digestion methods for elemental analysis in traditional

medicine products using atomic absorption spectrometry. Journal of analytical science and technology, 7, 1-7. https://doi.org/10.1186/s40543-016-0085-6

197. Le Troedec M, Sedan D, Peyratout C, et al (2008) Influence of various chemical treatments on the composition and structure of hemp fibres. Compos Part A Appl Sci Manuf 39:514–522. https://doi.org/10.1016/j.compositesa.2007.12.001

198. Rashid, S., & Dutta H (2020) . Characterization of nanocellulose extracted from short, medium and long grain rice husks. Industrial Crops and Products, 154, 112627. https://doi.org/10.1016/j.indcrop.2020.112627

199. Zhuang, J., Li, M., Pu, Y., Ragauskas, A. J., & Yoo CG (2020) . Observation of potential contaminants in processed biomass using fourier transform infrared spectroscopy. Applied Sciences, 10(12), 4345. https://doi.org/10.3390/app10124345

200. Tian, D., Chandra, R. P., Lee, J. S., Lu, C., & Saddler JN (2017) . A comparison of various lignin-extraction methods to enhance the accessibility and ease of enzymatic hydrolysis of the cellulosic component of steam-pretreated poplar. Biotechnology for biofuels, 10, 1-10. https://doi.org/10.1186/s13068-017-0846-5

201. Cheng, M., Qin, Z., Liu, Y., Qin, Y., Li, T., Chen, L., & Zhu M (2014) . Efficient extraction of carboxylated spherical cellulose nanocrystals with narrow distribution through hydrolysis of lyocell fibers by using ammonium persulfate as an oxidant. Journal of Materials Chemistry A, 2(1), 251-258. https://doi.org/10.1039/c3ta13653a

202. Tan, X. Y., Abd Hamid, S. B., & Lai CW (2015) . Preparation of high crystallinity cellulose nanocrystals (CNCs) by ionic liquid solvolysis. Biomass and Bioenergy, 81, 584-591. https://doi.org/10.1016/j.biombioe.2015.08.016

203. Panthapulakkal S, Zereshkian A, Sain M (2006) Preparation and characterization of wheat straw fibers for reinforcing application in injection molded thermoplastic composites. Bioresour Technol 97:265–272. https://doi.org/10.1016/j.biortech.2005.02.043

204. Ahvenainen P, Kontro I, Svedström K (2016) Comparison of sample crystallinity determination methods by X-ray diffraction for challenging cellulose I materials. Cellulose

23:1073–1086. https://doi.org/10.1007/s10570-016-0881-6

205. Sun X, Wu Q, Ren S, Lei T (2015) Comparison of highly transparent all-cellulose nanopaper prepared using sulfuric acid and TEMPO-mediated oxidation methods. Cellulose 22:1123–1133. https://doi.org/10.1007/s10570-015-0574-6

206. Nang An, V., Chi Nhan, H. T., Tap, T. D., Van, T. T. T., Van Viet, P., & Van Hieu L (2020) . Extraction of high crystalline nanocellulose from biorenewable sources of Vietnamese agricultural wastes. Journal of Polymers and the Environment, 28, 1465-1474. https://doi.org/10.1007/s10924-020-01695-x

207. Feng, Y. H., Cheng, T. Y., Yang, W. G., Ma, P. T., He, H. Z., Yin, X. C., & Yu XX (2018) . Characteristics and environmentally friendly extraction of cellulose nanofibrils from sugarcane bagasse. Industrial Crops and Products, 111, 285-291. https://doi.org/10.1016/j.indcrop.2017.10.041

208. Conti ME (2008) . Heavy metals in food packagings-the state of the art. https://doi.org/10.1201/9781420003987.ch9

209. van Putten EM (2011) Heavy metals in packaging: a literature survey. National Institute for Public Health and the Environment

210. Gbadeyan OJ, Linganiso LZ, Deenadayalu N (2022) Thermomechanical characterization of bioplastic films produced using a combination of polylactic acid and bionano calcium carbonate. Sci Rep 12:1–9. https://doi.org/10.1038/s41598-022-20004-1

211. Gbadeyan, O. J., Fagbemi, O. D., Andrew, J., Adali, S., Glen, B., & Sithole B (2022). (2023) Assessment and Optimization of Thermal Stability and Water Absorption of Loading Snail Shell Nanoparticles and Sugarcane Bagasse Cellulose Fibers on Polylactic Acid Bioplastic Films. Polymers, 15(6), 1557. https://doi.org/10.3390/polym15061557

212. Htwe YZN, Mariatti M (2020) Fabrication and characterization of silver nanoparticles/PVA composites for flexible electronic application. AIP Conf Proc 2267:. https://doi.org/10.1063/5.0016135

213. Krishnaraja, A. R., Kulanthaivel, P., Ramshankar, P., Wilson, V. H., Palanisamy, P., Vivek, S., ... & Jose S (2022) Performance of polyvinyl alcohol and polypropylene fibers under simulated cementitious composites pore solution. Advances in Materials Science and Engineering. https://doi.org/10.1155/2022/9669803

214. Zahid, M., Ali, S., Saleem, S., Salman, M., & Khan M (2020) . Carbon nanoparticles/polyvinyl alcohol composites with enhanced optical, thermal, mechanical, and flame-retardant properties. Journal of Applied Polymer Science, 137(41), 49261. https://doi.org/10.1002/app.49261

215. Cheng-an, T., Hao, Z., Fang, W., Hui, Z., Xiaorong, Z., & Jianfang W (2017) Mechanical properties of graphene oxide/polyvinyl alcohol composite film. Polymers and Polymer Composites, 25(1), 11-16. https://doi.org/10.1177/096739111702500102

216. Van der Schueren, B., El Marouazi, H., Mohanty, A., Lévêque, P., Sutter, C., Romero, T., & Janowska I (2020) . Polyvinyl alcohol-few layer graphene composite films prepared from aqueous colloids. Investigations of mechanical, conductive and gas barrier properties. Nanomaterials, 10(5), 858. https://doi.org/10.3390/nano10050858

217. Gbadeyan, O. J., Fagbemi, O. D., Andrew, J., Adali, S., Glen, B., & Sithole B (2022) Cellulose nanocrystals and snail shell-reinforced polyvinyl alcohol bioplastic films: Additive concentration optimization and mechanical properties assessment. Journal of Applied Polymer Science, 139(36), e52839.

218. Assefa EG, Kiflie Z, Dessalegn H (2023) Transition metal salt assisted dilute acid hydrolysis for synthesis of microcrystalline cellulose from Teff Straw. Cellulose. https://doi.org/10.1007/s10570-023-05270-0

219. Tănase EE, Popa ME, Râpă M, Popa O (2015) Preparation and characterization of biopolymer blends based on polyvinyl alcohol and starch. Rom Biotechnol Lett 20:10306–10315

220. El Achaby, M., El Miri, N., Aboulkas, A., Zahouily, M., Bilal, E., Barakat, A., & Solhy A (2017) (2017) . Processing and properties of eco-friendly bio-nanocomposite films filled

with cellulose nanocrystals from sugarcane bagasse. International journal of biological macromolecules, 96, 340-352. https://doi.org/10.1016/j.ijbiomac.2016.12.040

221. Sarebanha S, Farhan A (2018) Eco - friendly Composite Films Based on Polyvinyl Alcohol and Jackfruit Waste Flour. J Packag Technol Res 2:181–190. https://doi.org/10.1007/s41783-018-0043-4

222. Fahma F, Hori N, Iwata T, Takemura A (2017) PVA nanocomposites reinforced with cellulose nanofibers from oil palm empty fruit bunches (OPEFBs). Emirates J Food Agric 29:323–329. https://doi.org/10.9755/ejfa.2016-02-215

223. Khan, A., Khan, R. A., Salmieri, S., Le Tien, C., Riedl, B., Bouchard, J., ... & Lacroix M (2012) . Mechanical and barrier properties of nanocrystalline cellulose reinforced chitosan based nanocomposite films. Carbohydrate polymers, 90(4), 1601-1608. https://doi.org/10.1016/j.carbpol.2012.07.037

224. S. Erden, K. Sever, Y. Seki and MS (2010) . Enhancement of the mechanical properties of glass/polyester composites via matrix modification glass/polyester composite siloxane matrix modification. Fibers and polymers, 11, 732-737. https://doi.org/10.1007/s12221-010-0732-2

225. Lee, S. Y., Mohan, D. J., Kang, I. A., Doh, G. H., Lee, S., & Han SO (2009) . Nanocellulose reinforced PVA composite films: effects of acid treatment and filler loading. Fibers and Polymers, 10, 77-82. https://doi.org/10.1007/s12221-009-0077-x

226. Panaitescu, D. M., Vizireanu, S., Stoian, S. A., Nicolae, C. A., Gabor, A. R., Damian, C. M., ... & Dinescu G (2020) Poly (3-hydroxybutyrate) modified by plasma and TEMPO-oxidized celluloses. Polymers, 12(7), 1510.

227. Rhim JW (2011) Effect of clay contents on mechanical and water vapor barrier properties of agar-based nanocomposite films. Carbohydrate polymers, 86(2), 691-699. https://doi.org/10.1016/j.carbpol.2011.05.010

228. Ben Cheikh, S., Ben Cheikh, R., Cunha, E., Lopes, P. E., & Paiva MC (2018) . Production of cellulose nanofibers from Alfa grass and application as reinforcement for polyvinyl

alcohol. Plastics, Rubber and Composites, 47(7), 297-305. https://doi.org/10.1080/14658011.2018.1479822

229. Li, C. G., Zheng, B. G., Peng, W. G., Tian, W., & Zhang R (2012) . Preparation and Properties of Bagasses Cellulose Microcrystal Reinforced Poly (Vinyl alcohol) Composite Film. Advanced Materials Research, 399, 381-384. https://doi.org/10.4028/www.scientific.net/AMR.399-401.381

230. Fortunati, E., Luzi, F., Jiménez, A., Gopakumar, D. A., Puglia, D., Thomas, S., ... & Torre L (2016) . Revalorization of sunflower stalks as novel sources of cellulose nanofibrils and nanocrystals and their effect on wheat gluten bionanocomposite properties. Carbohydrate polymers, 149, 357-368. https://doi.org/10.1016/j.carbpol.2016.04.120

231. Wu, J., Du, X., Yin, Z., Xu, S., Xu, S., & Zhang Y. (2019) . Preparation and characterization of cellulose nanofibrils from coconut coir fibers and their reinforcements in biodegradable composite films. Carbohydrate polymers, 211, 49-56. https://doi.org/10.1016/j.carbpol.2019.01.093

232. Ji, T., Zhang, R., Dong, X., Sameen, D. E., Ahmed, S., Li, S., & Liu Y (2020) . Effects of ultrasonication time on the properties of polyvinyl alcohol/sodium carboxymethyl cellulose/nano-ZnO/multilayer graphene nanoplatelet composite films. Nanomaterials, 10(9), 1797. https://doi.org/10.3390/nano10091797

APPENDIX

Appendix A1: Supplementary Data for chapter 3

Table A1 Effect of solid to liquid ratio on the alkali treatment of raw fiber

Run	Solid to liquid ratio (g/ml)	Yield (%)	Residual lignin (%)
1	1:20	51.29 ±0.541	54.255 ±2.876
2	1:30	42.89 ±1.317	61.15 ±2.093
3	1:40	38.12 ±1.58	62.43 1.095

A preliminary experimental work was conducted to observe the effects of solid to liquid ratio (g/ml) at constant temperature (80 °C), and time (90min) on cellulose yield and lignin removal during the alkali treatment of *Teff* straw.

Appendix A2: Supplementary Data for chapter 3

Table A2 The effects of the bleaching parameters on cellulose yield and residual lignin content of the cellulose fiber

	Process condition				
Run	Ratio (g/ml)	Temperature (°C)	Time (min)	Yield (%)	Residual lignin content (%)
1	1:20	65	90	92.08 ±0.319	4 ±0.319
2	1:30	65	90	90.595 ±0.27	2.58 ±0.236
3	1:40	65	90	88.56 ±0.554	2.35 ±0.111
4	1:30	55	90	91.255 ±0.298	2.945 ±0.146
5	1:30	65	90	90.595 ±0.27	2.58 ±0.236

6	1:30	75	90	85.97 ±0.291	2.365 ±0.0901
7	1:30	65	60	92.315 ±0.381	3.12 ±0.263
8	1:30	65	90	90.595 ±0.27	2.58 ±0.236
9	1:30	65	120	89.45 ±0.263	2.435 ±0.132

In this preliminary work, the effects of the bleaching parameters (temperature, time and solid to liquid) on cellulose yield and residual lignin content of the cellulose fiber was observed.

Appendix A3: Supporting Information for Chapter 3

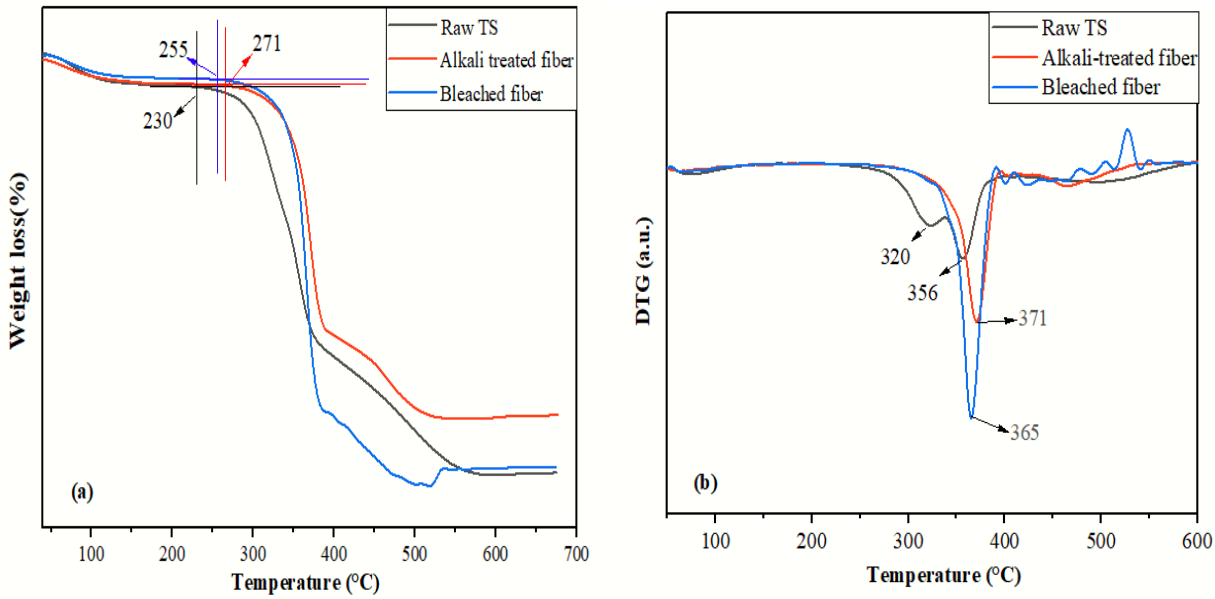

Fig. A3 (a) TGA and (b) DTG curve for the raw, alkali treated and bleached fibers

Appendix A4: Supporting Information for Chapter 3

The miller indices were assigned to the diffraction peaks according to the recent theoretical calculation [182]. The presence of diffraction peaks at 2θ = 16.0°, 22.0° and 34.0° indicates that the raw *Teff* straw showed the cellulose-I crystal structure. Thus, The miller indices were determined using a multi-step process where the observed peak positions, 2theta (2θ), were first converted into d_{hkl} values using Bragg's law, and the *miller indices (hkl)* values were then determined using the calculated d_{hkl} and predetermined parameters from the published references using Eq. A2.

Bragg's law is formulated as

$$d_{hkl} = \frac{\lambda}{2\sin\theta} \qquad Eq.\ A1$$

$$For\ \ 2\theta = \ 16.0°, and \lambda = 1.5$$

$$d_{hkl} = \frac{1.5}{2\sin(8.0)} = 5.36$$

From geometry relation [181]

$$d_{hkl} = \frac{a}{\sqrt{h^2 + k^2 + l^2}} \qquad Eq.\ A2$$

$$h^2 + k^2 + l^2 = \frac{a^2}{d_{hkl}^2} \quad = \frac{7.78^2}{5.36^2} = 2.1$$

$$1^2 + 1^2 + 0 = 2 \approx 2.1$$

Where α =7.78 for native cellulose structure from the literature [182]. Similarly, for the other 2θ values, the miller indices can be determined as

$$For\ \ 2\theta = 22°$$

$$d_{hkl} = \frac{1.5}{2\sin(11.0)} = 3.95 \quad then$$

$$h^2 + k^2 + l^2 = \frac{a^2}{d_{hkl}^2} \quad = \frac{7.78^2}{3.95^2} = 3.9 \quad this\ implies$$

$$2^2 + 0 + 0 = 4 \approx 3.9$$

$$For\ \ 2\theta = 34°$$

$$d_{hkl} = \frac{1.5}{2\sin(17.5)} = 2.59 \quad then$$

$$h^2 + k^2 + l^2 = \frac{a^2}{d_{hkl}^2} \quad = \frac{7.78^2}{2.59^2} = 9.0$$

$$4^2 + 0 + 0 = 8 \approx 9.0$$

Therefore, the determined miller indices were *110, 200,* and *400* illustrated the orientation of the cellulose crystallites along the raw fiber for 2θ = 16.0, 22,and 34° respectivily [182].

Appendix A5: Supporting Information for Chapter 3

- ***Determination of the lignin content***

The extractive free dried raw biomass will be weighed in glass test tubes and 72% H_2SO_4 will be added. Allow the sample to sit at room temperature for two hours, shaking gently every half hour to ensure thorough breakdown of the material. Once this initial breakdown is complete, add 84 milliliters of pure water to the sample. The next phase of the breakdown process will take place in a high-pressure steam chamber (autoclave) for one hour at a temperature of 121 °C. The mixture was allowed to cool to ambient temperature. Subsequently, the liquid portion was separated from the solid material by filtering it through a specialized crucible under vacuum conditions. The acid insoluble lignin will be determined by drying the residues at 105 ^oC and accounting for ash by incinerating the hydrolyzed samples at 575 ^oC in a muffle furnace. The acid soluble lignin fraction will be determined by measuring the absorbance of the acid hydrolyzed samples at 320 nm. Lignin content is determined by combining the quantities of acid-insoluble and acid-soluble lignin.

The acid insoluble lignin (AIL) fraction will be determined as

$$\%AIL = \frac{\left(W_{cru.+AIR} - W_{cru.}\right) - \left(W_{cru.+ash} - W_{cru.}\right)}{ODW_{sample}} x100 \qquad Eq.\ A3$$

Where AIR = acid insoluble residue, W_{cru}= weight of crucible, and $W_{cru+ash}$ = weight of crucible with ash.

Similarly, the acid soluble lignin (ASL) fraction will be calculated as

$$\%ASL = \frac{UV_{abs} * Volume_{filtrate} * Dilution}{\varepsilon * ODW_{sample} * pathlength} x100 \qquad Eq.\ A4$$

Where

UV_{abs} = average UV-Vis absorbance for the sample at appropriate wavelength,

ε= absorbity of biomass at specific wavelength,

ODW_{sample} = oven dry weight of sample,

Path length = path length of UV-Vis cell in cm and

$$Dilution = \frac{Volume_{sample} + Volume_{dilution\ solvent}}{Volume_{sample}}$$

$$ODW\ sample = \frac{Weight_{air\ dry\ sample} x\ \%\ Total\ solids}{100}$$

$$\%\ Total\ solids = \frac{\left(Weight_{dry\ samp + dry\ pan} - Weight_{dry\ pan}\right)}{weight_{sample\ as\ received}} x100$$

Therefore the total amount of lignin on an extractive free basis

$$\%\ \text{Lignin}_{\text{extractive free}} = \%\ \text{AIL} + \%\ \text{ASL} \qquad \text{Eq. A5}$$

Appendix B1: Supporting Information for Chapter 4

To confirm the removal of metals from the isolated cellulose, it has been conducted metal analysis using Atomic absorption spectroscopy. After determining the absorbance for all samples, a calibration curve was constructed as given in Figure B1 below. It have had a linear regressions, R = 0.99926 and a linear equation y =0.0034 + 0.0215 x for iron standard curve while, R = 0.99908 and a linear equation y =0.0002 + 0.0023 x for chrome curve. The absorbance of the prepared samples was then compared against the calibration to obtain the corresponding concentrations.

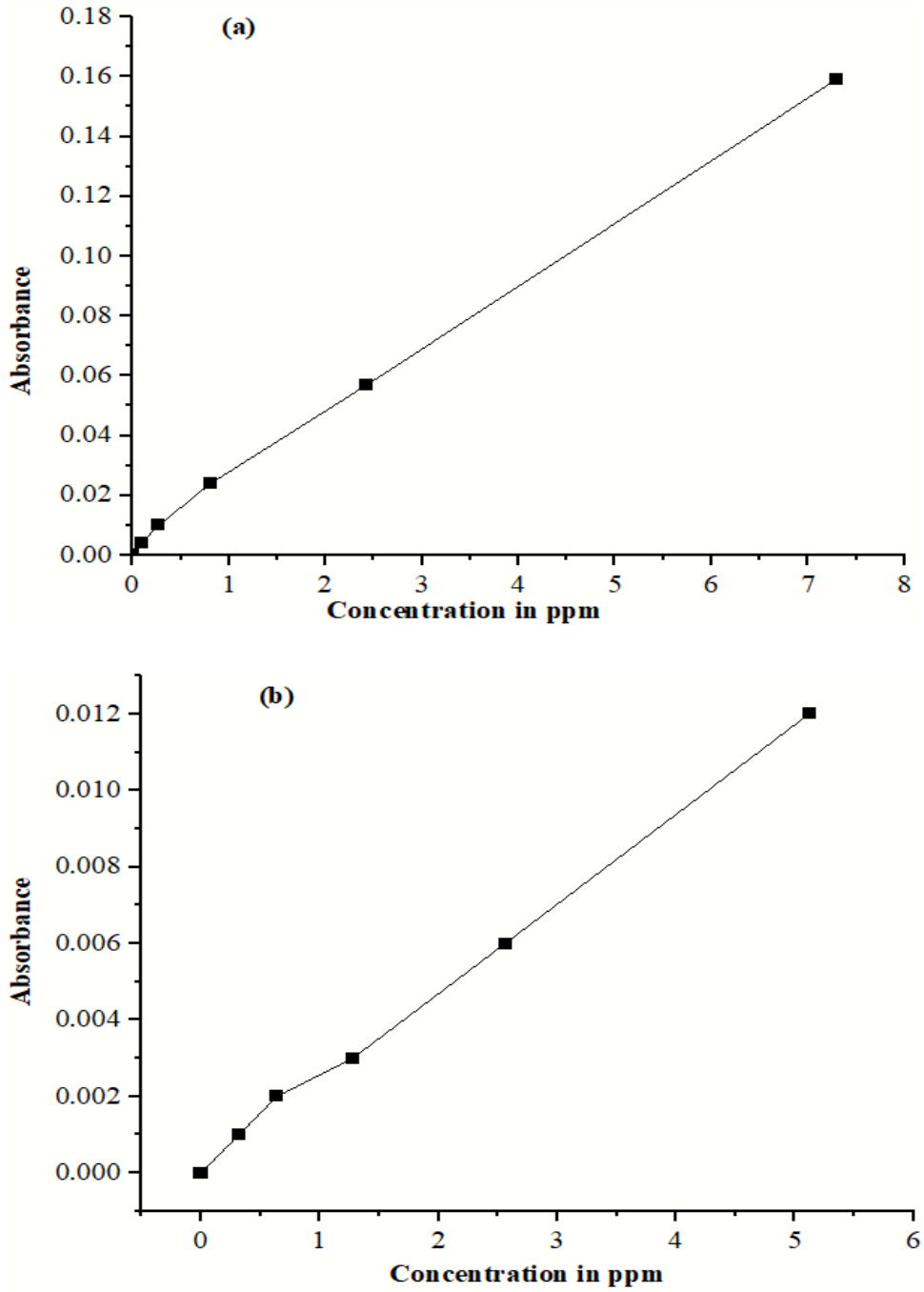

Fig. B1 Calibration curve (a) and (b) established after taking the absorbencies of all the standard solutions for iron and chrome, respectively using AAS